

การสังเคราะห์และสมบัติเชิงพื้นผิวของไดบล็อกโคพอลิเมอร์บรัซที่มีฟลูออรีน



นางสาวศิริโรจน์ เจียมรัตน์พิทักษ์

สถาบันวิทยบริการ

จุฬาลงกรณ์มหาวิทยาลัย

วิทยานิพนธ์นี้เป็นส่วนหนึ่งของการศึกษาตามหลักสูตรปริญญาวิทยาศาสตรมหาบัณฑิต

สาขาวิชาปิโตรเคมีและวิทยาศาสตร์พอลิเมอร์

คณะวิทยาศาสตร์ จุฬาลงกรณ์มหาวิทยาลัย

ปีการศึกษา 2548

ISBN 974-14-2193-1

ลิขสิทธิ์ของจุฬาลงกรณ์มหาวิทยาลัย

SYNTHESIS AND SURFACE PROPERTIES OF FLUORINE-  
CONTAINING DIBLOCK COPOLYMER BRUSH



Miss Sirorat Jeamrattanapitak

สถาบันวิทยบริการ  
จุฬาลงกรณ์มหาวิทยาลัย

A Thesis Submitted in Partial Fulfillment of the Requirements  
for the Degree of Master of Science Program in Petrochemistry and Polymer Science

Faculty of Science  
Chulalongkorn University


Academic Year 2005

ISBN 974-14-2193-1

**Thesis Title**            Synthesis and Surface Properties of Fluorine-Containing Diblock  
Copolymer Brush  
**By**                         Miss Sirorat Jeamrattanapitak  
**Field of Study**         Petrochemistry and Polymer Science  
**Thesis Advisor**        Assistant Professor Voravee P. Hoven, Ph.D.


---

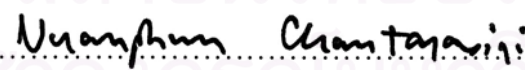
Accepted by the Faculty of Science, Chulalongkorn University in Partial  
Fulfillment of the Requirements for the Master's Degree

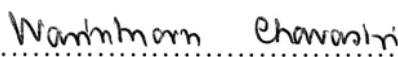
  
.....Dean of the Faculty of Science  
(Professor Piamsak Menasveta, Ph.D.)

THESIS COMMITTEE

  
.....Chairman  
(Associate Professor Supawan Tantayanon, Ph.D.)

  
.....Thesis Advisor  
(Assistant Professor Voravee P. Hoven, Ph.D.)

  
.....Member  
(Associate Professor Nuanphun Chantarasiri, Ph.D.)

  
.....Member  
(Assistant Professor Warinthorn Chavasiri, Ph.D.)

ศิริรัตน์ เจียมรัตน์พิทักษ์: การสังเคราะห์และสมบัติเชิงพื้นผิวของไดบล็อกโคพอลิเมอร์บรัชที่มีฟลูออรีน (SYNTHESIS AND SURFACE PROPERTIES OF FLUORINE-CONTAINING DIBLOCK COPOLYMER BRUSH) อาจารย์ที่ปรึกษา: ผศ.ดร.วรวิทย์ ไสวเณร; 99 หน้า ISBN 974-14-2193-1

สามารถสังเคราะห์ไดบล็อกโคพอลิเมอร์บรัชของพอลิ(2,2,2-ไตรฟลูออโรเอทิลเมทาคริเลต) และ พอลิ(เทอเทียรี-บิวทิลเมทาคริเลต) (พีทีเอฟเอ็มเอ-บล็อก-พีทีบีเอ็มเอ) บนพื้นผิวของซิลิกอนออกไซด์ได้โดยการริเริ่มปฏิกิริยาพอลิเมอไรเซชันจากพื้นผิวด้วยกลไกแบบอะตอมทรานส์เฟอร์เรดิคัลพอลิเมอไรเซชัน โดยใช้คอปเปอร์โบรไมด์/พีเอ็มดีซีทีเอเป็นระบบเร่งปฏิกิริยาสามารถติดตามการดำเนินไปของปฏิกิริยาด้วยอีฟไซเมตรี การวัดมุมสัมผัส โปรตอนเอ็นเอ็มอาร์ และเจลเพอมีเอชันโครมาโทกราฟี จากการทดลองพบว่าสามารถควบคุมน้ำหนักโมเลกุลและความหนาของพีทีเอฟเอ็มเอบรัชและพีทีบีเอ็มเอบรัชแยกจากกันด้วยการควบคุมเวลาที่ใช้ในการทำปฏิกิริยาและสัดส่วนของหมู่ริเริ่มปฏิกิริยาต่อมอนอเมอร์โดยโมลในสารละลาย นอกจากนี้ยังพบว่าปฏิกิริยาพอลิเมอไรเซชันมีกลไกเป็นแบบอมตะ การเติบโตของพอลิเมอร์บรัชในแต่ละบล็อกเป็นไปอย่างสม่ำเสมอ และความหนาของพอลิเมอร์บรัชเพิ่มขึ้นเมื่อบล็อกด้านบนของพีทีบีเอ็มเอถูกต่อเข้าไปที่บล็อกในของพีทีเอฟเอ็มเอ สำหรับไดบล็อกโคพอลิเมอร์บรัชของพอลิ(2,2,2-ไตรฟลูออโรเอทิลเมทาคริเลต) และ พอลิ(เมทาคริลิกแอซิด) (พีทีเอฟเอ็มเอ-บล็อก-พีเอ็มเอเอ) เตรียมได้โดยการทำปฏิกิริยาไฮโดรไลซิสด้วยกรดของ พีทีเอฟเอ็มเอ-บล็อก-พีทีบีเอ็มเอ และจากการศึกษาความสามารถในการเปียกของไดบล็อกโคพอลิเมอร์บรัชโดยการวัดมุมสัมผัสของของเหลวพบว่าทั้ง พีทีเอฟเอ็มเอ-บล็อก-พีทีบีเอ็มเอ และ พีทีเอฟเอ็มเอ-บล็อก-พีเอ็มเอเอ แสดงการจัดเรียงตัวใหม่ของพื้นผิวดตอบสนองต่อการสัมผัสกับไตรฟลูออโรโพลูอินซึ่งเป็นตัวทำละลายที่ดีของบล็อกด้านบนของพีทีเอฟเอ็มเอ และการจัดเรียงตัวใหม่นี้มีลักษณะแบบผันกลับได้

Field of study Petrochemistry and Polymer Science Student's signature Sirrat Jeamrattanapitak  
Academic year 2005 Advisor's signature Vp. Avorn

# # 4672520523: MAJOR PETROCHEMISTRY AND POLYMER SCIENCE

KEYWORD: POLYMER BRUSH/ SEMIFLUORINATED/ SURFACE-INITIATED POLYMERIZATION/ ATOM TRANSFER RADICAL POLYMERIZATION

SIRORAT JEAMRATTANAPITAK: SYNTHESIS AND SURFACE PROPERTIES OF FLUORINE-CONTAINING DIBLOCK COPOLYMER BRUSH. THESIS ADVISOR: ASSISTANT PROFESSOR VORAVEE P. HOVEN, Ph.D. 99 pp ISBN 974-14-2193-1

Diblock copolymer brushes of poly(2,2,2-trifluoroethyl methacrylate) and poly(*tert*-butyl methacrylate) (PTFMA-*b*-Pt-BMA) grafted on silicon oxide substrates were synthesized by surface-initiated polymerization *via* atom transfer radical polymerization using CuBr/PMDETA as a catalytic system. The reaction progress can be monitored by ellipsometry, contact angle analysis, <sup>1</sup>H-NMR analysis and gel permeation chromatography. The obtained results prompted that  $M_w$  and the thickness of both PTFMA and Pt-BMA brushes can be separately controlled as a function of reaction time and monomer to “free” initiator ratio in solution and the polymerization is living in character. The growth of each block was uniform and the thickness of the polymer brushes continuously increased after the outer block of Pt-BMA was consecutively added to the inner block of PTFMA. Diblock copolymer brushes of poly(2,2,2-trifluoroethyl methacrylate) and poly(methacrylic acid) (PTFMA-*b*-PMAA) were prepared by acid hydrolysis of PTFMA-*b*-Pt-BMA. As determined by contact angle analysis, responsive wettability of both PTFMA-*b*-Pt-BMA and PTFMA-*b*-PMAA brushes was observed after the treatment with  $\alpha,\alpha,\alpha$ -trifluorotoluene, a good solvent for the inner block of PTFMA. The surface rearrangement was found to be reversible.

Field of study Petrochemistry and Polymer Science Student's signature Sirorat Jeamrattanapitak  
 Academic year 2005 Advisor's signature Vp. Hoven

## ACKNOWLEDGEMENTS

I would like to express my heartfelt gratitude and appreciation to my advisor, Assistant Professor Dr. Voravee P. Hoven, for supporting me both in science and in life, and encouraging me throughout the course of my study. I am sincerely grateful to the members of the thesis committee, Associate Professor Dr. Supawan Tantayanon, Associate Professor Dr. Nuanphun Chantarasiri, Assistant Professor Dr. Warinthorn Chavasiri for their comments, suggestions and time to read the thesis.

Special thanks go to National Metal and Materials Technology Center for the contact angle goniometer and Capability Building Unit in Nanoscience and Nanotechnology, Department of Physics, Faculty of Science, Mahidol University for ellipsometry facility. A grateful acknowledgement also extends to the research funding for graduate students from Chulalongkorn University for financial support.

Many thanks go to all OSRU members for their assistance, suggestions concerning experimental techniques and their kind helps during my thesis work.

Finally, I would like to especially thank my family members: father, mother, three young sisters and relatives for their love, kindness and support throughout my entire study.

สถาบันวิทยบริการ  
จุฬาลงกรณ์มหาวิทยาลัย

# CONTENTS

	Page
ABSTRACT IN THAI.....	iv
ABSTRACT IN ENGLISH.....	v
ACKNOWLEDGEMENTS.....	vi
LIST OF FIGURES.....	xi
LIST OF TABLES.....	xv
LIST OF SCHEMES.....	xvii
LIST OF ABBREVIATIONS .....	xviii
CHAPTER I INTRODUCTION.....	1
1.1 Statement of Problem.....	1
1.2 Objectives.....	2
1.3 Scope of the Investigation.....	2
CHAPTER II THEORY AND LITERATURE REVIEW.....	4
2.1 Fluoropolymer.....	4
2.2 Living Polymerization.....	6
2.3 Polymer Brush.....	15
2.4 Diblock Copolymer Brushes.....	22
2.5 Characterization techniques.....	26
2.5.1 Ellipsometry.....	26
2.5.2 Contact Angle Measurement.....	27
2.5.3 Gel Permeation Chromatography (GPC).....	29
CHAPTER III EXPERIMENTAL.....	31
3.1 Materials.....	31
3.2 Equipments.....	32

	Page
3.2.1 Ellipsometry.....	32
3.2.2 Nuclear Magnetic Resonance Spectroscopy (NMR).....	33
3.2.3 Gel Permeation Chromatography (GPC)	33
3.2.4 Contact Angle Measurement.....	33
3.3 Synthesis of $\alpha$ -Bromoisobutyrate Initiators.....	34
3.3.1 Synthesis of 2-bromo-2-methyl propionic acid allyl ester.....	34
3.3.2 Synthesis of 2-bromo-2-methyl propionic acid 3-(ethoxydimethyl silanyl)propyl ester.....	35
3.3.3 Synthesis of 2-bromo-2-methylpropionic acid propyl ester as a “Sacrificial” Initiator.....	36
3.4 Pretreatment of Silicon Substrates.....	36
3.5 Preparation of Silicon-supported $\alpha$ -Bromoisobutyrate Monolayer .....	37
3.6 Preparation of Polymer Brushes.....	38
3.6.1 Homopolymer Brushes of Poly( <i>tert</i> -Butyl Methacrylate) ( <i>Pt</i> -BMA).....	38
3.6.2 Homopolymer Brushes of Poly(2,2,2-Trifluoroethyl Methacrylate) (PTFMA)..	39
3.6.3 Homopolymer Brushes of Poly(Methacrylic Acid) (PMAA).....	41
3.6.4 Diblock Copolymer Brushes of PTFMA- <i>b</i> - <i>Pt</i> -BMA .....	42
3.6.5 Diblock Copolymer Brushes of PTFMA- <i>b</i> -PMAA.....	43



	Page
CHAPTER IV RESULTS AND DISCUSSION.....	44
4.1 Synthesis of $\alpha$ -Bromoisobutyrate Initiators.....	44
4.1.1 Synthesis of 2-bromo-2-methyl propionic acid allyl ester .....	45
4.1.2 Synthesis of 2-bromo-2-methyl propionic acid 3-(ethoxydimethyl silanyl) propyl ester.....	45
4.1.3 Synthesis of 2-bromo-2-methyl propionic acid propyl ester as a “Sacrificial” Initiator.....	47
4.2 Preparation of Silicon-supported $\alpha$ -Bromoisobutyrate Monolayer .....	47
4.3 Preparation of Homopolymer Brushes.....	48
4.3.1 Homopolymer Brushes of Poly( <i>tert</i> - Butyl Methacrylate) ( <i>Pt</i> -BMA).....	49
4.3.2 Homopolymer Brushes of Poly(2,2,2- Trifluoroethyl Methacrylate) (PTFMA)...	54
4.3.3 Homopolymer Brushes of Poly(Metha- crylic Acid) (PMAA).....	59
4.4 Preparation of Diblock Copolymer Brushes.....	63
4.4.1 Diblock Copolymer Brushes of PTFMA- <i>b</i> - <i>Pt</i> -BMA.....	63
4.4.2 Diblock Copolymer Brushes of PTFMA- <i>b</i> -PMAA.....	68
4.5 Surface Wettability of Diblock Copolymer Brushes in Response to Solvent Treatment.....	71
CHAPTER V CONCLUSION AND SUGGESTION .....	77
REFERENCES.....	79

	Page
APPENDICES.....	88
APPENDIX A.....	89
APPENDIX B.....	92
VITAE.....	99



สถาบันวิทยบริการ  
จุฬาลงกรณ์มหาวิทยาลัย

## LIST OF FIGURES

Figure	Page
2.1 Molecular weight conversion curves for various kinds of polymerization methods: (A) living polymerization; (B) free radical polymerization; and (C) condensation polymerization.....	8
2.2 Architectural forms of polymers available by living polymerization techniques.....	9
2.3 Mechanism of ATRP.....	10
2.4 Equilibrium reaction in ATRP .....	11
2.5 Copper complexes used as ATRP catalysts.....	12
2.6 Examples of ligands used in copper-mediated ATRP.....	13
2.7 Rotation of the bpy ligands from the tetrahedral and co-ordination of halide at the Cu center.....	13
2.8 Proposed Cu(I) and Cu(II) species using PMDETA as ligand.....	14
2.9 Examples of polymer systems comprising polymer brushes.....	16
2.10 Classification of linear polymer brushes, (a <sub>1</sub> –a <sub>4</sub> ) homopolymer brushes; (b) mixed homopolymer brush; (c) random copolymer brush; (d) block copolymer brush.....	18
2.11 Preparation of polymer brushes by “physisorption”, “grafting to” and “grafting from”.....	20
2.12 Proposed responses of tethered PS- <i>b</i> -PMMA brushes to different solvent treatments.....	24
2.13 Atomic force microscopy (AFM) images of tethered Si/SiO <sub>2</sub> //PS- <i>b</i> -PMMA brushes after treatment with dichloromethane (a) and gradual treatment with cyclohexane (b).....	26
2.14 Schematic of the geometry of an ellipsometry experiment.....	27
2.15 Schematic representation of the Young’s equation.....	28
2.16 Schematic representation of wettability.....	28
2.17 Schematic representation of the gel permeation chromatography.....	30

Figure	Page
4.1 Ellipsometric thickness of <i>Pt</i> -BMA brushes as a function of polymerization time for targeted DP = 200 (●) and 100 (○).....	50
4.2 Water contact angle of <i>Pt</i> -BMA brushes as a function of polymerization time for targeted DP = 200: $\theta_A$ (●), $\theta_R$ (○) and 100: $\theta_A$ (■), $\theta_R$ (□).....	51
4.3 <sup>1</sup> H-NMR spectra of (a) <i>t</i> -BMA and (b) <i>Pt</i> -BMA in solution.....	52
4.4 Molecular weight ( $\overline{M}_n$ ) of free <i>Pt</i> -BMA for targeted DP = 200 (●) and 100 (■) and molecular weight distribution ( $\overline{M}_w/\overline{M}_n$ ) for targeted DP = 200 (○) and 100 (□) as a function of polymerization time.....	53
4.5 Ellipsometric thickness of PTFMA brushes as a function of polymerization time for targeted DP = 200 (●) and 100 (○).....	55
4.6 Water contact angle of PTFMA brushes as a function of polymerization time for targeted DP = 200: $\theta_A$ (●), $\theta_R$ (○) and 100: $\theta_A$ (■), $\theta_R$ (□).....	56
4.7 <sup>1</sup> H-NMR spectra of (a) TFMA and (b) PTFMA in solution.....	57
4.8 Molecular weight ( $\overline{M}_n$ ) of free PTFMA for targeted DP = 200 (●) and 100 (■) and molecular weight distribution ( $\overline{M}_w/\overline{M}_n$ ) for targeted DP = 200 (○) and 100 (□) as a function of polymerization time.....	58
4.9 Water contact angle of the silicon-supported <i>Pt</i> -BMA brushes after hydrolysis by a varied concentration of TFA in dichloromethane for 4h: $\theta_A$ (●), $\theta_R$ (○).....	60
4.10 Water contact angle of the silicon-supported <i>Pt</i> -BMA brushes as a function of hydrolysis time (h) using 5M TFA in dichloromethane: $\theta_A$ (●), $\theta_R$ (○).....	61
4.11 <sup>1</sup> H-NMR spectra of (a) <i>Pt</i> -BMA and (b) PMAA in solution.....	62
4.12 Ellipsometric thickness of PTFMA- <i>b</i> - <i>Pt</i> -BMA brushes as a function of <i>t</i> -BMA:TFMA ratio.....	64
4.13 Water contact angle of PTFMA- <i>b</i> - <i>Pt</i> -BMA brushes as a function of <i>t</i> -BMA:TFMA ratio: $\theta_A$ (●), $\theta_R$ (○).....	65

Figure	Page
4.14 Hexadecane contact angle of PTFMA- <i>b</i> -Pt-BMA brushes as a function of <i>t</i> -BMA:TFMA ratio: $\theta_A$ (●), $\theta_R$ (○).....	66
4.15 <sup>1</sup> H-NMR spectra of (a) PTFMA, (b) Pt-BMA, and (c) PTFMA- <i>b</i> -Pt-BMA ( <i>t</i> -BMA:TFMA = 1:1) in solution.....	67
4.16 <sup>1</sup> H-NMR spectra of (a) PTFMA- <i>b</i> -Pt-BMA and (b) PTFMA- <i>b</i> -PMAA in solution.....	70
4.17 Water contact angle of the silicon-supported PTFMA- <i>b</i> -Pt-BMA brushes ( <i>t</i> -BMA:TFMA = 1:1) before and after treatment with $\alpha,\alpha,\alpha$ - trifluorotoluene as a function of treatment time (min): $\theta_A$ (●), $\theta_R$ (○)...	71
4.18 Hexadecane contact angle of the silicon-supported PTFMA- <i>b</i> -Pt-BMA brushes ( <i>t</i> -BMA:TFMA = 1:1) before and after treatment with $\alpha,\alpha,\alpha$ - trifluorotoluene as a function of treatment time (min): $\theta_A$ (●), $\theta_R$ (○).....	72
4.19 Water contact angle of the silicon-supported PTFMA- <i>b</i> -Pt-BMA brushes after treatment with $\alpha,\alpha,\alpha$ - trifluorotoluene for 120 min as a function of <i>t</i> -BMA:TFMA ratio in the diblock copolymer: $\theta_A$ (●), $\theta_R$ (○).....	73
4.20 Hexadecane contact angle of the silicon-supported PTFMA- <i>b</i> -Pt-BMA brushes after treatment with $\alpha,\alpha,\alpha$ – trifluorotoluene for 120 min as a function of <i>t</i> -BMA:TFMA ratio in the diblock copolymer: $\theta_A$ (●), $\theta_R$ (○).....	73
4.21 Water contact angle of the silicon-supported PTFMA- <i>b</i> -Pt-BMA brushes after 3 cycles of solvent treatment: $\theta_A$ (●), $\theta_R$ (○).....	74
4.22 Hexadecane contact angle of the silicon-supported PTFMA- <i>b</i> -Pt-BMA brushes after 3 cycles of solvent treatment: $\theta_A$ (●), $\theta_R$ (○).....	75
A.1 <sup>1</sup> H-NMR spectrum (400 MHz, CDCl <sub>3</sub> ) of 2-bromo-2-methylpropionic acid allyl ester.....	90
A.2 <sup>1</sup> H-NMR spectrum (400 MHz, CDCl <sub>3</sub> ) of 2-bromo-2-methylpropionic acid 3-(ethoxydimethylsilyl)propyl ester.....	90

Figure	Page
A.3 $^1\text{H-NMR}$ spectrum (400 MHz, $\text{CDCl}_3$ ) of 2-bromo-2-methylpropionic acid propyl ester.....	91



สถาบันวิทยบริการ  
จุฬาลงกรณ์มหาวิทยาลัย

## LIST OF TABLES

Table	Page
4.1 Information from $^1\text{H-NMR}$ spectrum of PTFMA- <i>b</i> -Pt-BMA.....	68
4.2 Contact angle data of the silicon-supported polymer brushes.....	76
B.1 Average thickness of Pt-BMA brushes for targeted DP = 100 and 200 calculated from ellipsometric data as a function of polymerization time	93
B.2 Advancing and receding water contact angle data of Pt-BMA brushes for targeted DP = 100 and 200 as a function of polymerization time.....	93
B.3 Average molecular weight and molecular weight distribution of Pt- BMA brushes for targeted DP = 100 and 200 analyzed by GPC as a function of polymerization time.....	94
B.4 Average thickness of PTFMA brushes for targeted DP = 100 and 200 calculated from ellipsometric data as a function of polymerization time	94
B.5 Advancing and receding water contact angle data of PTFMA brushes for targeted DP = 100 and 200 as a function of polymerization time.....	95
B.6 Average molecular weight and molecular weight distribution of PTFMA brushes for targeted DP = 100 and 200 analyzed by GPC as a function of polymerization time.....	95
B.7 Advancing and receding water contact angle data of Pt-BMA brushes after hydrolysis by a varied concentration of TFA in dichloromethane for 4h.....	96
B.8 Advancing and receding water contact angle data of Pt-BMA brushes after hydrolysis by a varied hydrolysis time using 5M TFA in dichloromethane.....	96
B.9 Average thickness of PTFMA- <i>b</i> -Pt-BMA brushes calculated from ellipsometric data as a function of <i>t</i> -BMA:TFMA ratio.....	96
B.10 Advancing and receding water and hexadecane contact angle data of PTFMA- <i>b</i> -Pt-BMA brushes as a function of <i>t</i> -BMA:TFMA ratio.....	97

Table	Page
B.11 Advancing and receding water and hexadecane contact angle data of PTFMA- <i>b</i> - <i>Pt</i> -BMA brushes (mole ratio = 1:1) before and after treatment with $\alpha,\alpha,\alpha$ -trifluorotoluene as a function of treatment time..	97
B.12 Advancing and receding water and hexadecane contact angle data of PTFMA- <i>b</i> - <i>Pt</i> -BMA brushes after treatment with $\alpha,\alpha,\alpha$ -trifluorotoluene for 120 min as a function of <i>t</i> -BMA:TFMA ratio.....	98
B.13 Advancing and receding water and hexadecane contact angle data of PTFMA- <i>b</i> - <i>Pt</i> -BMA brushes (mole ratio = 1:1) after 3 cycles of solvent treatment.....	98



**LIST OF SCHEMES**

Scheme	Page
4.1 Mechanism of hydrosilylation using chloroplatinic acid as a catalyst....	46
4.2 Activation/deactivation cycles of ATRP process.....	49



สถาบันวิทยบริการ  
จุฬาลงกรณ์มหาวิทยาลัย

## LIST OF ABBREVIATIONS

ATRP	: Atom transfer radical polymerization
Å	: Ångström = 0.1 nm.
<i>t</i> -BMA	: <i>tert</i> -Butyl methacrylate
CDCl <sub>3</sub>	: Deuteriochloroform
CuBr	: Copper (I) bromide
°C	: Degree Celsius
<i>DP</i>	: Degree of polymerization
Eq.	: Equation
GPC	: Gel permeation chromatography
$k_{act}$	: The activation rate parameter
$k_{deact}$	: The deactivation rate parameter
MeOH	: Methanol
μL	: microliter
mg	: milligram
min	: minute
mL	: milliliter
mm	: millimeter
mM	: millimolar
mmol	: millimole

$\overline{M}_n$	: Number average molecular weight
$\overline{M}_w$	: Weight average molecular weight
nm	: nano meter
NMR	: Nuclear magnetic resonance spectroscopy
PDI	: Polydispersity Index
Pt-BMA	: Poly( <i>tert</i> -butyl methacrylate)
PTFMA	: Poly(2,2,2-trifluoroethyl methacrylate)
ppm	: part per million
S.D.	: Standard deviation
TFMA	: 2,2,2-trifluoroethyl methacrylate
THF	: Tetrahydrofuran

สถาบันวิทยบริการ  
จุฬาลงกรณ์มหาวิทยาลัย

# CHAPTER I

## INTRODUCTION

### 1.1 Statement of Problem

Formation of polymer brushes is recognized as one of novel routes for surface modification. In principle, the most versatile approach used for generating polymer brushes is the “grafting from” or the “surface-initiated polymerization”, in which polymerization is initiated from initiators coupled covalently to the surface. From this technique, one can grow very high-density and high-stability polymer brushes on a substrate if proper conditions are employed.

There is growing interest in atom transfer radical polymerization (ATRP) since it was discovered in 1995. The living characteristic and the compatibility with a variety of functional monomer render ATRP an attractive method for surface-initiated polymerization in producing well-defined polymer brushes. The process not only allows a better control of target molecular weight and molecular weight distribution but can also be used for the synthesis of block copolymer.

Diblock copolymer brushes have many attractive properties such as phase separation, ability to form nanopattern surface. Because of the different physical properties such as solubility and glass transition temperature, the diblock copolymer brushes are capable to response to the external stimuli such as solvent, temperature. Fluoropolymers are known to exhibit an affinity for the air interface in polymeric materials. If the fluoropolymer is incorporated into the diblock copolymer brushes, the migration of its fluorine moieties to the polymer-air interface is believed to constitute a novel surface rearrangement mechanism in response to the external stimuli.

In this research, two series of homopolymer brushes of poly(2,2,2-trifluoroethyl methacrylate) (PTFMA) and poly(*tert*-butyl methacrylate) (*Pt*-BMA)

and one series of diblock copolymer brushes of poly(2,2,2-trifluoroethyl methacrylate) and poly(*tert*-butyl methacrylate) (PTFMA-*b*-Pt-BMA) were prepared by surface-initiated ATRP from  $\alpha$ -bromoisobutyrate-based initiator anchored onto silicon oxide substrates, using CuBr/PMDETA as a catalytic system. By subsequent acid hydrolysis, homopolymer brushes of poly(methacrylic acid) and diblock copolymer brushes of poly(2,2,2-trifluoroethyl methacrylate) and poly(methacrylic acid) (PTFMA-*b*-PMAA) can be generated. The growth of homopolymer and diblock copolymer brushes is monitored by contact angle measurement, ellipsometry and gel permeation chromatography.

The diblock copolymer brushes are subjected to solvent treatment. Effects of the relative block length of the copolymer and treatment time are explored. We anticipate that the diblock copolymer brushes can respond to the solvent treatment as a rearrangement mechanism and capitalize on the wettability of the diblock copolymer brushes.

## 1.2 Objectives

1. To synthesize fluorine-containing diblock copolymer brushes by surface-initiated atom transfer radical polymerization
2. To study wettability of fluorine-containing diblock copolymer brushes in response to solvent treatment

## 1.3 Scope of Investigation

The stepwise investigation was carried out as follows.

1. Literature survey for related research work.
2. To immobilize  $\alpha$ -bromoester-containing initiator on silicon oxide surfaces.

3. To synthesize homopolymer brushes of PTFMA and *Pt*-BMA by surface-initiated polymerization from silicon oxide surfaces containing  $\alpha$ -bromoester groups.
4. To synthesize diblock copolymer brushes of PTFMA-*b*-*Pt*-BMA by surface-initiated polymerization from silicon oxide surfaces containing  $\alpha$ -bromoester groups.
5. To synthesize diblock copolymer brushes of PTFMA-*b*-PMAA by acid hydrolysis of PTFMA-*b*-*Pt*-BMA
6. To investigate the wettability of diblock copolymer brushes in response to solvent treatment



สถาบันวิทยบริการ  
จุฬาลงกรณ์มหาวิทยาลัย

## CHAPTER II

### THEORY AND LITERATURE REVIEW

#### 2.1 Fluoropolymer

Fluoropolymers, the polymers consisting of fluorine atom, are widely applicable because of their heat and chemical resistance, weatherability, low refractive index [1], a low relative permittivity [2], non-cohesiveness, a low friction coefficient [3] and electric insulating properties [4]. Due to these unique properties, fluorinated polymers find diverse applications in electronics, optics, biomaterials [5], lubricants and surfactants and coatings [6]. Furthermore, a fluorinated block plays a role in the construction of ordered structures as a component different from a hydrophilic or oleophilic block [7]. When the surface is uniformly covered with a trifluoromethyl (CF<sub>3</sub>) array, a very low energy surface can be achieved. It is known to exhibit an affinity for the air interface in polymeric materials [8]. Fluoropolymers bring about dramatic changes in their physical properties with respect to the corresponding fully hydrogenated materials. Up to date synthesis and properties of various types of fluorine-containing polymers have been reviewed. Incorporation of fluorinated moieties in polymers is carried out using different methods: (1) participation of fluorinated unit in main chain, (2) modification of polymer terminals by fluorinated derivatives, and (3) fluorination of polymer side chains.

In 2004, Jennings and Brantley [9] reported a strategy to prepare partially fluorinated polymer films by utilizing surface-initiated films of poly(2-hydroxyethyl methacrylate) (PHEMA) grown onto gold surfaces *via* atom transfer radical polymerization (ATRP). And polymer films were fluorinated by the acylation between hydroxyl side chains of PHEMA and fluorinated acid chlorides to yield partially fluorinated surface-initiated polymer films. Film properties depend on the chemical composition and length of the fluorinated side chains. A longer fluoroalkyl side group on PHEMA greatly improves the film properties in all areas-higher

resistance, lower capacitance and critical surface tension, and better defined structures as compared with a shorter fluoroalkyl chain.

In the same year, Ober and co-workers [10] synthesized styrene-based homopolymer and diblock copolymer brushes bearing semifluorinated alkyl side groups by surface-initiated nitroxide-mediated controlled radical polymerization (NMP) on planar silicon oxide surfaces. Water contact angle measurements showed that, in the case of the diblock copolymer brushes, the second block to be added was always exposed at the polymer-air interface regardless of its surface energy. These results support the idea that after grafting the first block onto the surface of the nitroxide-end capped polymer chains were able to polymerize the second block in a “living” fashion and the stretched brush so formed was dense enough that the outermost block in all cases completely covers the surface. The surface behavior observed for these brushes holds very important implications for the stability of such surfaces toward reconstruction when exposed to different environments, which is a crucial requirement in application fields, ranging from the coating technology to biotechnology, where stable and non-reconstructing surfaces are needed. Time-dependent water contact angle measurements revealed that the orientation of the side chains of the brush improved the surface stability toward reconstruction upon prolonged exposure to water.

Brittain et al. [11] used “grafting from” surface-initiated atom transfer radical polymerization (ATRP) technique to synthesize a series of semifluorinated diblock copolymer brushes, consisting either of polystyrene (PS) or poly(methyl acrylate) (PMA) as first (inner) block and poly(semifluorinated acrylates) (outer) block. Four poly(semifluorinated acrylates) such as poly(pentafluorostyrene) (PPFS), poly(heptadecafluorodecyl acrylate) (PHFA), poly(pentafluoropropyl acrylate) (PPFA), and poly(trifluoroethyl acrylate) (PTFA) were used. The diblock copolymer brushes were treated with a good and poor fluoropolymer solvent to induce rearrangement of the chains at the surface. Tensiometry data indicate the polymer brush layers reversibly rearrange to form either a hydrocarbon polymer enriched or a fluoropolymer enriched air-polymer interface depending upon the nature of the



solvent. All the diblock systems except the systems containing PHFA were shown to exhibit water contact angles typical for the hydrocarbon polymer block after solvent treatment. The highly fluorinated PHFA diblock copolymer systems exhibited incomplete surface rearrangement.

Recently, Baker and colleagues [12] employed the acylation method to prepare porous alumina membranes coated with fluorinated poly(HEMA) films. Fluorinated monomers were also directly grafted from surfaces. They reported derivatization of poly(2-hydroxyethyl methacrylate) (PHEMA) coatings with octyl (C8-PHEMA), hexadecyl (C16-PHEMA), or pentadecafluorooctyl (fluorinated PHEMA) side chains provides films that are sufficiently hydrophobic to allow selective pervaporation of volatile organic compounds (VOCs) from water. For all of these derivatized PHEMA membranes, VOC/water selectivities generally increase with decreasing solubility of the VOC in water.

## 2.2 Living Polymerization

Synthetic polymers are long-chain molecules possessing uniform repeat units (mers). The chains are not all the same length. These giant molecules are of interest because of their physical properties, in contrast to low molecular weight molecules, which are of interest due to their chemical properties. Possibly the most useful physical property of polymers is their low density versus strength.

When synthetic polymers were first introduced, they were made by free radical initiation of single vinyl monomers or by chemical condensation of small difunctional molecules. The range of their properties was understandably merger. Random copolymers are greatly expanding in the range of useful physical properties such as toughness, hardness, elasticity, compressibility, and strength, however, polymer chemists realized that their materials could not compare with the properties of natural polymers, such as wool, silk, cotton, rubber, tendons, and spider webbing. The natural polymers are generally condensation polymers made by addition of monomer units one at a time to the ends of growing polymer chains. Polymerization

of all chains stops at identical molecular weights. For some time polymer chemists have realized that to approach nature's degree of sophistication, new synthetic techniques would be needed.

Conventional chain-growth polymerizations, for example, free radical synthesis, consist of four elementary steps: initiation, propagation, chain transfer, and termination. As early as 1936, Ziegler proposed that anionic polymerization of styrene and butadiene, consecutive addition of monomer to an alkyl lithium initiator occurred without chain transfer or termination. During transferless polymerization, the number of polymer molecules remains constant. Since there is no termination, active anionic chain ends remain after all of the monomer has been polymerized. When fresh monomer is added, polymerization resumes. The name "living polymerization" was coined for the method by Szwarc [13], because the chain ends remain active until killed. The term has nothing to do with living in the biological sense. Before Szwarc's classic work, Flory [14] had described the properties associated with living polymerization of ethylene oxide initiated with alkoxides. Flory noted that since all of the chain ends grow at the same rate, the molecular weight is determined by the amount of initiator used versus monomer (Eq.1)

$$\text{Degree of polymerization} = [\text{monomer}]/[\text{initiator}] \quad (2.1)$$

Another property of polymers produced by living polymerization is the very narrow molecular weight distribution. The polydispersity ( $D$ ) has a Poisson distribution,  $D = \overline{M}_w/\overline{M}_n = 1 + (1/dp)$ ;  $\overline{M}_w$  is the average molecular weight determined by light scattering,  $\overline{M}_n$  is the average molecular weight determined by osmometry, and  $dp$  is the degree of polymerization (the number of monomer units per chain). The values of  $\overline{M}_w$  and  $\overline{M}_n$  can also be determined by gel permeation chromatography (GPC). A living polymerization can be distinguished from free radical polymerization or from a condensation polymerization by plotting the molecular weight of the polymer versus conversion. In a living polymerization, the molecular weight is directly proportional to conversion (Figure 2.1, line A). In a free radical or other nonliving polymerization, high molecular weight polymer is formed

in the initial stages (line B), and in a condensation polymerization, high molecular weight polymer is formed only as the conversion approaches 100% (line C).

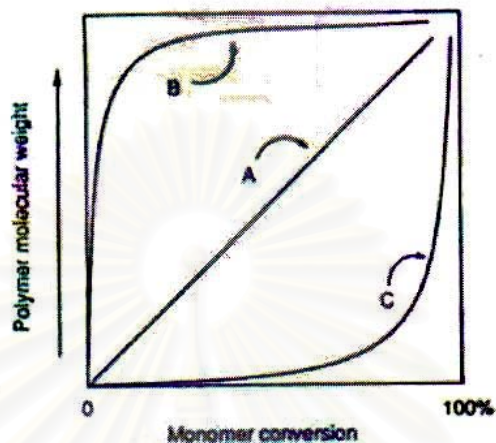


**Figure 2.1** Molecular weight conversion curves for various kinds of polymerization methods: (A) living polymerization; (B) free radical polymerization; and (C) condensation polymerization.

Living polymerization techniques give the synthetic chemist two particularly powerful tools for polymer chain design: the synthesis of block copolymers by sequential addition of monomers and the synthesis of functional-ended polymers by selective termination of living ends with appropriate reagents. The main architectural features available starting with these two basic themes are listed in Figure 2.2 along with applications for the various polymer types. Although living polymerization of only a few monomers is nearly perfect, a large number of other systems fit theory close enough to be useful for synthesis of the wide variety of different polymer chain structures. In general, the well-behaved living systems need only an initiator and monomer, as occurs in the anionic polymerization of styrene, dienes, and ethylene oxide. For an increasing number of monomers, more complex processes are needed to retard chain transfer and termination. These systems use initiators, catalysts, and sometimes chain-end stabilizers. The initiator begins chain growth and in all systems is attached (or part of it, at least) to the nongrowing chain end. The catalyst is necessary for initiation and propagation but is not consumed. The chain-end

stabilizer usually decreases the polymerization rate. When the catalyst is a Lewis acid (electron-pair acceptor), the stabilizer will likely be a Lewis base (electron-pair donor), and vice versa. In all systems, the initiation step must be faster than or the same rate as chain propagation to obtain molecular weight control. If the initiation rate is slower than the propagation rate, the first chains formed will be longer than the last chains formed. If an initiator with a structure similar to that of the growing chain is chosen, the initiation rate is assured of being comparable to the propagation rate. A number of living systems operate better if excess monomer is present. A possible explanation is that the living end is stabilized by complexation with monomer [15]. Large counterions tend to be more effective than small counterions in living polymerization systems even when the ionic center is only indirectly involved.

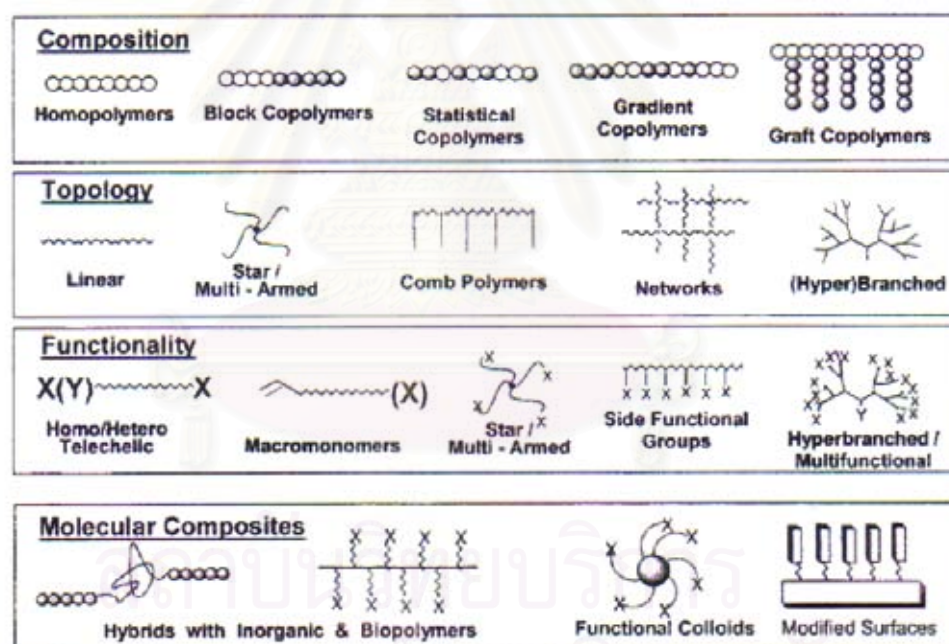


**Figure 2.2** Architectural forms of polymers available by living polymerization techniques.

In this research, free radical process for living polymerization is selected and described. The concept of using stable free radicals, such as nitroxides, to reversibly react with the growing polymer radical chain end can be traced back to the pioneering work of Rizzardo and Mozd [16]. After further refinement by Georges [17], the basic blueprint for all subsequent work in the area of “living” free radical

polymerization was developed. Subsequently, the groups of Sawamoto[18], Matyjaszewski [19], Percec [20] and others [21-22] have replaced the stable nitroxide free radical with transition metal species to obtain a variety of copper-, nickel-, or ruthenium-mediated “living” free radical systems. These systems were called atom transfer radical polymerization (ATRP). This mechanism is an efficient method for carbon-carbon bond formation in organic synthesis. In some of these reactions, a transition-metal catalyst acts as a carrier of the halogen atom in a reversible redox process (Figure 2.3). Initially, the transition-metal species,  $M_t^n$ , abstracts halogen atom X from the organic halide, RX, to form the oxidized species,  $M_t^{n+1}X$ , and the carbon-centered radical  $R^\bullet$ . In the subsequent step, the radical  $R^\bullet$  participates in an inter- or intramolecular radical addition to alkene, Y, with the formation of the intermediate radical species,  $RY^\bullet$ . The reaction between  $M_t^{n+1}X$  and  $RY^\bullet$  results in a target product, RYX, and regenerates the reduced transition-metal species,  $M_t^n$ , which further promotes a new redox process. The fast reaction between  $RY^\bullet$  and  $M_t^{n+1}X$  apparently suppresses bimolecular termination between alkyl radicals and efficiently introduces a halogen functional group X into the final product in good to excellent yields.

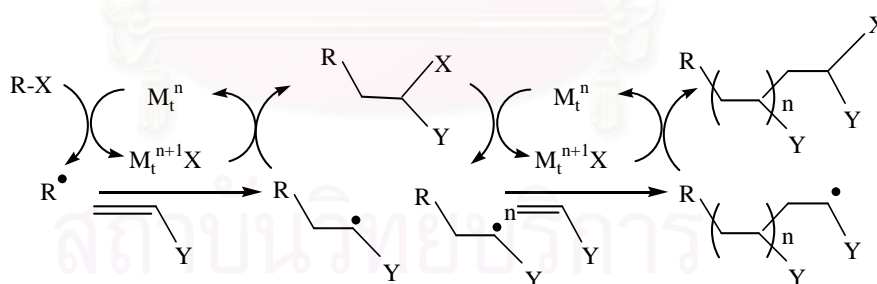


**Figure 2.3** Mechanism of ATRP.

The ATRP system relies on one equilibrium reaction in addition to the classical free-radical polymerization scheme (Figure 2.4). In this equilibrium, a dormant species, RX, reacts with the activator,  $M_t^n$ , to form a radical  $R^\bullet$  and deactivating species,  $M_t^{n+1}X$ . The activation and deactivation rate parameters are  $k_{act}$  and  $k_{deact}$ , respectively. Since deactivation of growing radicals is reversible, control

over the molecular weight distribution and, in the case of copolymers, over chemical composition can be obtained if the equilibrium meets several requirements [23-24].

1. The equilibrium constant,  $k_{\text{act}}/k_{\text{deact}}$ , must be low in order to maintain a low stationary concentration of radicals. A high value would result in a high stationary radical concentration, and as a result, termination would prevail over reversible deactivation.

2. The dynamics of the equilibrium must be fast; i.e. deactivation must be fast compared to propagation in order to ensure fast interchange of radicals in order to maintain a narrow molecular weight distribution.

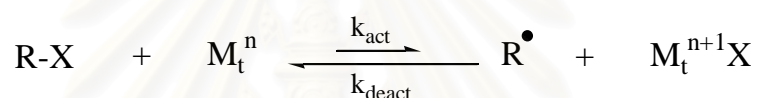


**Figure 2.4** Equilibrium reaction in ATRP [25].

Transition metal complexes (catalyst) are perhaps the most important components of ATRP. It is the key to ATRP since it determines the position of the atom transfer equilibrium and the dynamics of exchange between the dormant and active species. There are several prerequisites for an efficient transition metal catalyst. First, the metal center must have at least two readily accessible oxidation states separated by one electron. Second, the metal center should have reasonable affinity toward a halogen. Third, the coordination sphere around the metal should be expandable upon oxidation to selectively accommodate a (pseudo)-halogen. Fourth, the ligand should complex the metal relatively strongly. Eventually, the position and dynamics of the ATRP equilibrium should be appropriate for the particular system. A variety of transition-metal complexes have been studied as ATRP catalysts.

Copper catalysts are superior in ATRP in terms of versatility and cost. Styrenes, (meth)acrylate esters and amides, and acrylonitrile have been successfully

polymerized using copper-mediated ATRP. Examples of copper complexes used in ATRP are shown in Figure 2.5.

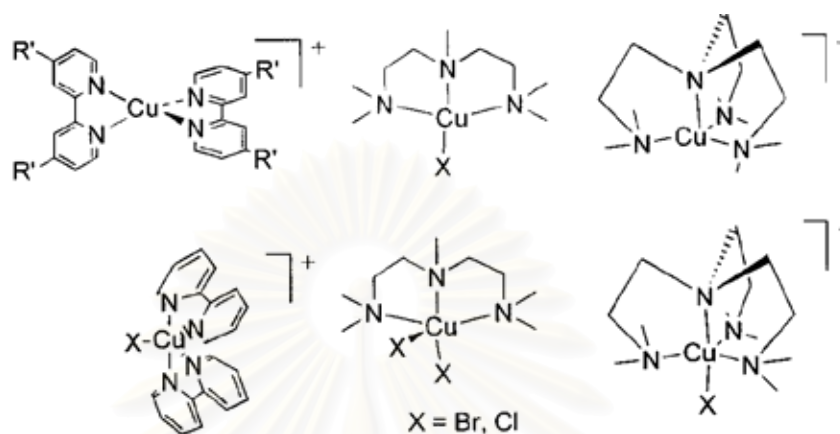


**Figure 2.5** Copper complexes used as ATRP catalysts [26].

Nitrogen ligands have been used in copper-mediated ATRP. The monodentate (e.g.,  $N(nBu)_3$ ), bidentate (e.g.,  $dNbpy$ ), and multidentate nitrogen ligands have been applied to copper-based ATRP. The electronic and steric effects of the ligands are important. Reduced catalytic activity or efficiency is observed when there is excessive steric hindrance around the metal center or the ligand has strongly electron-withdrawing substituents. A recent survey summarized different ligands employed in copper-mediated ATRP. The effect of the ligands and guidelines for ligand design were reviewed. Activity of N-based ligands in ATRP decreases with the number of coordinating sites  $N4 > N3 > N2 \gg N1$  and with the number of linking C-atoms  $C2 > C3 \gg C4$ . It also decreases in the order  $R_2N- \approx PyrEnDash- > R-N= > Ph-N= > Ph-NR-$ . Activity is usually higher for bridged and cyclic systems than for linear analogues. Examples of some N-based ligands used successfully in Cu-based ATRP are shown in Figure 2.6.

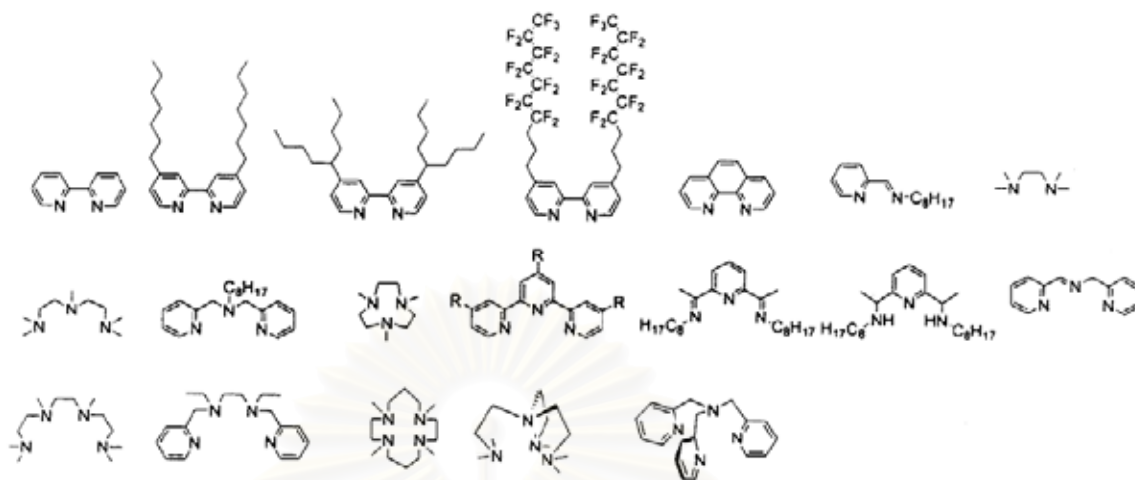


**Figure 2.6** Examples of ligands used in copper-mediated ATRP [26].

In 1995, Matyjaszewski has described the use of  $\text{Cu}^{\text{I}}\text{X}$  ( $\text{X} = \text{Br}, \text{Cl}$ ) with 2,2'-bipyridine (bpy) as a “solubilizing” ligand. The active species has been described as “ $\text{CuBr}\cdot\text{bpy}$ ”. This system is active toward styrene, acrylates, and methacrylates under the appropriate condition [19]. Percec has also described the role of bpy as partially solubilizing the  $\text{Cu}(\text{I})/\text{Cu}(\text{II})$  catalyst [27]. The role of the bpy is to coordinate to  $\text{Cu}(\text{I})$  to give a *pseudo*-tetrahedral  $\text{Cu}(\text{I})$  center in solution (Figure 2.7).

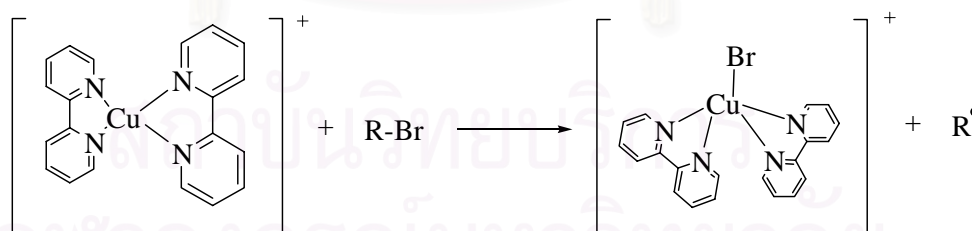


**Figure 2.7** Rotation of the bpy ligands from the tetrahedral and co-ordination of halide at the Cu center.



Furthermore, in 1997, Matyjaszewski and coworkers [28] has described the use of simple amines as ligands for the copper mediated atom transfer radical polymerization (ATRP) of styrene, methyl acrylate and methyl methacrylate. The simple amines are of interest in ATRP for three general reasons. First, most of the simple amines are less expensive, more accessible and more tunable than 2,2'-bipyridine (bpy) ligands. Second, due to the absence of the extensive  $\pi$ -bonding in the simple amines, the subsequent copper complexes are less colored. Third, since the coordination complexes between copper and simple amines tend to have lower redox potentials than the copper-bpy complex, the employment of simple amines as the ligand in ATRP may lead to faster polymerization rates. The example of simple amine ligand is *N,N,N',N',N''*-pentamethyldiethylenetriamine (PMDETA). When this ligand was employed in ATRP, all the polymerizations were well controlled with a linear increase of molecular weights with conversion and relatively low polydispersities throughout the reactions. The rate of polymerization showed a significant increase, as compared to the corresponding bpy system. The higher polymerization rate of PMDETA as the ligand is partially attributed to the lower redox potential of the copper(I)-PMDETA complex than the copper(I)-bpy complex, which shifts the equilibrium from the dormant species toward the active species resulting in the generation of more radicals in the system. The structure of copper complex using PMDETA as the ligand was shown in Figure 2.8.



**Figure 2.8** Proposed Cu(I) and Cu(II) species using PMDETA as ligand.

### 2.3 Polymer Brush

Polymer brushes refer to an assembly of polymer chains which are tethered by one end to a surface or an interface [29]. Tethering is sufficiently dense that the polymer chains are crowded and forced to stretch away from the surface or interface to avoid overlapping, sometimes much further than the typical unstretched size of a chain. These stretched configurations are found under equilibrium conditions; neither a confining geometry nor an external field is required. This situation, in which polymer chains stretch along the direction normal to the grafting surface, is quite different from the typical behavior of flexible polymer chains in solution where chains adopt a random-walk configuration. A series of discoveries show that the deformation of densely tethered chains affects many aspects of their behavior and results in many novel properties of polymer brushes [29].

Polymer brushes are a central model for many practical polymer systems such as polymer micelles, block copolymers at fluid–fluid interfaces (e.g. microemulsions and vesicles), grafted polymers on a solid surface, adsorbed diblock copolymers and graft copolymers at fluid–fluid interfaces. All of these systems, illustrated in Figure 2.9, have a common feature: the polymer chains exhibit deformed configurations. Solvent can be either present or absent in polymer brushes. In the presence of a good solvent, the polymer chains try to avoid contact with each other to maximize contact with solvent molecules. With solvent absent (melt conditions), polymer chains must stretch away from the interface to avoid overfilling incompressible space.

The interface to which polymer chains are tethered in the polymer brushes may be a solid substrate surface or an interface between two liquids, between a liquid and air, or between melts or solutions of homopolymers. Tethering of polymer chains on the surface or interface can be reversible or irreversible. For solid surfaces, the polymer chains can be chemically bonded to the substrate or may be just adsorbed onto the surface. Physisorption on a solid surface is usually achieved by block copolymers with one block interacting strongly with the substrate and another block interacting weakly. For interfaces between fluids, the attachment may be

achieved by similar adsorption mechanisms in which one part of the chain prefers one medium and the rest of the chain prefers the other.

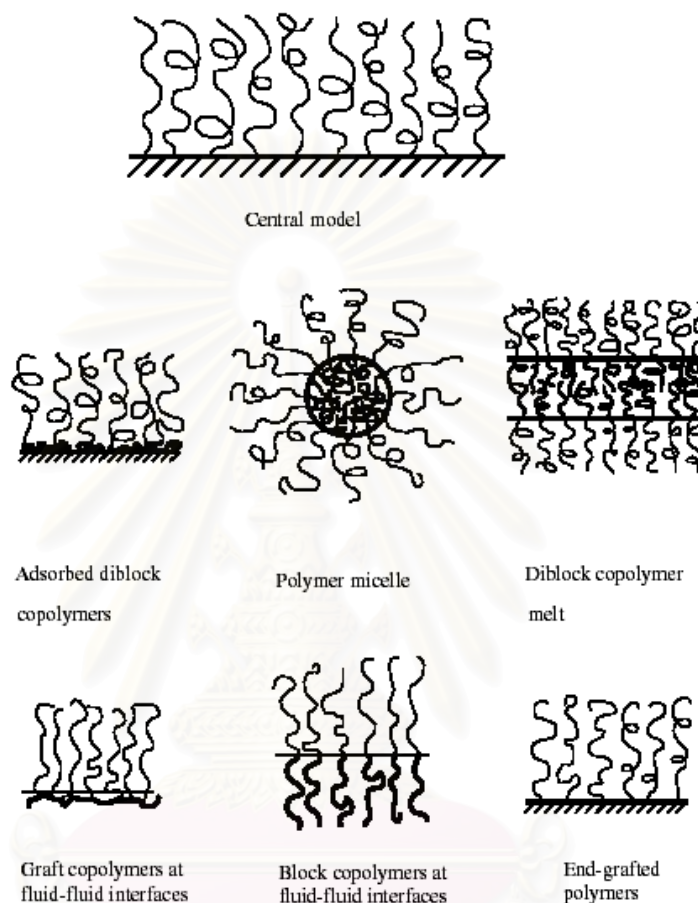


**Figure 2.9** Examples of polymer systems comprising polymer brushes.

Polymer brushes (or tethered polymers) attracted attention in 1950s when it was found that grafting polymer molecules to colloidal particles was a very effective way to prevent flocculation [29]. In other words, one can attach polymer chains which prefer the suspension solvent to the colloidal particle surface; the brushes of two approaching particles resist overlapping and colloidal stabilization is achieved. The repulsive force between brushes arises ultimately from the high osmotic pressure inside the brushes. Subsequently it was found that polymer brushes can be useful in other applications such as new adhesive materials [30-31], protein-resistant

biosurfaces [32], chromatographic devices [33], lubricants [34], polymer surfactants [29] and polymer compatibilizers [29]. Tethered polymers which possess low critical solution temperature (LCST) properties exhibit different wetting properties above and below LCST temperature [35]. A very promising field that has been extensively investigated is using polymer brushes as chemical gates. Ito and coworkers [36-38] have reported pH sensitive, photosensitive, oxidoreduction sensitive polymer brushes covalently tethered on porous membranes, which are used to regulate the liquid flowing rate through porous membranes. Suter and coworkers [39-40] have prepared polystyrene brushes on high surface area mica for the fabrication of organic-inorganic hybrids. Cation-bearing peroxide free-radical initiators were attached to mica surfaces *via* ion exchange and used to polymerize styrene. This process is important in the field of nanocomposites. Patterned thin organic films could be useful in microelectronics [41], cell growth control [42-43], biomimetic material fabrication [44], microreaction vessel and drug delivery [45].

In terms of polymer chemical compositions, polymer brushes tethered on a solid substrate surface can be divided into homopolymer brushes, mixed homopolymer brushes, random copolymer brushes and block copolymer brushes. Homopolymer brushes refer to an assembly of tethered polymer chains consisting of one type of repeat unit. Mixed homopolymer brushes are composed of two or more types of homopolymer chains [46]. Random copolymer brushes refer to an assembly of tethered polymer chains consisting of two different repeat units which are randomly distributed along the polymer chain [47]. Block copolymer brushes refer to an assembly of tethered polymer chains consisting of two or more homopolymer chains covalently connected to each other at one end [48]. Homopolymer brushes can be further divided into neutral polymer brushes and charged polymer brushes. They may also be classified in terms of rigidity of the polymer chain and would include flexible polymer brushes, semiflexible polymer brushes and liquid crystalline polymer brushes. These different polymer brushes are illustrated in Figure 2.10.

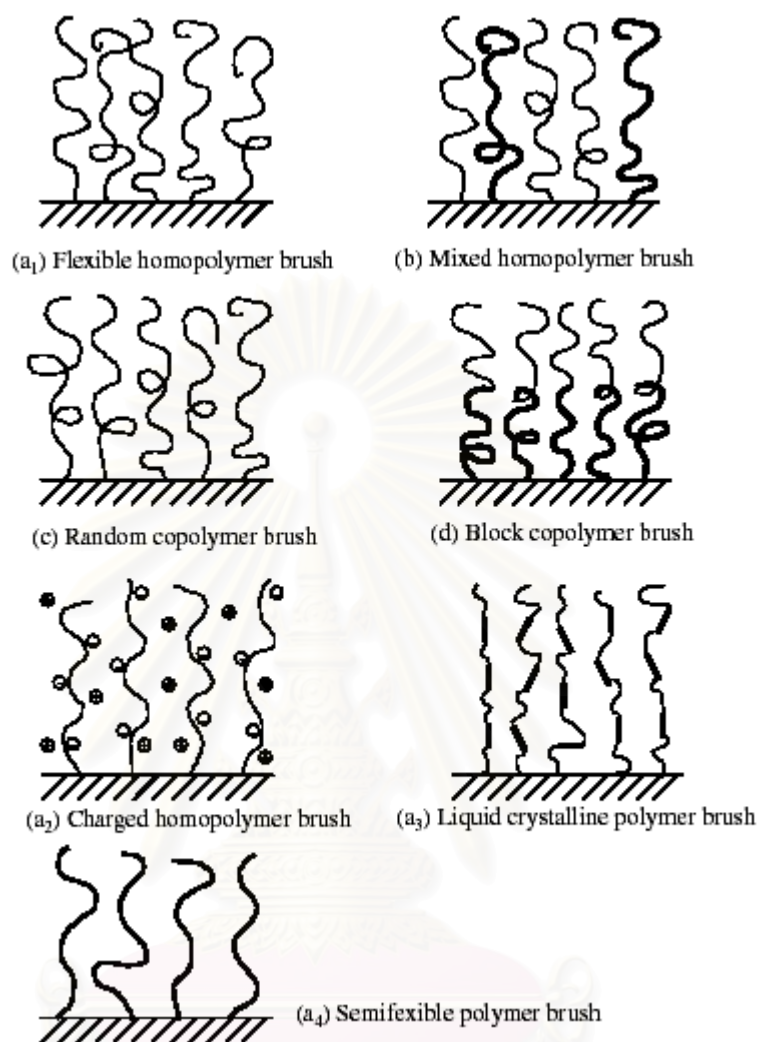


**Figure 2.10** Classification of linear polymer brushes, (a<sub>1</sub>–a<sub>4</sub>) homopolymer brushes; (b) mixed homopolymer brush; (c) random copolymer brush; (d) block copolymer brush.

Generally, there are two ways to fabricate polymer brushes: physisorption and covalent attachment (Figure 2.11). For polymer physisorption, block copolymers adsorb onto a suitable substrate with one block interacting strongly with the surface and the other block interacting weakly with the substrate. The disadvantages of physisorption include thermal and solvolytic instabilities due to the non-covalent nature of the grafting, poor control over polymer chain density and complications in

synthesis of suitable block copolymers. Tethering of the polymer chains to the surface is one way to surmount some of these disadvantages. Covalent attachment of polymer brushes can be accomplished by either “grafting to” or “grafting from” approaches. In a “grafting to” approach, preformed end-functionalized polymer molecules react with an appropriate substrate to form polymer brushes. This technique often leads to low grafting density and low film thickness, as the polymer molecules must diffuse through the existing polymer film to reach the reactive sites on the surface. The steric hindrance for surface attachment increases as the tethered polymer film thickness increases. To overcome this problem, the “grafting from” approach is a more promising method in the synthesis of polymer brushes with a high grafting density. “Grafting from” can be accomplished by treating a substrate with plasma or glow-discharge to generate immobilized initiators onto the substrate followed by in situ surface-initiated polymerization. However “grafting from” well-defined self-assembled monolayers (SAMs) is more attractive due to a high density of initiators on the surface and a well-defined initiation mechanism. Also progress in polymer synthesis techniques makes it possible to produce polymer chains with controllable lengths. Polymerization methods that have been used to synthesize polymer brushes include cationic, anionic, TEMPO-mediated radical, atom transfer radical polymerization (ATRP) and ring opening polymerization.

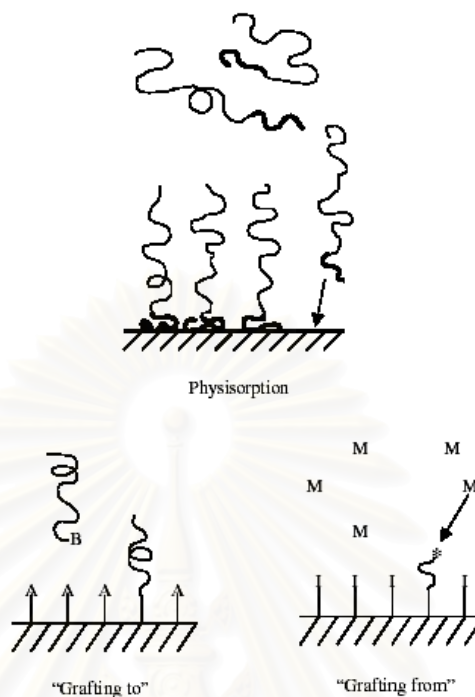


**Figure 2.11** Preparation of polymer brushes by “physisorption”, “grafting to” and “grafting from”.

In order to achieve a better control of molecular weight and molecular weight distribution and to obtain novel polymer brushes like block copolymer brushes, controlled radical polymerizations including ATRP, reverse ATRP, TEMPO-mediated and iniferter radical polymerizations have been used to synthesize tethered polymer brushes on solid substrate surfaces [49-54].

ATRP, the most robust “living” free radical polymerization, has been recognized in recent years as a versatile method for generating polymer brushes having well-defined thickness and architecture *via* surface initiated polymerization. [50]. This approach has also enabled the synthesis of a wide range of polymer brushes where polymers of precise molar mass, composition, and architecture are covalently attached to either curved or flat surfaces. ATRP is compatible with a variety of functionalized monomers, and the living/controlled character of the ATRP process yields polymers with a low polydispersity ( $M_w/M_n$ ) that are end functionalized and so can be used as macroinitiators for the formation of di- and triblock copolymers. In 1998, Fukuda and coworkers prepared poly(methyl

methacrylate) brushes on silicon surface *via* surface initiated atom transfer radical polymerization. The addition of free initiator to the polymerization solution yields free polymers which can be characterized by conventional methods. The relatively narrow polydispersities of these polymers in conjunction with the molecular weights were proportional to monomer conversion points towards the surface polymerization being controlled. The thickness of the polymer brushes was related to the concentration of the free initiator, the lower concentration of free initiator the thicker the films being achieved [50, 55]. Husseman and coworkers [51] applied ATRP in the synthesis of tethered polymer brushes on silicon wafers and achieved great success. They prepared SAMs of 5-trichlorosilylpentyl-2-bromo-2-methylpropionate on silicate substrates. The  $\alpha$ -bromoester is a good initiator for ATRP. They have successfully synthesized PMMA brushes by the polymerization of MMA initiated from the SAMs. It has also been reported that tethered polyacrylamide has been obtained from surface initiated ATRP of acrylamide on a porous silica gel surface [52].

Recently, Matyjaszewski and coworkers [56] reported a detailed study of polymer brush synthesis using ATRP in controlled growth of homopolymer and block copolymers from silicon surfaces. They described that the persistent radical effect must be considered in controlled radical polymerizations. In other words, a sufficient concentration of deactivation must be available to provide control over chain lengths and distributions. The Cu(II) can be supplied by termination of initiator molecules in the early stages of the polymerization or by addition of the transition metal complex prior to commencement of the reaction. Moreover, the only factor affected is the kinetics of the reaction; in the former case, first-order consumption of monomer is dictated by the chains generated from the free initiator while in the latter, due to the extremely low concentration of alkyl halide bound to the surface and low monomer conversion, growth of polymer chains scales linearly with reaction time. Their conclusion suggested that the design of such complex structures whether in solution or at an interface, understanding of the relative rates of chain propagation, equilibrium constants, and the influences of the end group, metal, and ligand in crossover reaction are important. Factors such as initiator functionality and



blocking efficiency can have a profound influence on the physical properties of the resulting material.

In 2001, *von Werne* and Patten [57] reported the preparation of structurally well-defined polymer-nanoparticle hybrids by modifying the surface of silica nanoparticles with initiators for ATRP and by using these initiator-modified nanoparticles as macroinitiators. They found that polymerizations of styrene and methyl methacrylate (MMA) using the nanoparticle initiators displayed the diagnostic criteria for a controlled / “living” radical polymerization: an increase in the molecular weight of the pendant polymer chains with monomer conversion and a narrow molecular weight distribution for the grafted chains. Polymerization of styrene from smaller silica nanoparticles (75-nm-diameter) exhibited good molecular weight control, while polymerization of MMA from the same nanoparticles exhibited good molecular weight control only when a small amount of free initiator was added to the polymerization solution. For the polymerization of both styrene and MMA from larger silica nanoparticles (300-nm-diameter) did not exhibit molecular weight control. Molecular weight control was induced by the addition of a small amount of free initiator to the polymerization but was not induced when 5-15 mol% of deactivator (Cu(II) complex) was added. These findings provide guidance for efforts in using ATRP for the controlled grafting of polymers from high and low surface area substrates.

#### **2.4 Diblock Copolymer Brushes**

Block copolymer brushes refer to an assembly of tethered polymer chains consisting of two or more homopolymer chains covalently connected to each other at one end [48]. Block copolymer brushes are the most interesting architectures produced to date [48, 53, 56, 58-61], and this is due mainly to vertical phase separation occurring when the block copolymer chains are tethered by one end to a surface or substrate.

Diblock copolymer brushes tethered to flat silicon substrates have been synthesized using ATRP technique. In 1999, Brittain and Zhao synthesized the first diblock copolymer brushes by a combination of carbocationic polymerization and ATRP [48]. They have characterized films by tensiometry, FTIR, XPS, and ellipsometry. In the same year, Matyjaszewski et al. [56] reported the preparation of diblock copolymer brushes of polystyrene and poly(*tert*-butyl acrylate) (PS-*b*-PtBA) on Si wafers using a surface-initiated ATRP approach. Hydrolysis of *t*-butyl groups yielded a polystyrene-*block*-poly(acrylic acid) brushes, and demonstrated a versatile approach to tune film properties and wettability [56]. Modification of the hydrophilicity of the surface layer was confirmed by a decrease in water contact angle from 86° to 18°. They observed the thickness of the layer consisting of chains grown from the surface increased linearly with the molecular weight of chains polymerization in solution. Other novel diblock copolymer brushes have been synthesized using sequential ATRP from wafers possessing diblock copolymers tethered to various substrates (e.g., Si, Au) [62-64].

In 2000, Zhao and Brittain [61] synthesized diblock copolymer brushes consisting of a tethered chlorine-terminated polystyrene (PS) block, produced using carbocationic polymerization, on top of which was added a block of either poly(methyl methacrylate) (PMMA), poly(methyl acrylate) (PMA) or poly((*N,N'*-dimethylamino)ethyl methacrylate) (PDMAEMA), synthesized using ATRP. The thickness of the outer poly(meth)acrylate block was controlled by adding varying amounts of free initiator to the ATRP media. They reported the response of these diblock copolymer brushes to different solvent treatments and illustrated proposed responses of tethered PS-*b*-PMMA brushes as shown in Figure 2.12. Upon treatment with different solvents, these tethered diblock copolymer brushes exhibit reversible changes in surface properties, which are revealed by water contact angle. For PS-*b*-PMMA and PS-*b*-PMA brushes, treatment with CH<sub>2</sub>Cl<sub>2</sub> resulted in localization of PMMA and PMA at the air interface and treatment with cyclohexane localized the PS block at the air interface. PS-*b*-PDMAEMA brushes exhibited a similar behavior, using cyclohexane and THF/H<sub>2</sub>O (v/v = 1:1).

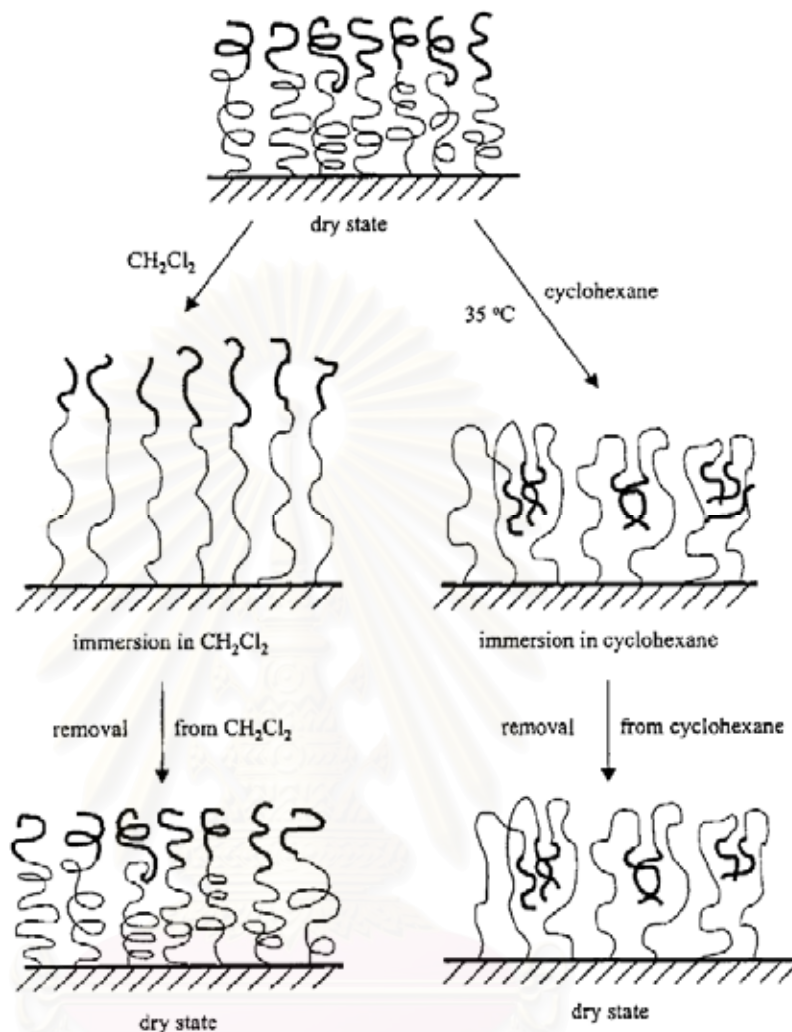


**Figure 2.12** Proposed responses of tethered PS-*b*-PMMA brushes to different solvent treatments.

Granville and colleagues [11] were able to synthesize diblock copolymer brushes using ATRP in 2004. They synthesized semifluorinated diblock copolymer brushes. Either a polystyrene (PS) or poly(methyl acrylate) (PMA) block was firstly formed (inner block) followed by polymerization of the fluorinated monomers (outer block). The outer block consisted either of poly(pentafluorostyrene) (PPFS), poly(heptafluorodecyl acrylate) (PHFA), poly(pentafluoropropyl acrylate), or poly(trifluoethyl acrylate). Solvent-induced diblock rearrangement experiments were performed using a selective solvent for the hydrocarbon polymer block to generate a

fluorine-deficient surface. All the diblock systems were shown to exhibit water contact angles typical for the hydrocarbon polymer block after solvent treatment. With the exception of the systems containing PHFA, poor rearrangement was observed when compared to all other semifluorinated diblock copolymer systems.

Experimentally, very few investigations have been conducted into the rearrangement of tethered diblock copolymer brushes. The first report of nanopattern formation from a tethered diblock copolymer brush was reported by Zhao and co-workers [58-59, 61] in 2000. They produced a tethered Si/SiO<sub>2</sub>//PS-*b*-PMMA brush where the PS thickness was 23 nm and the PMMA thickness was 14 nm. When this diblock copolymer brush was treated with dichloromethane (which is a good solvent for both PS and PMMA), water contact angle results indicated a characteristic advancing contact angle of PMMA, 74°, while atomic force microscopy (AFM) analysis indicated that the surface of the brush was smooth (Figure 2.13 (a)) [59]. When the same sample was treated with mixed solvents of dichloromethane and cyclohexane, and the percentage of cyclohexane was gradually increased, the advancing water contact angle of the brush increased to 120°, and the tethered diblock copolymer brush was seen to reorganize, resulting in the formation of a regular nanopattern on the surface. Zhao and colleagues speculated that, with an increasing cyclohexane content, the PMMA blocks would collapse and aggregate to form a core, so as to avoid contact with the cyclohexane (Figure 2.13 (b)) [59].

Granville et al. [11] used thermal treatment of samples that had been rearranged using solvent, to reorganize the surface composition. Thermal treatment of the solvent-rearranged Si/SiO<sub>2</sub>//PS-*b*-PPFS brush at 100 °C for 20 min, after it had been treated with cyclohexane at 35 °C, resulted in an increase in the advancing contact angle from 101° to 121°. Similar results were seen for the Si/SiO<sub>2</sub>//PMA-*b*-PPFS brush, although thermal treatment at 60 °C for 5 min was all that was required to increase the advancing contact angle from 80° to 118°.

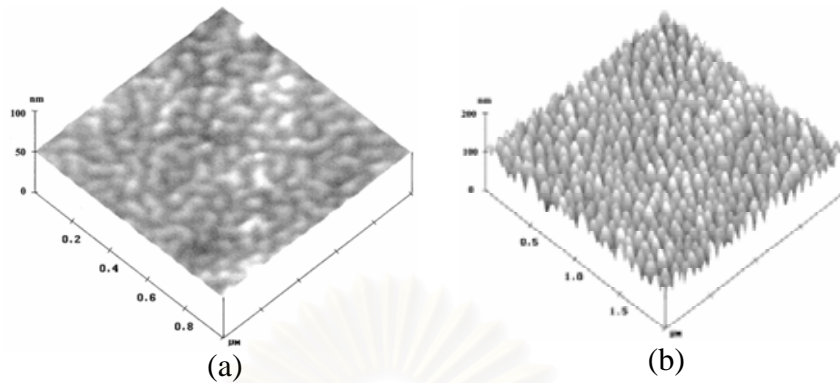


**Figure 2.13** Atomic force microscopy (AFM) images of tethered Si/SiO<sub>2</sub>//PS-*b*-PMMA brushes after treatment with dichloromethane (a) and gradual treatment with cyclohexane (b).

## 2.5 Characterization Techniques

### 2.5.1 Ellipsometry [65]

Ellipsometry is a sensitive optical technique for determining properties of surfaces and thin films. If linearly polarized light of a known orientation is reflected at oblique incidence from a surface then the reflected light is elliptically polarized. The shape and orientation of the ellipse depend on the angle of incidence, the direction of the polarization of the incident light, and the reflection properties of the surface. Ellipsometry measures the polarization of the reflected light with a quarter-wave plate followed by an analyzer; the orientations of the quarter-wave plate and the analyzer are varied until no light passes through the analyzer. From these orientations and the direction of polarization of incident light are expressed as the relative phase change,  $\Delta$ , and the relative amplitude change,  $\Psi$ , introduced by reflection from the surface. These values are related to the ratio of Fresnel reflection coefficients,  $R_p$  and  $R_s$ , for *p* and *s*- polarized light, respectively.

$$\tan(\Psi) e^{i\Delta} = \frac{R_p}{R_s} \quad (2.2)$$

An ellipsometer measures the changes in the polarization state of light when it is reflected from a sample. If the sample undergoes a change, for example, a thin film on the surface changes its thickness, then its reflection properties is also changed. Measuring these changes in the reflection properties allow us to deduce the actual change in the film's thickness.

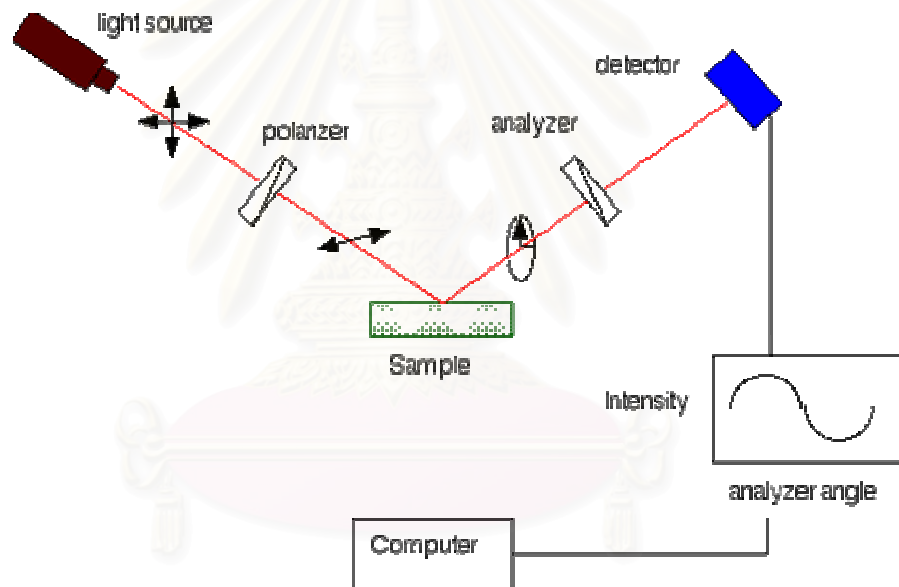


**Figure 2.14** Schematic of the geometry of an ellipsometry experiment.

### 2.5.2 Contact Angle Measurement [66]

Contact angle measurements are often used to assess changes in the wetting characteristics of a surface and hence indicate a change in surface energy. The technique is based on the three-phase boundary equilibrium described by Young's equation.

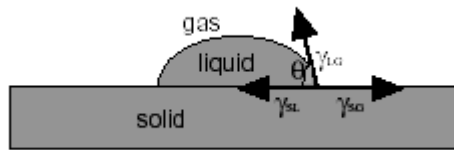


**Figure 2.15** Schematic representation of the Young's equation.

$$\gamma_{LG}\cos\theta = \gamma_{SG} - \gamma_{SL} \quad (2.3)$$

where  $\gamma_{LG}$ ,  $\gamma_{SG}$  and  $\gamma_{SL}$  are the interfacial tension between the phases with subscripts L, G, S corresponding to liquid, gas, and solid phase, respectively and  $\theta$  refers to the equilibrium contact angle. The Young's equation applies for a perfectly homogeneous atomically flat and rigid surface and therefore supposes many simplifications. In the case of real surfaces, the contact angle value is affected by surface roughness, heterogeneity, vapor spreading pressure, and chemical contamination of the wetting liquid. Although the technique to measure contact angles is easy, data interpretation is not straightforward and the nature of different contributions to the surface is a matter of discussion. Generally, we can define the complete wetting, wetting, partial wetting, and nonwetting according to Figure 2.16.

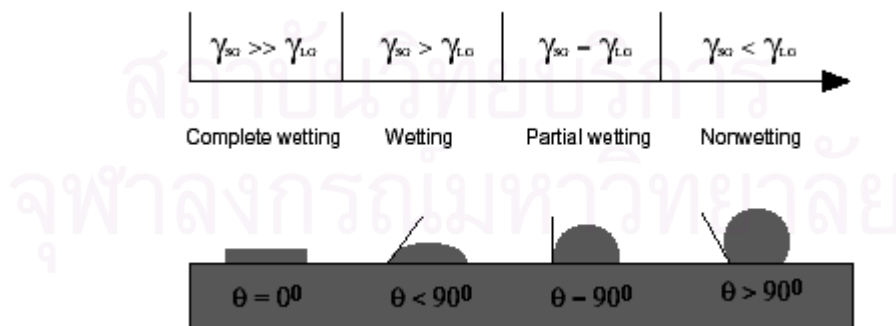


**Figure 2.16** Schematic representation of wettability.

### 2.5.3 Gel Permeation Chromatography (GPC) [67]

Gel permeation chromatography, more correctly termed *size exclusion chromatography*, is a separation method for high polymers, similar to but advanced in practice over *gel filtration* as carried out by biochemists, that has become a prominent and widely used method for estimating molecular-weight distributions since its discovery just over two decades ago in 1961. The separation takes place in a chromatographic column filled with beads of a rigid porous “gel”; highly cross-linked porous polystyrene and porous glass are preferred column-packing materials. The pores in these gels are of the same size as the dimensions of polymer molecules.

A sample of a dilute polymer solution is introduced into a solvent stream flowing through the column. As the dissolved polymer molecules flow past the porous beads, they can diffuse into the internal pore structure of the gel to an extent depending on their size and the pore-size distribution of the gel. Larger molecules can enter only a small fraction of the internal portion of the gel, or are completely excluded; smaller polymer molecules penetrate a larger fraction of the interior of the gel. The larger the molecule, therefore, the less time it spends inside the gel, and the sooner it flows through the column. The different molecular species are eluted from the column in order of their molecular size as distinguished from their molecular weight, the largest emerging first.

A complete theory predicting retention times or volumes as a function of molecular size has not been formulated for gel permeation chromatography. A specific column or set of columns (with gels of different pore sizes) is calibrated empirically to give such a relationship, by means of which a plot of amount of solute versus retention volume can be converted into a molecular-size-distribution curve.

As in all chromatographic processes, the band of solute emerging from the column is broadened by a number of processes, including contributions from the apparatus, flow of the solution through the packed bed of gel particles, and the permeation process itself. Corrections for this zone broadening can be made empirically; it usually becomes unimportant when the sample has  $\overline{M}_w/\overline{M}_n > 2$ .



Gel permeation chromatography is extremely valuable for both analytic and preparative work with a wide variety of systems ranging from low to very high molecular weights. The method can be applied to a wide variety of solvents and polymers, depending on the type of gel used. With polystyrene gels, relatively nonpolar polymers can be measured in solvents such as tetrahydrofuran, toluene, or (at high temperatures) *o*-dichlorobenzene; with porous glass gels, more polar systems, including aqueous solvents, can be used. A few milligrams of sample suffices for analytic work, and the determination is complete in as short a time as a few minutes using modern high-pressure, high-speed equipment.

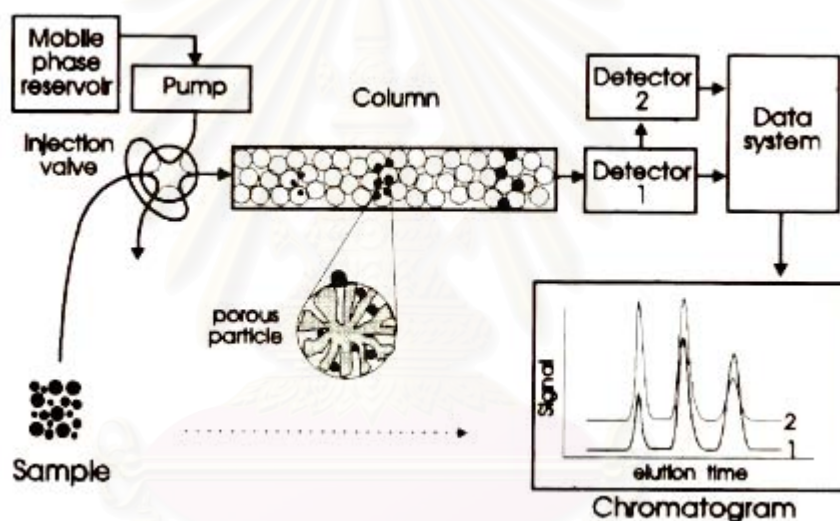


**Figure 2.17** Schematic representation of the gel permeation chromatography.

สถาบันวิทยบริการ  
จุฬาลงกรณ์มหาวิทยาลัย

# CHAPTER III

## EXPERIMENTAL

### 3.1 Materials

All reagents and materials are analytical grade

1. 2-Bromo-2-methylpropionyl bromide : Fluka
2. *tert*-Butyl methacrylate : Aldrich
3. Copper (I) bromide : Fluka
4. Dichloromethane : Merck
5. Dimethoxyethane : Fluka
6. Ethanol : Merck
7. Ethoxydimethylsilane : Gelest
8. Ethyldiisopropylamine : Fluka
9. Hexadecane : Aldrich
10. Hexane : Merck
11. Hydrochloric acid : Merck
12. Hydrogen hexachloroplatinate (IV) hydrate : Aldrich
13. Hydrogen peroxide : Merck
14. *N, N, N', N'', N'''*-pentamethyldiethylenetriamine : Aldrich
15. Prop-2-en-1-ol : Merck

16. Propan-1-ol	: Univar
17. Pyridine	: Fluka
18. Silica gel 60 (0.063-0.200 mm)	: Merck
19. Silicon wafer (Single-sided)	: Siltron Inc. Korea
20. Sodium sulfate anhydrous	: Fluka
21. Sulfuric acid	: Merck
22. Tetrahydrofuran	: Labscan
23. Toluene	: Carlo
24. Toluene anhydrous 99%	: Aldrich
25. Trifluoroacetic acid	: Fluka
26. 2,2,2-Trifluoroethyl methacrylate	: Aldrich
27. $\alpha,\alpha,\alpha$ -Trifluorotoluene	: Fluka
28. Ultrapure distilled water	: Mill-Q Lab system

## 3.2 Equipments

### 3.2.1 Ellipsometry

The ellipsometry was studied by using L115C WAFER<sup>TM</sup> ELLIPSOMETER. The thicknesses were determined in air with a 70° of incidence angle at 632.8 nm. The thickness of the adsorbed film was calculated by using the software “Dafibm” Rudolph Research, Double Absorbing Films Calculations. The calculation was based on a refractive index of  $N_{\text{initiator}} = 1.443$ ,  $N_{t\text{-BMA}} = 1.460$ ,  $N_{\text{TFMA}} = 1.415$ ,  $N_{\text{hydroxyl}} =$

1.462 and a silicon substrate refractive index  $N_{\text{substrate}} = 3.858$ . At least five different locations on each sample were measured and the average thickness was calculated.

### 3.2.2 Nuclear Magnetic Resonance Spectroscopy (NMR)

The  $^1\text{H}$ -NMR spectra was recorded in  $\text{CDCl}_3$  using Varian, model Mercury-400 nuclear magnetic resonance spectrometer operating at 400 MHz. Chemical shifts ( $\delta$ ) are reported in part per million (ppm) relative to tetramethylsilane (TMS) or using the residual protonated solvent signal as a reference.

### 3.2.3 Gel Permeation Chromatography (GPC)

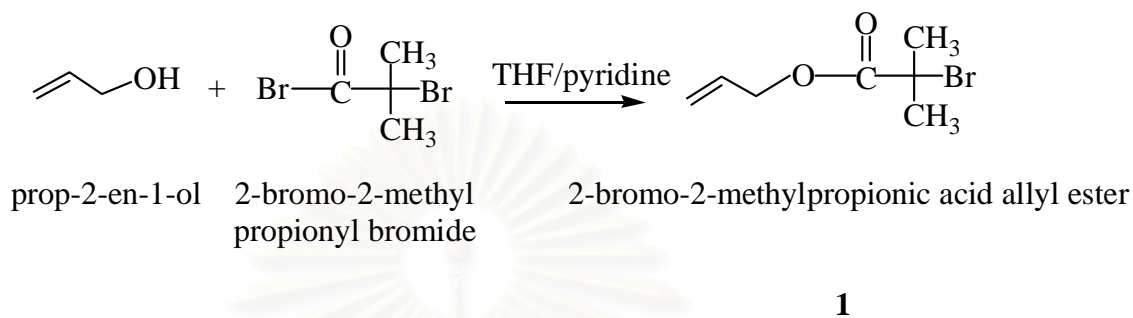
The molecular weight and molecular weight distributions of the TFMA and *t*-BMA homopolymers was determined by Waters gel permeation chromatography (GPC) equipped with HR4, HR3, HR1 THF column using THF as eluant connected to the RI detector. The flow rate was 1.0 mL/min. Calibration was based on polystyrene(PS) standards ranging from 500 to 43,000  $\text{g mol}^{-1}$ .

### 3.2.4 Contact Angle Measurement

Contact angle Goniometer model 100-00 and a Gilmont syringe with a 24-gauge flat-tipped needle (Ramé-Hart, Inc., USA) was used for the determination of water and hexadecane contact angles. The measurements were carried out in air at ambient temperature. Dynamic advancing and receding angles were recorded while the probe fluid (water or hexadecane) was added to and withdrawn from the drop, respectively. The reported angle is an average of 5 measurements on different area of each sample.

### 3.3 Synthesis of $\alpha$ -Bromoisobutyrate Initiators

#### 3.3.1 Synthesis of 2-bromo-2-methylpropionic acid allyl ester (1)

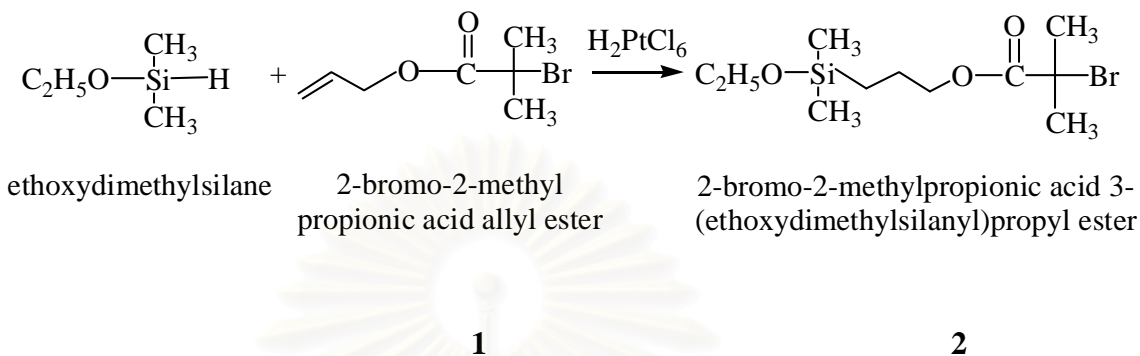


To a solution of 25 mmol of prop-2-en-1-ol (1.7 mL) in 25 mL of tetrahydrofuran, pyridine (2.1 mL, 26.5 mmol) was added, followed by a dropwise addition of 2-bromo-2-methylpropionyl bromide (3.10 mL, 25 mmol). The mixture was stirred at room temperature overnight, diluted with hexane and then washed once with 2N HCl and twice with deionized water. The organic phase was dried over sodium sulfate and filtered. After the solvent was removed from the filtrate under reduced pressure, the colorless oily residue was purified by filtering through a silica gel column chromatography to give the product (1) in 90 % yield.

**$^1\text{H NMR}$  ( $\text{CDCl}_3$ ) of (1):**  $\delta$  1.98 (6H,  $\text{C}(\text{CH}_3)_2$ , s), 4.71 (2H,  $\text{OCH}_2$ , d,  $J = 5.46$  Hz), 5.25 (1H,  $=\text{CH}_2$ , d,  $J = 11.70$  Hz), 5.39 (1H,  $=\text{CH}_2$ , d,  $J = 18.72$ ), 5.93-6.0 (1H,  $=\text{CH}$ , complex m).

สถาบันวิทยบริการ  
จุฬาลงกรณ์มหาวิทยาลัย

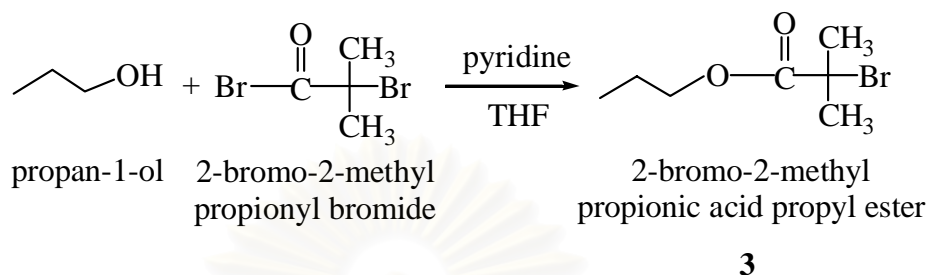
### 3.3.2 Synthesis of 2-bromo-2-methylpropionic acid 3-(ethoxydimethylsilyl)propyl ester (2)



To a solution of the alkene derivative (1) (2.07 g, 10 mmol) in ethoxy dimethylsilane (1.2 mL, 10 mmol), a 1:1 ethanol/dimethoxyethane solution of chloroplatinic acid,  $\text{H}_2\text{PtCl}_6$  (1.1 mg, 0.002 mmol, 0.2 mL) was added. The reaction mixture was stirred at room temperature under nitrogen atmosphere in the dark for 14 h. Dry toluene (3 mL) was then added and the excess ethoxydimethylsilane was removed under reduced pressure. Dry dichloromethane was added and then removed under reduced pressure. The crude product was passed through a short column of dry sodium sulfate, the column was washed with dry dichloromethane and the dichloromethane was removed under reduced pressure to give the desired product as yellow viscous liquid (2) in 93 % yield.

**$^1\text{H NMR}$  ( $\text{CDCl}_3$ ) of (2):**  $\delta$  0.04 (6H,  $\text{Si}(\text{CH}_3)_2$ , s), 0.93 (3H,  $\text{SiOCH}_2\text{CH}_3$ , t,  $J = 7.04$  Hz), 1.24 (2H,  $\text{OCH}_2\text{CH}_2\text{CH}_2$ , t,  $J = 7.04$  Hz), 1.66 (2H,  $\text{OCH}_2\text{CH}_2\text{CH}_2$ , complex m), 1.88 (6H,  $\text{C}(\text{CH}_3)_2$ , s), 3.60 (2H,  $\text{SiOCH}_2\text{CH}_3$ , q,  $J = 6.45$  Hz), 4.06 (2H,  $\text{OCH}_2\text{CH}_2\text{CH}_2$ , t,  $J = 6.45$  Hz).

### 3.3.3 Synthesis of 2-bromo-2-methylpropionic acid propyl ester (3) as a “Sacrificial” Initiator



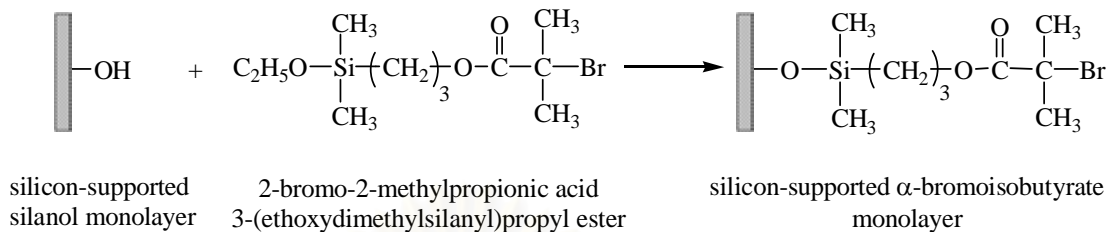
To a solution of propan-1-ol (1.5 mL, 25 mmol) in 25 mL of tetrahydrofuran, pyridine (3.1 mL, 26.5 mmol) was added, followed by a dropwise addition of 2-bromo-2-methylpropionyl bromide (3.10 mL, 25 mmol). The mixture was stirred at room temperature overnight and then diluted with hexane and washed once with 2N HCl and twice with deionized water. The organic phase was dried over sodium sulfate and filtered. The solvent was removed from the filtrate under reduced pressure, and the colorless oily residue was purified by filtering through a silica gel column chromatography to give the desired product in 90% yield.

**$^1\text{H}$  NMR ( $\text{CDCl}_3$ ) of (3):**  $\delta$  1.0 (3H,  $\text{OCH}_2\text{CH}_2\text{CH}_3$ , t,  $J = 7.02$  Hz), 1.72 (2H,  $\text{OCH}_2\text{CH}_2\text{CH}_3$ , complex m), 1.95 (6H,  $\text{C}(\text{CH}_3)_2$ , s), 4.15 (2H,  $\text{OCH}_2\text{CH}_2\text{CH}_3$ , t,  $J = 6.24$  Hz).

### 3.4 Pretreatment of Silicon Substrates

Silicon wafers were cut into  $1.5 \times 1.5 \text{ cm}^2$  substrates. The substrates held in a slotted hollow glass cylinder (custom designed holder) were put in a freshly prepared mixture of 7 parts of concentrated sulfuric acid and 3 parts of 30% hydrogen peroxide. Substrates were submerged in the solution at room temperature for 2h, then removed and rinsed with five to seven aliquots of deionized water followed by drying in a clean oven at  $120^\circ\text{C}$  for 2h. Silanization reaction was carried out immediately after treating the substrates in this fashion.

### 3.5 Preparation of Silicon-supported $\alpha$ -Bromoisobutyrate Monolayer



2

4

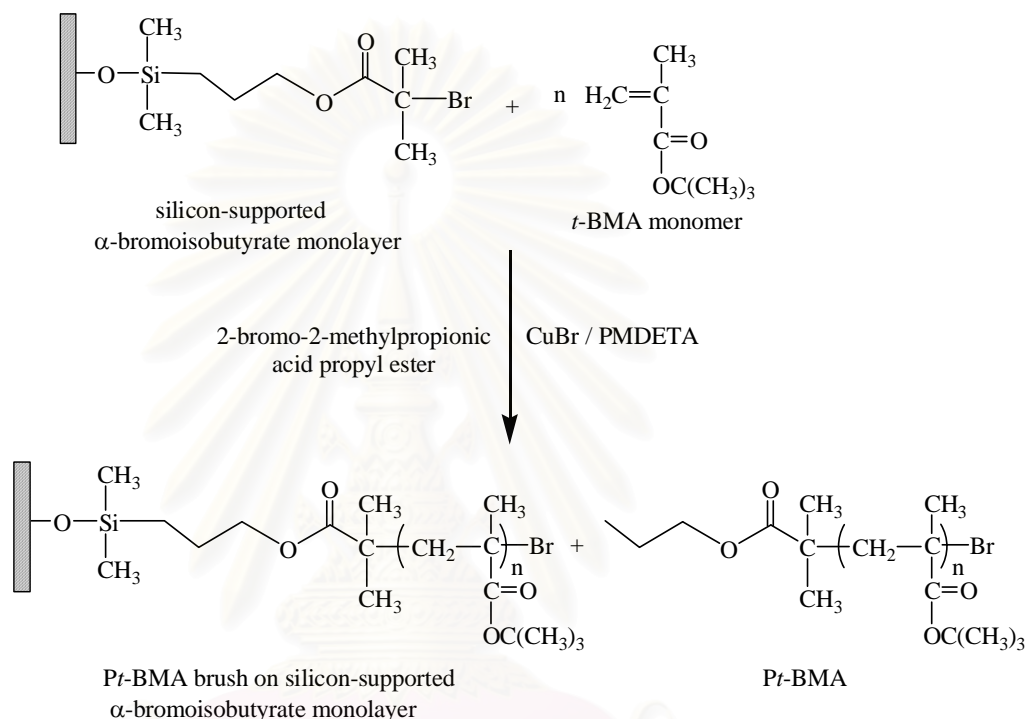
Freshly cleaned and dried silicon substrates held in a slotted hollow glass cylinder were covered with 10 mL of anhydrous toluene in a Schlenk flask. 2-bromo-2-methylpropionic acid 3-(ethoxydimethylsilyl)propyl ester (2) (33  $\mu$ L, 4 mmol) was added by a syringe. Reactions were carried out under nitrogen atmosphere at ambient temperature for 24h. The substrates were removed and sequentially rinsed with 3 x 10 mL of toluene, 3 x 10 mL of ethanol, 2 x 10 mL of ethanol-water (1:1), 2 x 10 mL of water, 2 x 10 mL of ethanol and 2 x 10 mL of water and dried under vacuum.

สถาบันวิทยบริการ  
จุฬาลงกรณ์มหาวิทยาลัย



### 3.6 Preparation of Polymer Brushes

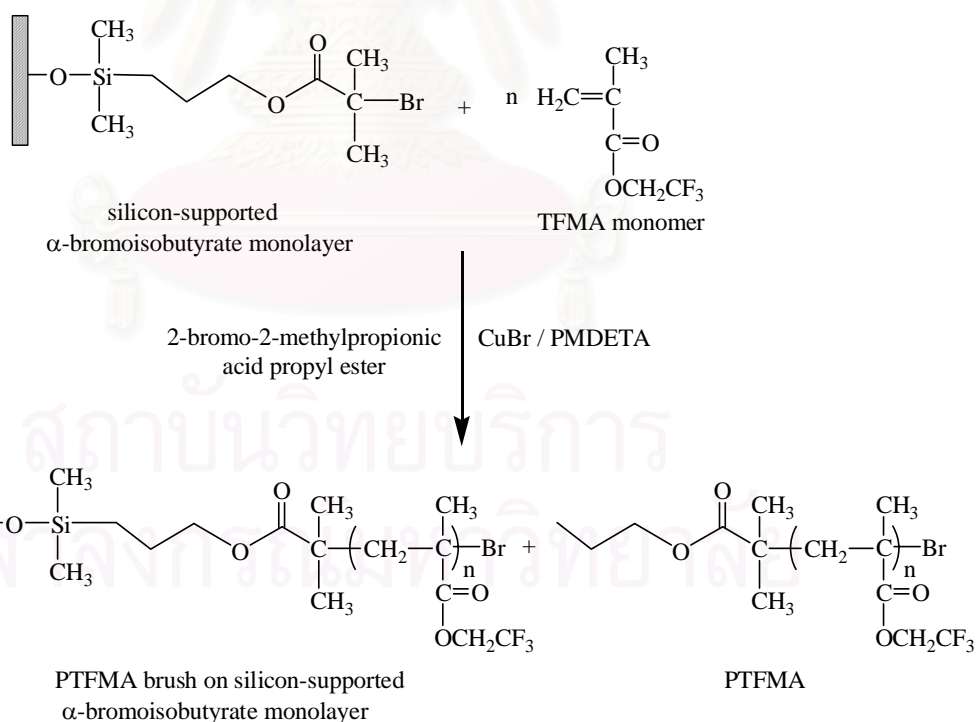
#### 3.6.1 Homopolymer Brushes of Poly(*tert*-Butyl Methacrylate) (*Pt*-BMA)



The silicon-supported  $\alpha$ -bromoisobutyrate monolayer (4) held in a slotted hollow glass cylinder were placed in a 100 mL Schlenk flask and sealed with a rubber septum. The flask was degassed and back-filled with nitrogen three times and left under a nitrogen atmosphere. Copper (I) bromide (29 mg, 0.20 mmol), anhydrous toluene (10 mL), and *t*-BMA (1.0 mL, 0.006 mol or 2.0 mL, 0.012 mol) were added to a separate 100 mL Schlenk flask with a magnetic stir bar. The flask was sealed with a rubber septum and degassed by purging with nitrogen for 1h. Anhydrous toluene (5 mL) containing PMDETA (41.8  $\mu$ L, 0.20 mmol) was added to the mixture *via* a syringe, and the solution was stirred at 90  $^{\circ}$ C until it became homogeneous (approximately 15 min). The solution was then transferred to the flask containing silicon-supported  $\alpha$ -bromoisobutyrate monolayer *via* a cannula, followed by the addition of 2-bromo-2-methylpropionic acid propyl ester (3) (12.5 mg, 0.060

mmol) as a “added” initiator in anhydrous toluene (5 mL) *via* a syringe. The polymerization was allowed to proceed at 90-100 °C until the desired reaction time, after which the silicon substrates were removed from the polymerization mixture then rinsed with copious amount of anhydrous toluene before soxhlet-extracted by THF for 24h to remove untethered polymer chains and dried under vacuum. The solution containing *Pt*-BMA formed from the “added” initiator was past through a silica column to remove the copper catalyst. Solid *Pt*-BMA was obtained after toluene was removed under reduced pressure.

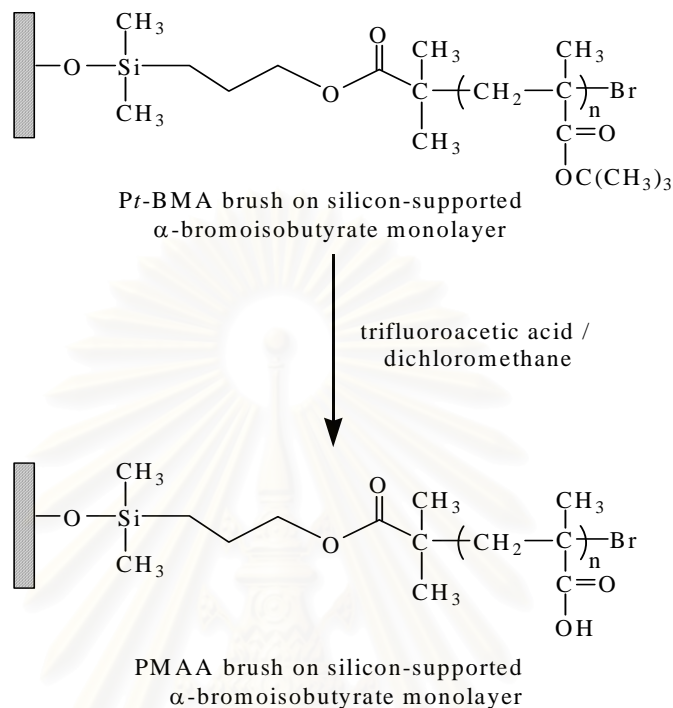
### 3.6.2 Homopolymer Brushes of Poly(2,2,2-Trifluoroethyl Methacrylate) (PTFMA)



The silicon-supported  $\alpha$ -bromoisobutyrate monolayer (4) held in a slotted hollow glass cylinder were placed in a 100 mL Schlenk flask and sealed with a rubber septum. The flask was degassed and back-filled with nitrogen three times and

left under a nitrogen atmosphere. Copper (I) bromide (7.2 mg, 0.05 mmol) ,  $\alpha,\alpha,\alpha$ -trifluorotoluene (10 mL), and TFMA (0.7 mL, 5.0 mmol or 1.4 mL, 10.0 mmol) were added to a separate 100 mL Schlenk flask with a magnetic stir bar. The flask was sealed with a rubber septum and degassed by purging with nitrogen for 1h.  $\alpha,\alpha,\alpha$ -Trifluorotoluene (5 mL) containing PMDETA (10.5  $\mu$ l, 0.05 mmol) was added to the mixture *via* a syringe, and the solution was stirred at 90 °C until it became homogeneous (approximately 15 min). The solution was then transferred to the flask containing silicon-supported  $\alpha$ -bromoisobutyrate monolayer *via* a cannula, followed by the addition of 2-bromo-2-methylpropionic acid propyl ester (3) (10.5 mg, 0.05 mmol) as a “sacrificial” initiator in  $\alpha,\alpha,\alpha$ -trifluorotoluene (5 mL) *via* a syringe. The polymerization was allowed to proceed at 90-100 °C until the desired reaction time, after which the silicon substrates were removed from the polymerization mixture then rinsed with copious amount of  $\alpha,\alpha,\alpha$ -trifluorotoluene before soxhlet-extracted by THF for 24h to remove untethered polymer chains and dried under vacuum. PTFMA formed in the solution from the “added” initiator was precipitated in mixture of methanol and water (5:1). The viscous PTFMA was re-dissolved in THF. The PTFMA solution was past through a silica column to remove the copper catalyst. Solid PTFMA was obtained after THF was removed under reduced pressure.

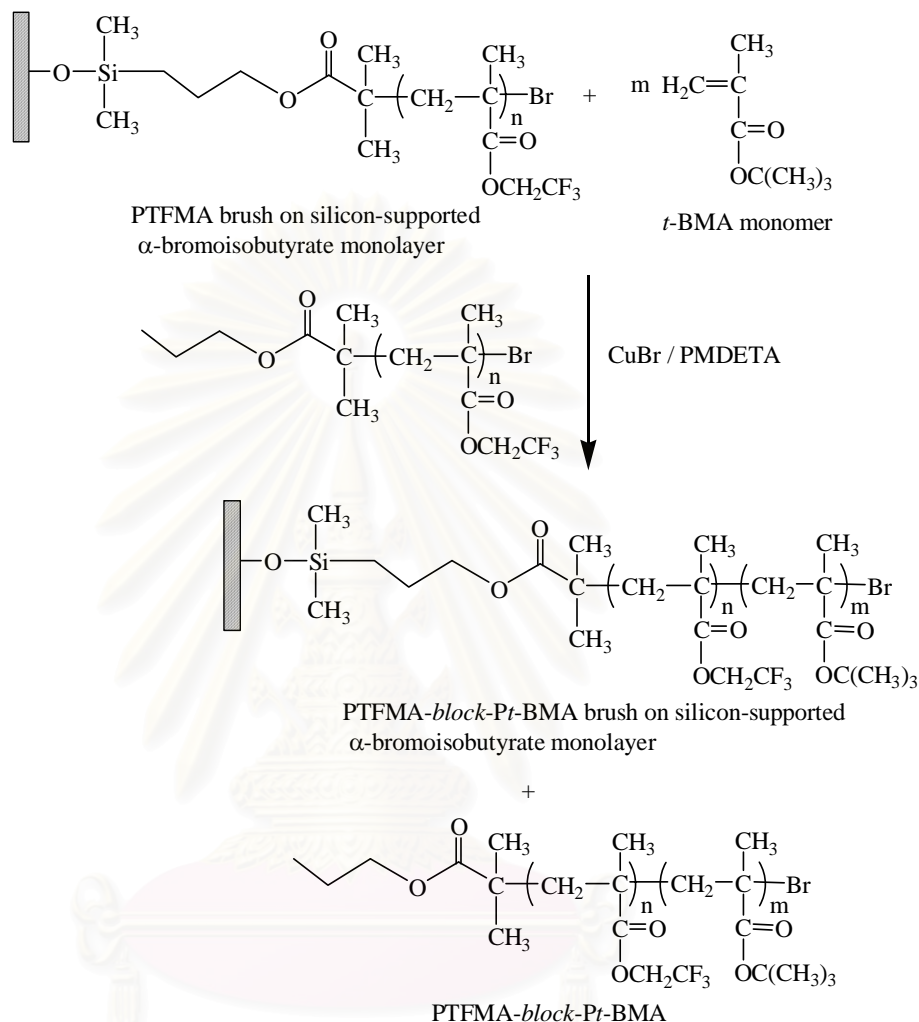
### 3.6.3 Homopolymer Brushes of Poly(Methacrylic Acid) (PMAA)



The silicon-supported Pt-BMA brushes held in a slotted hollow glass cylinder were placed in a 100 mL Schlenk flask containing dichloromethane (10 mL). Trifluoroacetic acid (0.38-5.7 mL) was added and the mixture was stirred for a desired period of time. The substrates were removed then rinsed with copious amount of dichloromethane and dried under vacuum.

สถาบันวิทยบริการ  
จุฬาลงกรณ์มหาวิทยาลัย

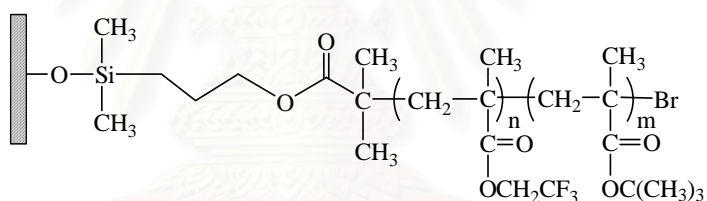
### 3.6.4 Diblock Copolymer Brushes of PTFMA-*b*-Pt-BMA



The silicon-supported PTFMA brush held in a slotted hollow glass cylinder were placed in a 100 mL Schlenk flask and sealed with a rubber septum. The flask was degassed and back-filled with nitrogen three times and left under a nitrogen atmosphere. Copper (I) bromide (7.2 mg, 0.05 mmol),  $\alpha,\alpha,\alpha$ -trifluorotoluene (10 mL), and *t*-BMA (0.16 mL, 1 mmol or 0.32 mL, 2 mmol) were added to a separate 100 mL Schlenk flask with a magnetic stir bar. The flask was sealed with a rubber septum and degassed by purging with nitrogen for 1h.  $\alpha,\alpha,\alpha$ -Trifluorotoluene (5 mL) containing PMDETA (10.5  $\mu\text{L}$ , 0.05 mmol) was added to the mixture *via* a syringe, and the solution was stirred at 90°C until it became homogeneous (approximately 15 min). The solution was then transferred to the flask containing silicon-supported PTFMA brush *via* a cannula, followed by the addition of solution of solid PTFMA

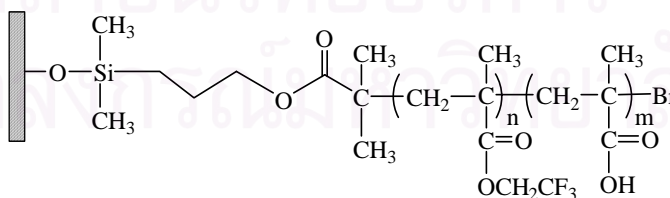
(168.1 mg, 0.01 mmol) as “macroinitiator” dissolved in  $\alpha,\alpha,\alpha$ -trifluorotoluene (10 mL) *via* a cannula. The polymerization was allowed to proceed at 90-100°C until the desired reaction time, after which the silicon substrates were removed from the polymerization mixture then rinsed with copious amount of  $\alpha,\alpha,\alpha$ -trifluorotoluene before soxhlet-extracted by THF for 24h to remove untethered polymer chains and dried under vacuum. PTFMA-*b*-Pt-BMA formed in the solution from the “macroinitiator” was precipitated in a mixture of methanol and water (5:1). The viscous diblock copolymer was re-dissolved in THF then past through a silica column to remove the copper catalyst. Solid PTFMA-*b*-Pt-BMA was obtained after THF was removed under reduced pressure.

### 3.6.5 Diblock Copolymer Brushes of PTFMA-*b*-PMAA



PTFMA-*block*-Pt-BMA brush on silicon-supported  $\alpha$ -bromoisobutyrate monolayer

trifluoroacetic acid/  
dichloromethane



PTFMA-*block*-PMAA brush on silicon-supported  $\alpha$ -bromoisobutyrate monolayer

The same procedure as described in section 3.6.3 was employed using the silicon-supported PTFMA-*b*-Pt-BMA brushes as substrates.

## CHAPTER IV

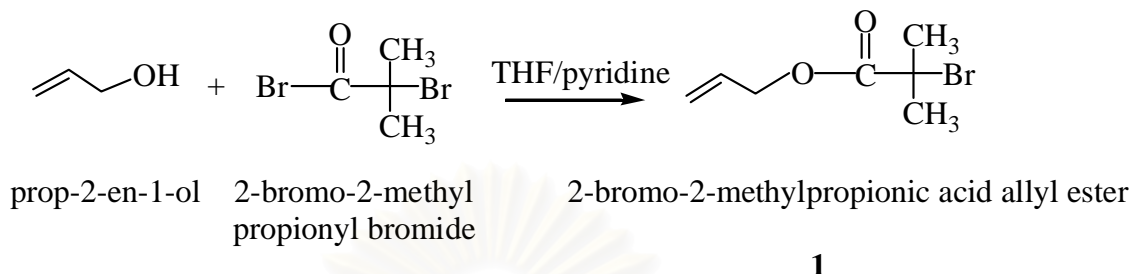
### RESULTS AND DISCUSSION

In this chapter, the results are divided into five sections. The first section mainly focuses on the synthesis of  $\alpha$ -bromoisobutyrate-containing silane compound and  $\alpha$ -bromoisobutyrate derivative to be used as surface-tethered initiator and “sacrificial” initiator, respectively. The second section involves the preparation of silicon-supported  $\alpha$ -bromoisobutyrate monolayer for the synthesis of surface-tethered polymer brushes. The third and fourth sections are devoted to the preparation of homopolymer brushes (poly(*tert*-butyl methacrylate); Pt-BMA, poly(methacrylic acid); PMAA, and poly(2,2,2-trifluoroethyl methacrylate); PTFMA) and diblock copolymer brushes (PTFMA-*b*-Pt-BMA and PTFMA-*b*-Pt-PMAA), respectively. The final section studies surface properties of diblock copolymer brushes upon a treatment with  $\alpha,\alpha,\alpha$ -trifluorotoluene.

#### 4.1 Synthesis of $\alpha$ -Bromoisobutyrate Initiators

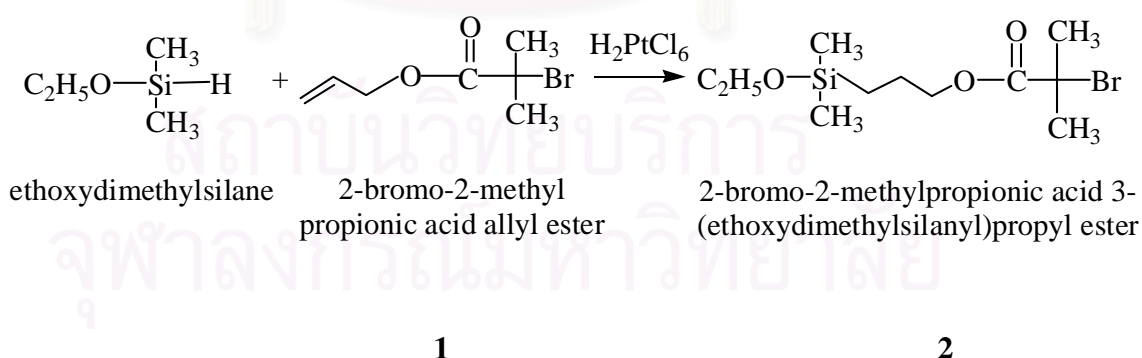
Esterification of prop-2-en-1-ol with 2-bromo-2-methylpropionyl bromide was followed by hydrosilylation with ethoxydimethylsilane to yield 2-bromo-2-methylpropionic acid 3-(ethoxydimethylsilyl)propyl ester having one end capable of bonding to silanol groups on a silicon surface and the other end carrying latent  $\alpha$ -bromo ester which can later be used to initiate the ATRP of vinyl monomers.

#### 4.1.1 Synthesis of 2-bromo-2-methylpropionic acid allyl ester (1)



Nucleophilic substitution of prop-2-en-1-ol with 2-bromo-2-methylpropionyl bromide in tetrahydrofuran gave 2-bromo-2-methylpropionic acid allyl ester as colorless liquid products which were sufficiently pure for the next synthesis without further purification after the work-up process. The characteristic  $^1\text{H-NMR}$  peak of product is a singlet signal of methyl protons of  $\text{C}(\text{CH}_3)_2$  at 1.98 ppm indicating the success of the reaction between prop-2-en-1-ol and 2-bromo-2-methylpropionyl bromide.  $^1\text{H-NMR}$  spectrum of the product is displayed in Figure A.1.

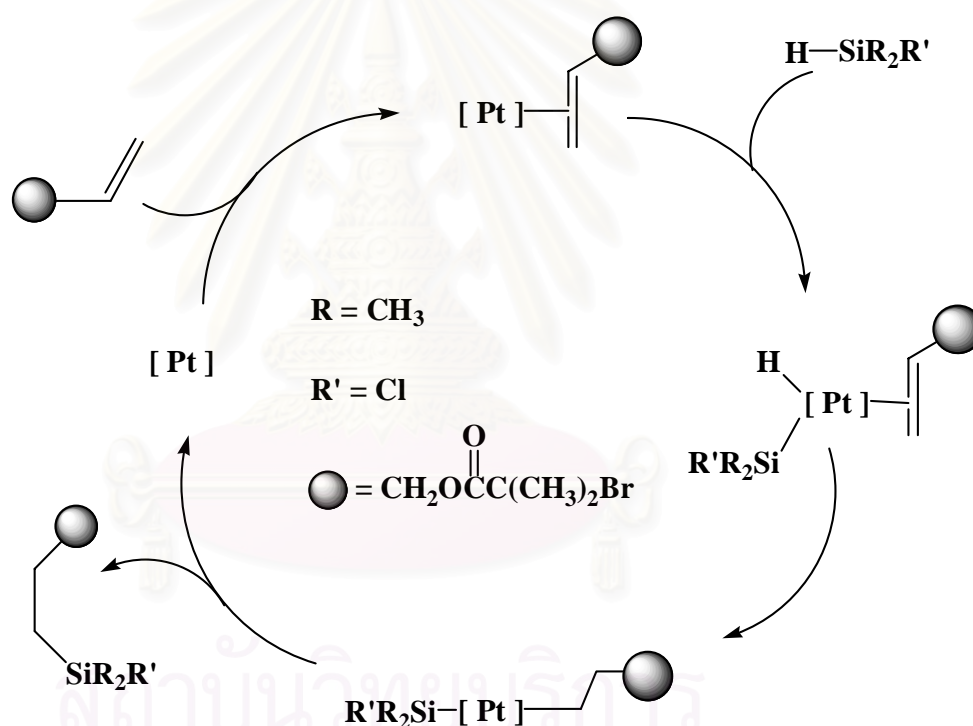
#### 4.1.2 Synthesis of 2-bromo-2-methylpropionic acid 3-(ethoxydimethyl silanyl)propyl ester (2)



Hydrosilylation of ethoxydimethylsilane with 2-bromo-2-methylpropionic acid allyl ester (1) was carried out in the dark in the presence of chloroplatinic acid,  $\text{H}_2\text{PtCl}_6$  at room temperature for 24h. Scheme 4.1 illustrates hydrosilylation mechanism using chloroplatinic acid as a catalyst. The reaction yielded yellow viscous liquid as a crude product which was sufficiently pure for the next synthesis

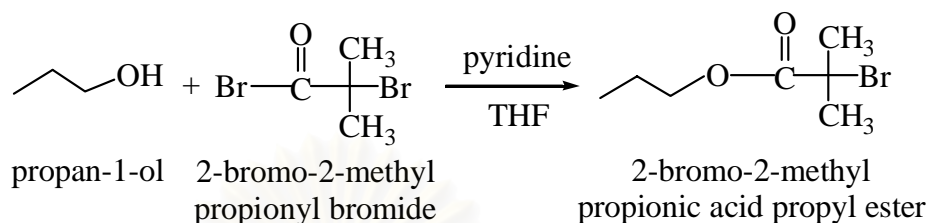


without further purification after the work-up process.  $^1\text{H-NMR}$  spectrum of the product (Figure A.2) shows a singlet signal of methyl protons of  $\text{C}(\text{CH}_3)_2$  adjacent to bromine at 1.88 ppm together with a triplet signal and a multiplet signal of the methylene protons ( $(\text{SiCH}_2\text{CH}_2\text{CH}_2\text{O})$  and  $(\text{SiCH}_2\text{CH}_2\text{CH}_2\text{O})$ ) at 0.93 and 1.66 ppm, respectively. Signals from three vinylic protons ( $\text{CH}_2=\text{CH}$  and  $\text{CH}_2=\text{CH}$ ) previously appeared in 2-bromo-2-methylpropionic acid allyl ester substrate in the range of 4-6 ppm are also absent. The evidence from  $^1\text{H-NMR}$  analysis conclusively suggests that the reaction was successful and gave 2-bromo-2-methylpropionic acid 3-(ethoxy dimethylsilyl)propyl ester as the desired product.



**Scheme 4.1** Mechanism of hydrosilylation using chloroplatinic acid as a catalyst

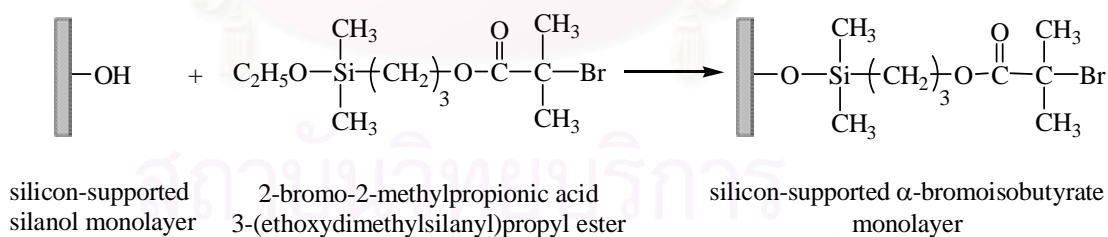
### 4.1.3 Synthesis of 2-bromo-2-methylpropionic acid propyl ester as a “Sacrificial” Initiator



3

Nucleophilic substitution of propan-1-ol with 2-bromo-2-methylpropionyl bromide in tetrahydrofuran gave 2-bromo-2-methylpropionic acid propyl ester (3) as a pale yellow viscous liquid (90 % yield).  $^1\text{H-NMR}$  spectrum of the product (Figure A.3) shows a singlet signal of the methyl proton from  $\text{C}(\text{CH}_3)_2$  at 1.96 ppm indicating the success of reaction. This product was used as an “added” or “sacrificial” initiator for the polymerization of polymer brushes.

### 4.2 Preparation of Silicon-supported $\alpha$ -Bromoisobutyrate Monolayer



2

4

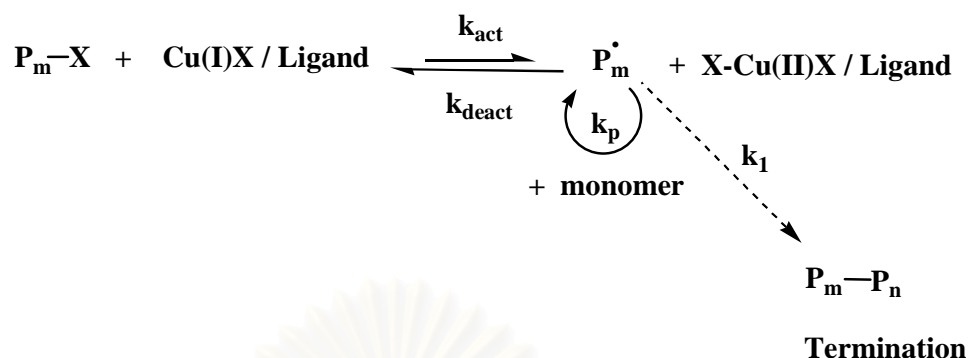
Silicon-supported  $\alpha$ -bromoisobutyrate monolayers were prepared by silanization of silanol groups on the silicon surface by the silane compound having end-functionalized  $\alpha$ -bromoisobutyrate (2). Using the optimized condition previously reported [57],  $\alpha$ -bromoisobutyrate monolayer having maximum graft density was formed on silicon substrates with a thickness of  $9.25 \pm 0.1 \text{ \AA}$  as

measured by ellipsometry. Advancing/receding water contact angle of silicon-supported  $\alpha$ -bromoisobutyrate monolayer was  $72^\circ/63^\circ$  which was significantly different from the value of  $29^\circ/15^\circ$  for the cleaned and dried hydrophilic silicon substrates.

### 4.3 Preparation of Homopolymer Brushes

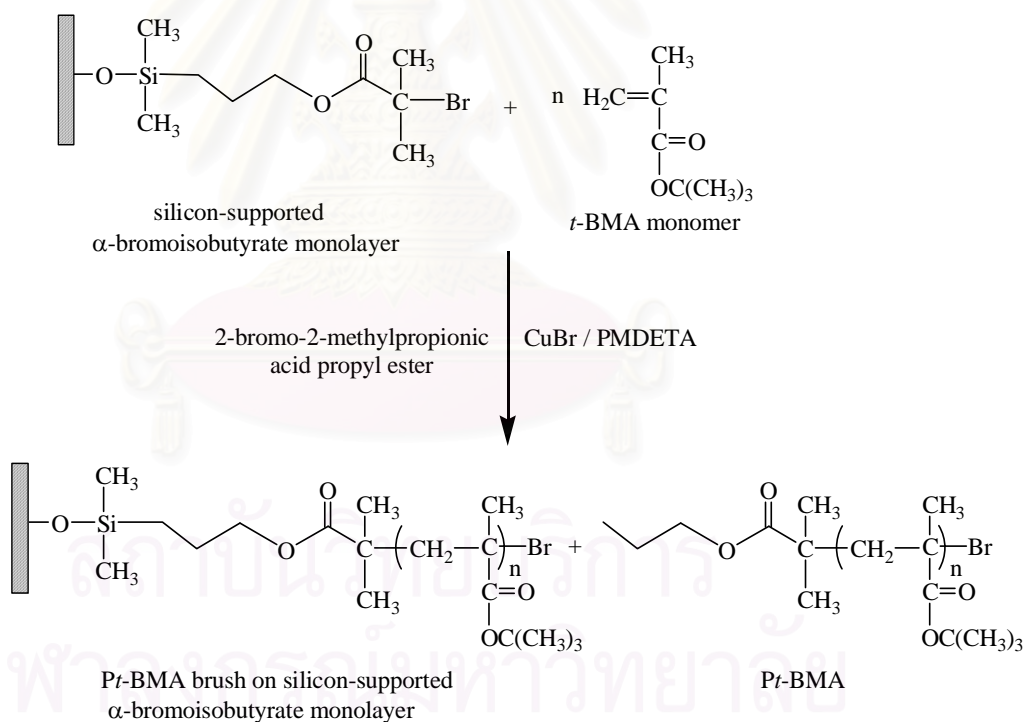
This part of research focuses on surface-initiated polymerization of *tert*-butyl methacrylate (*t*-BMA) and 2,2,2-trifluoroethyl methacrylate (TFMA) in the presence of a “sacrificial” or “added” initiator to prepare homopolymer brushes of poly(*tert*-butyl methacrylate) (*Pt*-BMA) and poly(2,2,2-trifluoroethyl methacrylate) (PTFMA). The subsequent hydrolysis of *Pt*-BMA yielded homopolymer brushes of poly(methacrylic acid) (PMAA).

The word “sacrificial” initiator or “added” initiator represents free initiator which is not attached to the surface. It was intentionally added in the solution during surface-initiated polymerization due to 2 major reasons. The first reason is to use this free initiator (2-bromo-2-methylpropionic acid propyl ester, in this case) to simultaneously initiate polymerization in the solution. Previous work reported by Fukuda has demonstrated that the molecular weight of this “free” polymer formed in the solution closely resembled that of the grafted polymer brushes cleaved from the surface. Thus, it can be used to monitor the surface-initiated polymerization process [50, 55]. The free initiator plays a role not only as an indicator of the polymerization but also as a controller for the ATRP on the surface. The second reason has a lot to do with the activation/deactivation cycles of ATRP process (Scheme 4.2). The concentration of the  $\text{Cu}^{\text{II}}$  complex produced from the reaction at the substrate surface is too low to reversibly deactivate polymer radicals with a sufficiently high rate. The addition of the free initiator creates the necessary concentration of the  $\text{Cu}(\text{II})$  complex, which in turn controls polymerization from the substrate as well as in solution.



Scheme 4.2 Activation/deactivation cycles of ATRP process

#### 4.3.1 Homopolymer Brushes of Poly(*tert*-Butyl Methacrylate) (Pt-BMA)



*Pt*-BMA brushes were grown from the surface bearing  $\alpha$ -bromoisobutyrate monolayer *via* ATRP mechanism in the presence of CuBr/PMDETA at 90°C using anhydrous toluene as a solvent. The CuBr/PMDETA catalyst system was commonly used in the metal-catalyzed living radical polymerization because the catalyst complex is (i) highly active, (ii) easily available, (iii) cost-effective and (iv) can be

easily separated from the polymer [68]. 2-bromo-2-methylpropionic acid propyl ester (3) was also used as an “added” initiator.

Figure 4.1 depicts the development of *Pt*-BMA thickness as a function of time at two targeted degrees of polymerization (DP), 100 and 200. The mole ratio of added initiator:CuBr:PMDETA of 1:1:1 was fixed while the mole ratio of added initiator:*t*-BMA was varied (1:200 and 1:100). The thickness of *Pt*-BMA layer increased with the increase of the targeted DP. For both targeted DPs, the thickness increased linearly with time. This result clearly indicates that both polymerization time and [added initiator]:[*t*-BMA] ratio can be used as tools for controlling the growth of polymer brushes. The linear increase of thickness as a function of polymerization time evidently suggests that the polymerization is living in character.

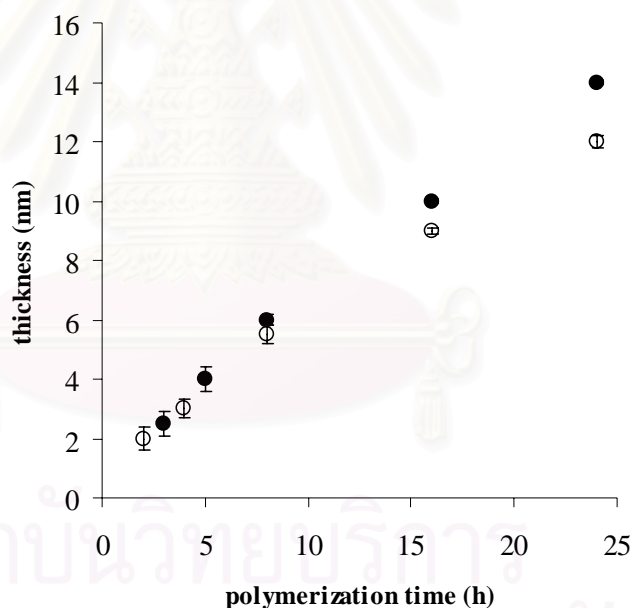


**Figure 4.1** Ellipsometric thickness of *Pt*-BMA brushes as a function of polymerization time for targeted DP = 200 (●) and 100 (○).

The growth of *Pt*-BMA brushes can also be monitored by water contact angle analysis. Figure 4.2 shows advancing ( $\theta_A$ ) and receding ( $\theta_R$ ) water contact angles of the silicon-supported *Pt*-BMA brushes as a function of polymerization time for two target DPs (200 and 100). Both  $\theta_A$  and  $\theta_R$  increased with time from 72°/63° of the

silicon-supported  $\alpha$ -bromoisobutyrate monolayer to  $90^\circ/70^\circ$  of the hydrophobic silicon-supported *Pt*-BMA brushes after 5 h of reaction. The fact that the contact angle hysteresis ( $\theta_A - \theta_R$ ) remaining relatively constant  $\sim 20^\circ$  regardless of the thickness also implies that the surface bearing *Pt*-BMA brushes is quite homogeneous and smooth.

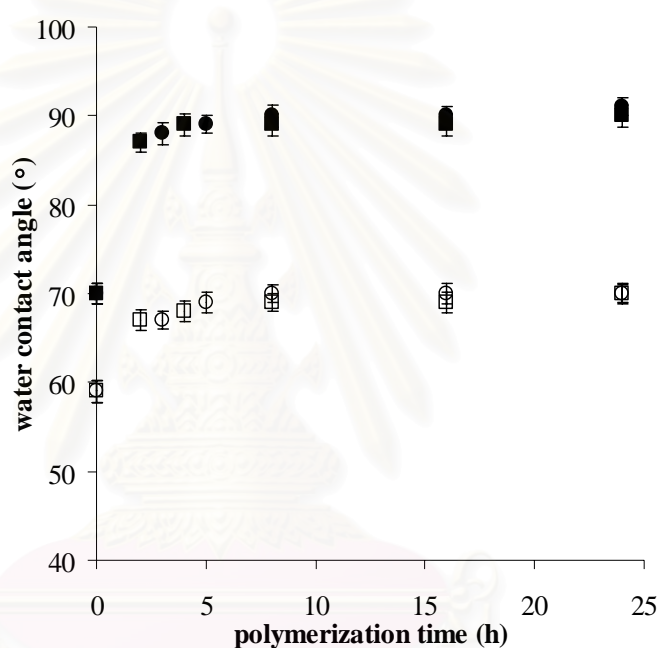


**Figure 4.2** Water contact angle of *Pt*-BMA brushes as a function of polymerization time for targeted DP = 200:  $\theta_A$ (●),  $\theta_R$ (○) and 100:  $\theta_A$ (■),  $\theta_R$ (□).

The free *Pt*-BMA generated from the “added” initiator in solution were subjected to  $^1\text{H-NMR}$  and GPC analyses.  $^1\text{H-NMR}$  spectra of *t*-BMA and *Pt*-BMA are shown in Figure 4.3. Signals of vinylic protons from *t*-BMA at 5.5 and 6.0 ppm obviously disappeared while methylene protons ( $\text{CH}_2$ ) of *Pt*-BMA appeared at 1.1 and 1.2 ppm indicating the success of the polymerization.

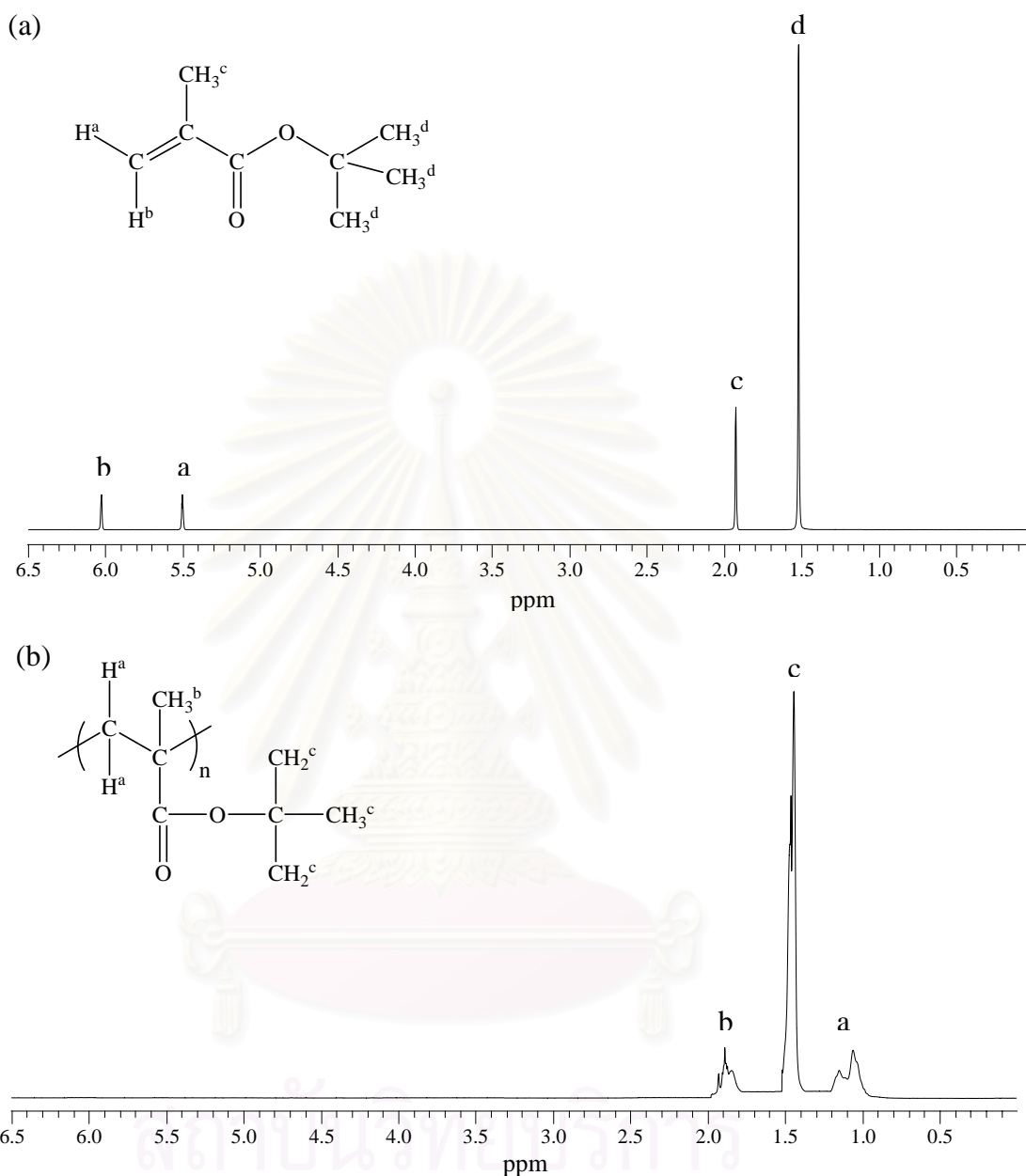


**Figure 4.3**  $^1\text{H-NMR}$  spectra of (a) *t*-BMA and (b) *Pt*-BMA in solution.

Figure 4.4 illustrates the change in the molecular weight ( $\overline{M}_n$ ) and molecular weight distribution ( $\overline{M}_w/\overline{M}_n$ ) of the free *Pt*-BMA as a function of polymerization time for both target DPs (200 and 100). The molecular weight increased linearly with increasing polymerization time. The highest molecular weight obtained was in accord with the targeted molecular weight. The molecular weight distribution being in the range of 1.2-1.6 is reasonably acceptable for living polymerization.

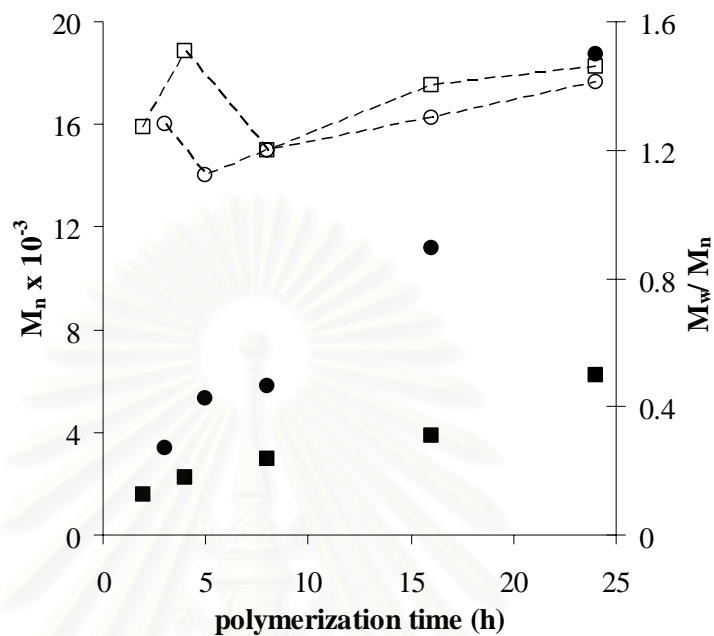
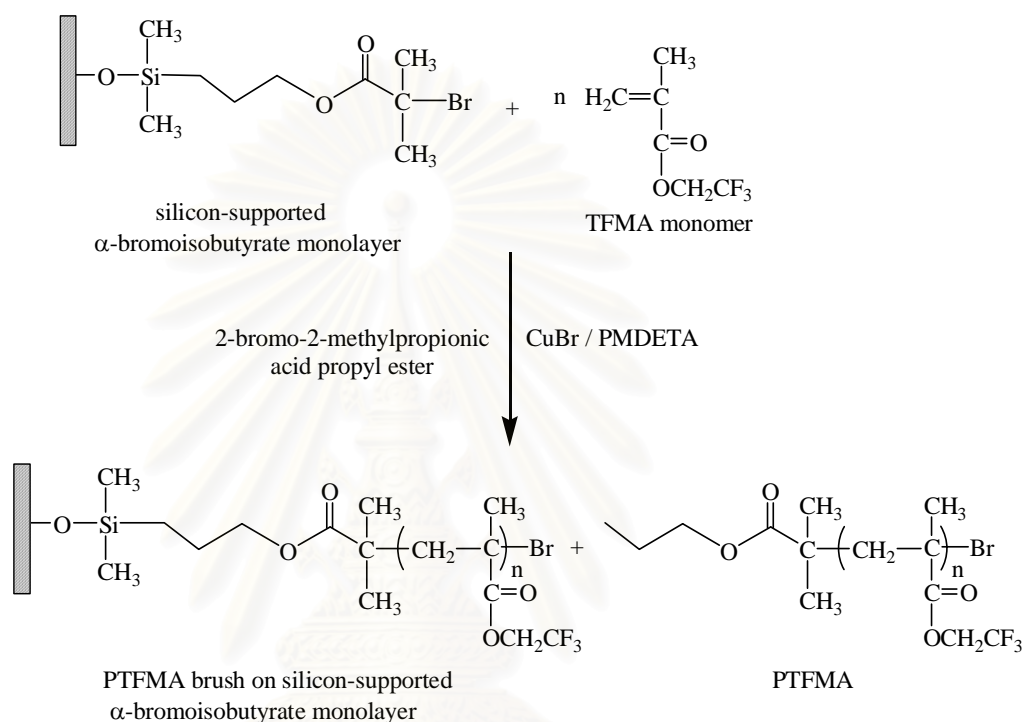


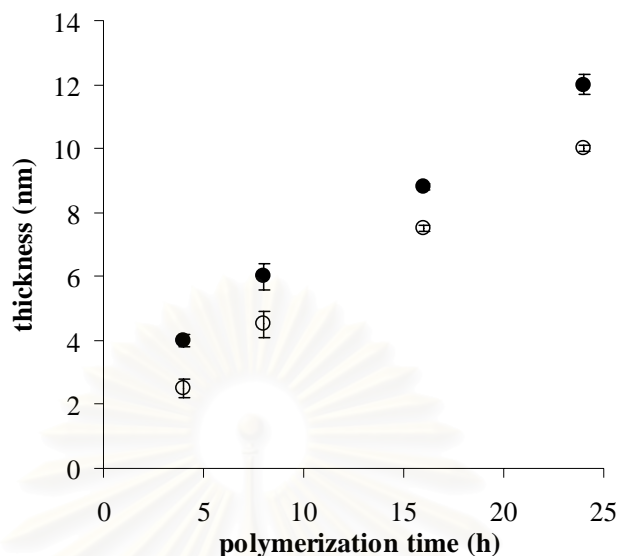
**Figure 4.4** Molecular weight ( $\bar{M}_n$ ) of free Pt-BMA for targeted DP = 200 (●) and 100 (■) and molecular weight distribution ( $\bar{M}_w/\bar{M}_n$ ) for targeted DP = 200 (○) and 100 (□) as a function of polymerization time.



### 4.3.2 Homopolymer Brushes of Poly(2,2,2-Trifluoroethyl Methacrylate) (PTFMA)



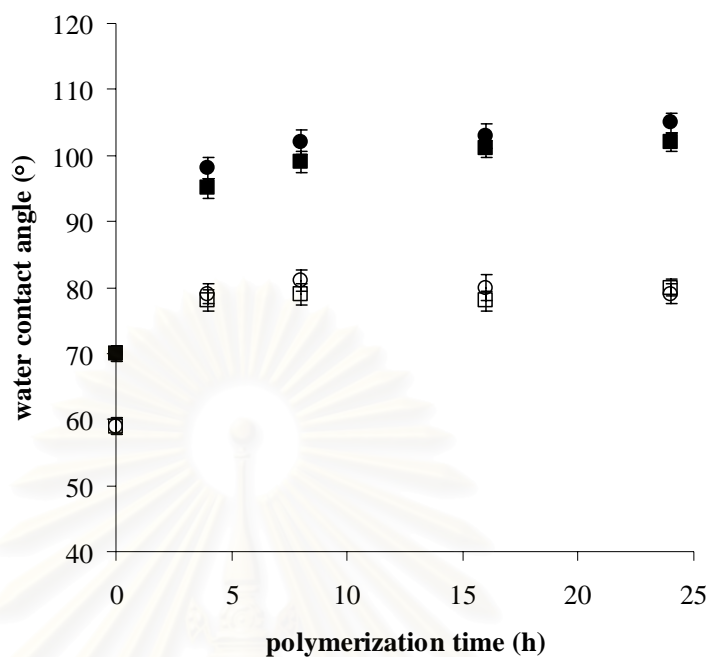
PTFMA brushes were grown from the surface bearing  $\alpha$ -bromoisobutyrate monolayer *via* ATRP mechanism in the presence of  $\text{CuBr/PMDETA}$  at  $90^\circ\text{C}$  using  $\alpha,\alpha,\alpha$ -trifluorotoluene as a solvent. Figure 4.5 shows the development of PTFMA thickness as a function of time at two targeted DPs, 100 and 200. The mole ratio of added initiator: $\text{CuBr:PMDETA}$  of 1:1:1 was fixed while the mole ratio of added initiator:TFMA was varied (1:200 and 1:100). The thickness of PTFMA layer increased with the increase of the targeted DP. For both targeted DPs, the thickness increased linearly as a function of polymerization time suggesting that the polymerization is living.



**Figure 4.5** Ellipsometric thickness of PTFMA brushes as a function of polymerization time for targeted DP = 200 (●) and 100 (○).

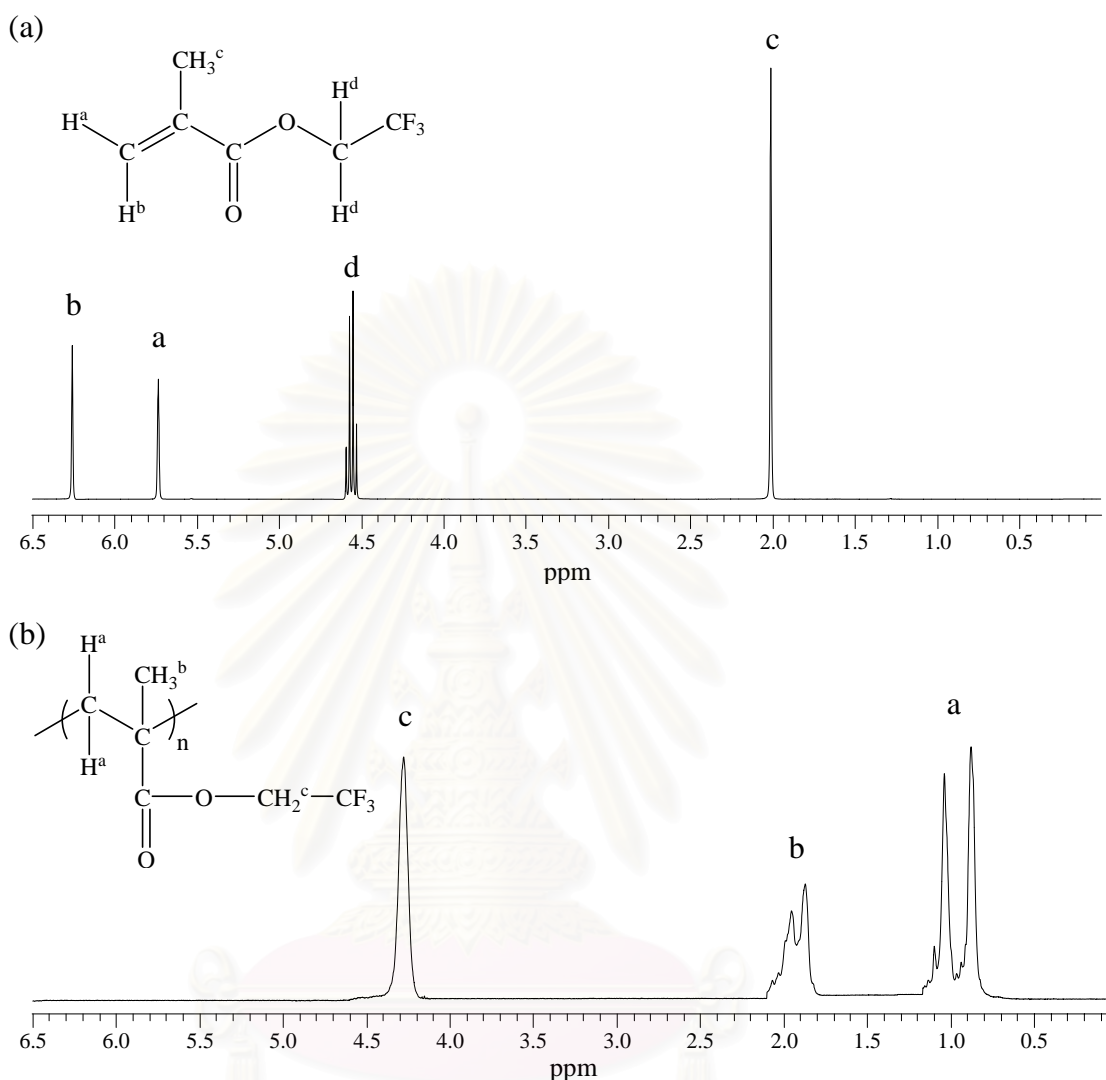
The growth of PTFMA brushes can also be monitored by water contact angle analysis. Figure 4.6 demonstrates  $\theta_A$  and  $\theta_R$  of the silicon-supported PTFMA brushes as a function of polymerization time for two target DPs (200 and 100). Both  $\theta_A$  and  $\theta_R$  increased with time from  $72^\circ/63^\circ$  of the silicon-supported  $\alpha$ -bromoisobutyrate monolayer to  $102^\circ/79^\circ$  of the hydrophobic silicon-supported PTFMA brushes after 8 h of reaction. Once again, The fact that the contact angle hysteresis ( $\theta_A - \theta_R$ ) remaining relatively constant  $\sim 20^\circ$  regardless of the thickness suggests that the surface bearing PTFMA brushes is quite homogeneous and smooth.

จุฬาลงกรณ์มหาวิทยาลัย



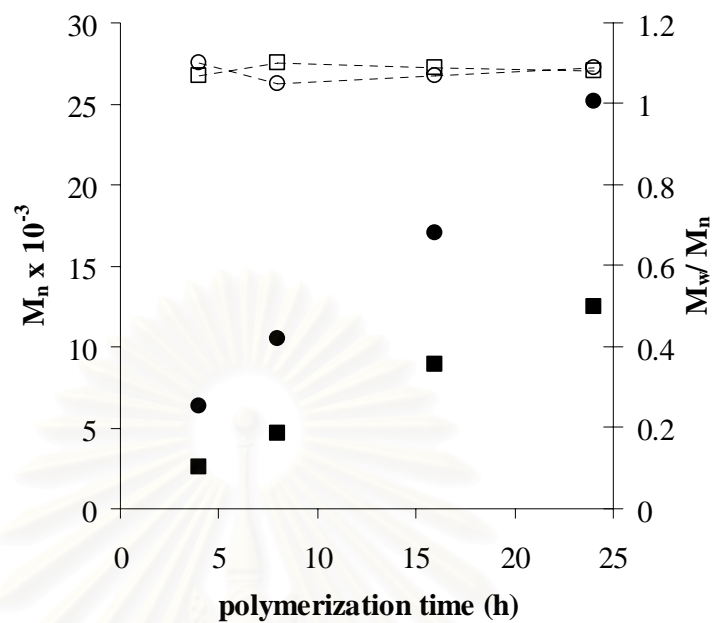
**Figure 4.6** Water contact angle of PTFMA brushes as a function of polymerization time for targeted DP = 200:  $\theta_A$  (●),  $\theta_R$  (○) and 100:  $\theta_A$  (■),  $\theta_R$  (□).

The free PTFMA generated from the “added” initiator in solution were subjected to  $^1\text{H-NMR}$  and GPC analyses.  $^1\text{H-NMR}$  spectra of TFMA and PTFMA are shown in Figure 4.7. Signals of vinylic protons from TFMA at 5.7 and 6.2 ppm obviously disappeared while methylene protons ( $\text{CH}_2$ ) of *Pt*-BMA appeared at 0.9 and 1.1 ppm indicating the success of the polymerization.



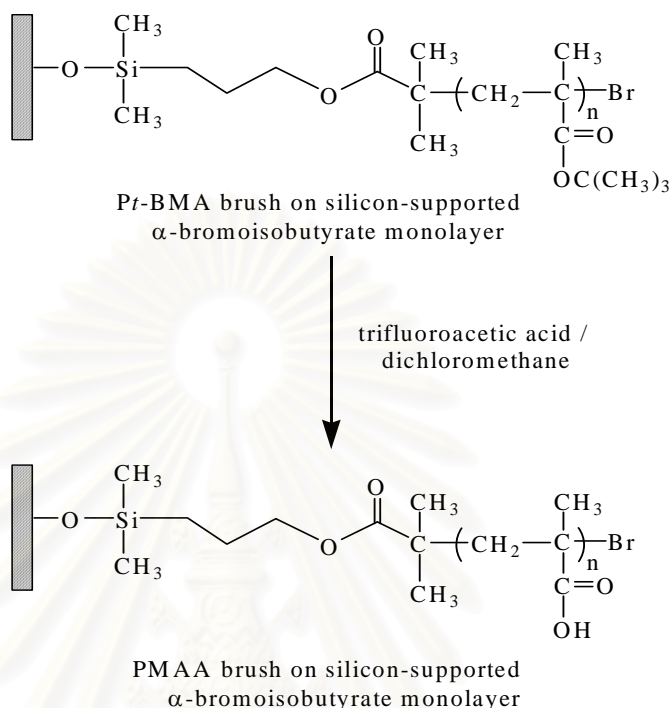
**Figure 4.7**  $^1\text{H}$ -NMR spectra of (a) TFMA and (b) PTFMA in solution.

Figure 4.8 illustrates the change in the molecular weight ( $\overline{M}_n$ ) and molecular weight distribution ( $\overline{M}_w/\overline{M}_n$ ) of free PTFMA as a function of polymerization time for both target DPs (200 and 100). The molecular weight increased linearly with increasing polymerization time. The highest molecular weight obtained was in accord with the targeted molecular weight. The molecular weight distribution being close to 1.0 suggested that polymerization mechanism is living.



**Figure 4.8** Molecular weight ( $\bar{M}_n$ ) of free PTFMA for targeted DP = 200 (●) and 100 (■) and molecular weight distribution ( $\bar{M}_w/\bar{M}_n$ ) for targeted DP = 200 (○) and 100 (□) as a function of polymerization time.

### 4.3.3 Homopolymer Brushes of Poly(Methacrylic Acid) (PMAA)



The ultimate goal of this research is, in fact, to prepare 2 series of diblock copolymer brushes. One is PTFMA-*b*-Pt-BMA which can be prepared by sequential polymerization of TFMA and *t*-BMA. The other is PTFMA-*b*-PMAA can be prepared by acid hydrolysis of PTFMA-*b*-Pt-BMA. It is thus important to seek for a suitable condition for hydrolysis which can effectively convert Pt-BMA to PMAA. For this reason, two experimental variables affecting hydrolysis were investigated: acid concentration and hydrolysis time. The silicon-supported Pt-BMA brushes and their corresponding free Pt-BMA obtained in solution were used as substrates. Trifluoroacetic acid was selected because it is known to selectively remove *t*-butyl groups without disturbing the ester linkage in the polymer chain. [69] Hydrolysis was performed at ambient temperature using dichloromethane as a solvent. The extent of hydrolysis of Pt-BMA brushes attached on the surface was monitored by water contact angle measurements. Figure 4.9 shows  $\theta_A$  and  $\theta_R$  of the silicon-supported Pt-BMA brushes after hydrolysis by a varied concentration of TFA solution for 4h. The contact angles dropped rapidly as a function of TFA

concentration up to 3M and decreased slightly further until they reached a minimum values of  $62^\circ/54^\circ$  when 5M TFA was used.

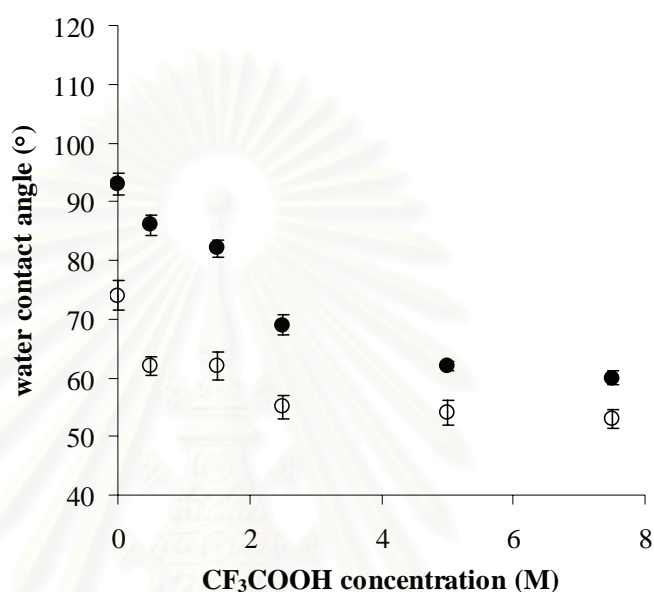


**Figure 4.9** Water contact angle of the silicon-supported *Pt*-BMA brushes after hydrolysis by a varied concentration of TFA in dichloromethane for 4h:  $\theta_A$  (●),  $\theta_R$  (○).

Using 5M TFA, effect of hydrolysis time was studied. According to Figure 4.10, the long exposure of the silicon-supported *Pt*-BMA to TFA solution seems to cause an adverse effect to the hydrolysis. The  $\theta_A$  tended to rise back up to  $62^\circ/53^\circ$  after 4h treatment. This value closely resembles the water contact angle of the silicon-supported  $\alpha$ -bromoisobutyrate monolayer which was used as the initiator. It is highly possible that TFA is capable of removing the *Pt*-BMA from the silicon surface upon the extensive hydrolysis. To verify this speculation, more evidences from other techniques are necessary.

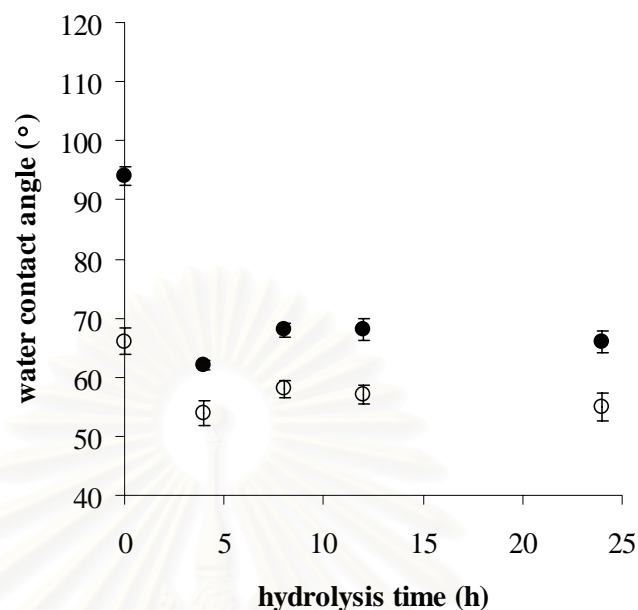


**Figure 4.10** Water contact angle of the silicon-supported *Pt*-BMA brushes as a function of hydrolysis time (h) using 5M TFA in dichloromethane:  $\theta_A$  (●),  $\theta_R$  (○).

Thus, the optimal condition for hydrolysis was 5M TFA in dichloromethane for 4h. The hydrolysis of the *Pt*-BMA in solution can also be confirmed by  $^1\text{H-NMR}$  analysis. Figure 4.11 demonstrates  $^1\text{H-NMR}$  spectra of *Pt*-BMA and PMAA obtained after hydrolysis. The disappearance of the  $-\text{C}(\text{CH}_3)_3$  peak at 1.50 ppm in the  $^1\text{H-NMR}$  spectrum of the PMAA strongly suggested that the *tert*-butyl groups of *Pt*-BMA were removed as a result of acid hydrolysis.



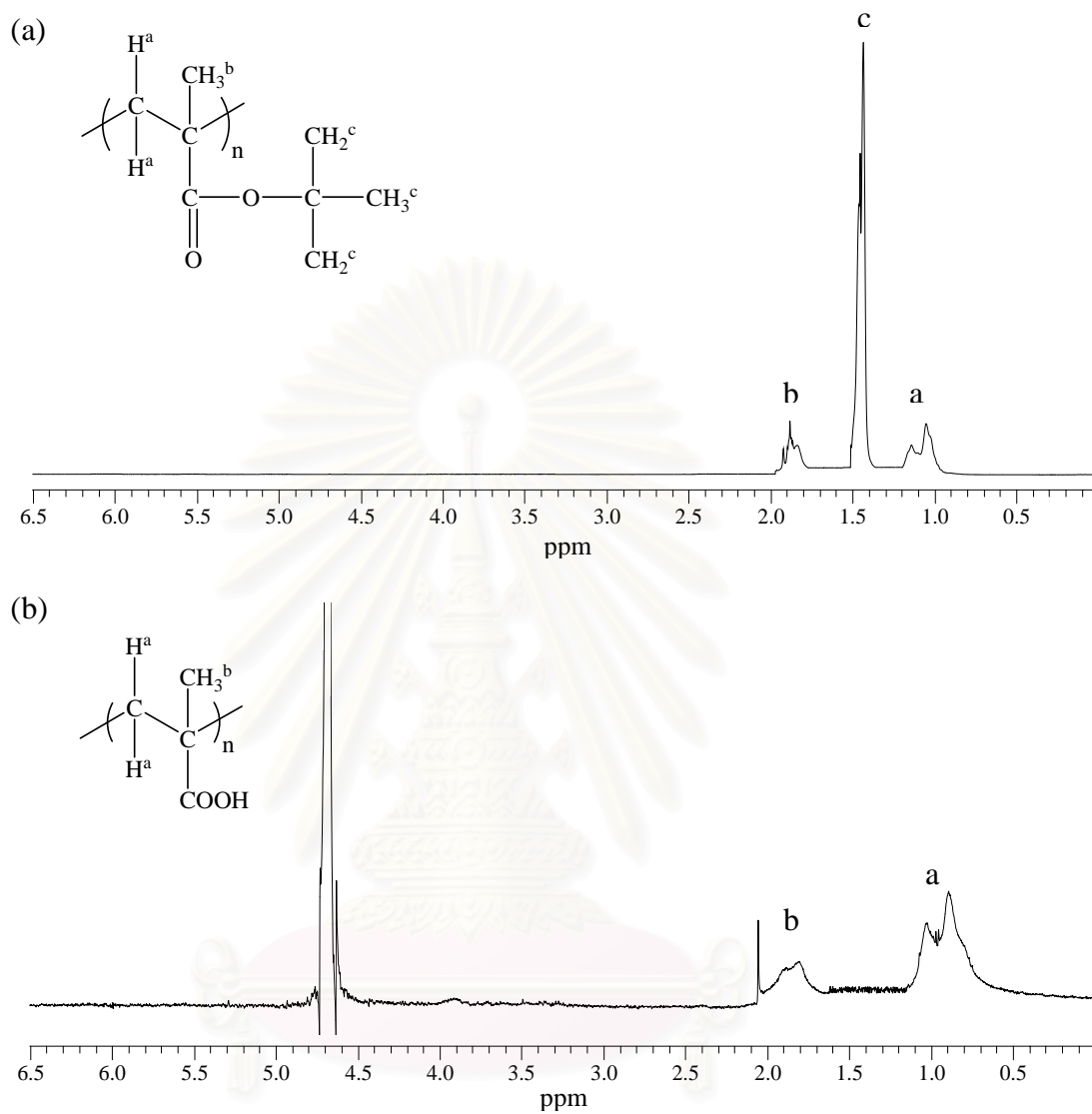
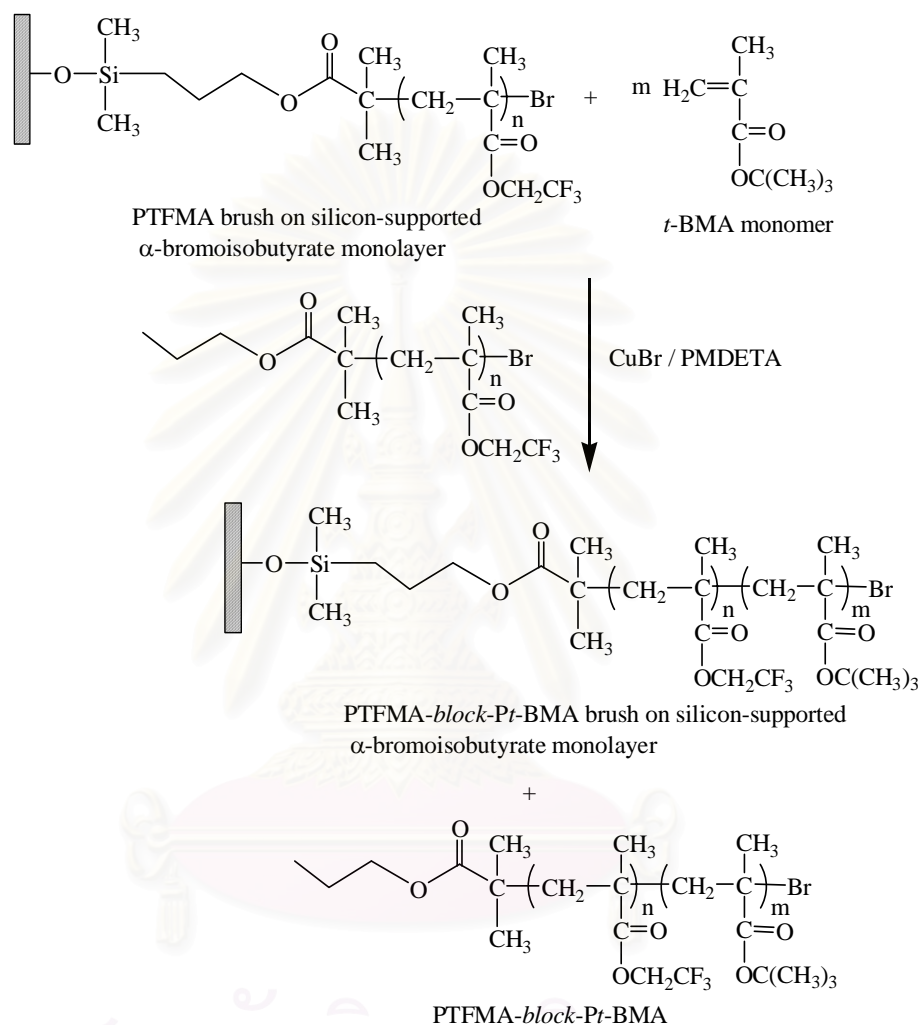


**Figure 4.11**  $^1\text{H-NMR}$  spectra of (a) *Pt*-BMA and (b) PMAA in solution.

สถาบันวิทยบริการ  
จุฬาลงกรณ์มหาวิทยาลัย

## 4.4 Preparation of Diblock Copolymer Brushes

### 4.4.1 Diblock Copolymer Brushes of PTFMA-*b*-Pt-BMA



The diblock copolymer brushes of PTFMA-*b*-Pt-BMA were generated by the surface-initiated polymerization of *t*-BMA from the silicon-supported PTFMA (the inner block) *via* sequential ATRP, using  $\alpha,\alpha,\alpha$ -trifluorotoluene as a solvent at 90°C. CuBr/PMDETA was also used as a catalyst system. The free polymer of PTFMA was used as a macroinitiator. The mole ratio of macroinitiator:CuBr:PMDETA of 1:5:5 was fixed while the mole ratio of macroinitiator:*t*-BMA were varied (1:0.5, 1:1, 1:2 and 1:3). As shown in Figure 4.12, the thickness of PTFMA-*b*-Pt-BMA layer proportionally increased with a mole ratio between the added *t*-BMA to TFMA of PTFMA (*t*-BMA:TFMA).

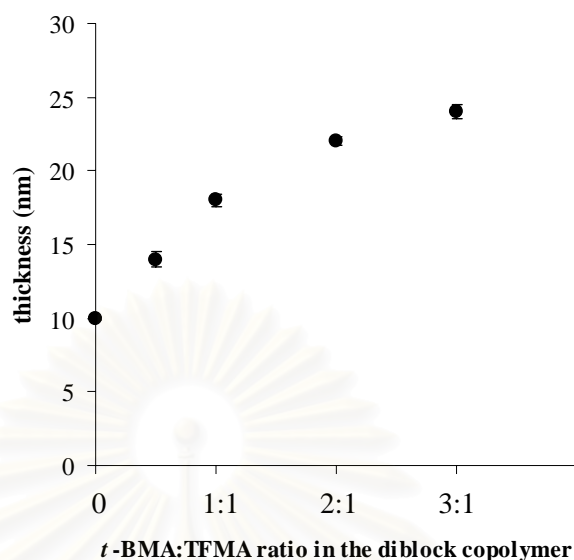


**Figure 4.12** Ellipsometric thickness of PTFMA-*b*-*Pt*-BMA brushes as a function of *t*-BMA:TFMA ratio.

The change in water and hexadecane contact angle also reflected the growth of *Pt*-BMA (outer block) from PTFMA (inner block). Figure 4.13 shows  $\theta_A$  and  $\theta_R$  of the silicon-supported PTFMA-*b*-*Pt*-BMA brushes as a function of *t*-BMA:TFMA mole ratio. Both  $\theta_A$  and  $\theta_R$  decreased from  $102^\circ/79^\circ$  of the silicon-supported PTFMA (inner block) to  $90^\circ/70^\circ$ . This evidence strongly suggested that the wettability of the silicon-supported PTFMA-*b*-*Pt*-BMA brushes was dominated by the outer block of *Pt*-BMA brushes independent of the *t*-BMA:TFMA. The fact that the contact angle hysteresis ( $\theta_A - \theta_R$ ) remaining relatively constant  $\sim 20^\circ$  also indicates that the surface bearing PTFMA-*b*-*Pt*-BMA brushes is quite homogeneous and smooth.

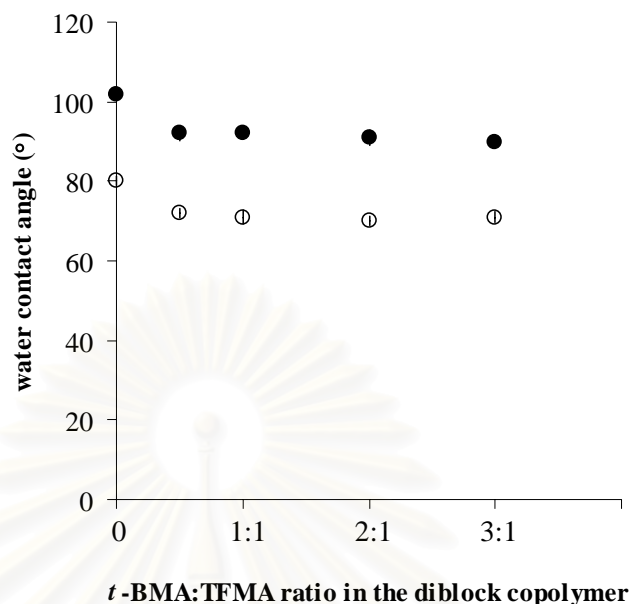


**Figure 4.13** Water contact angle of PTFMA-*b*-*Pt*-BMA brushes as a function of *t*-BMA:TFMA ratio:  $\theta_A$  (●),  $\theta_R$  (○).

Advancing ( $\theta_A$ ) and receding ( $\theta_R$ ) hexadecane contact angles of the silicon-supported PTFMA-*b*-*Pt*-BMA brushes as a function of *t*-BMA:TFMA demonstrated in Figure 4.14 also pointed in the same direction. After the introduction of the outer block of *Pt*-BMA, both  $\theta_A$  and  $\theta_R$  decreased from  $76^\circ/52^\circ$  of the oleophobic silicon-supported PTFMA to  $30^\circ/19^\circ$  of the oleophilic silicon-supported PTFMA-*b*-*Pt*-BMA brushes. These values are exactly the same as that was measured on the silicon-supported *Pt*-BMA brushes. Once again, it can be assumed that the wettability of the diblock copolymer brushes was governed by the outer block which is *Pt*-BMA in this particular case.

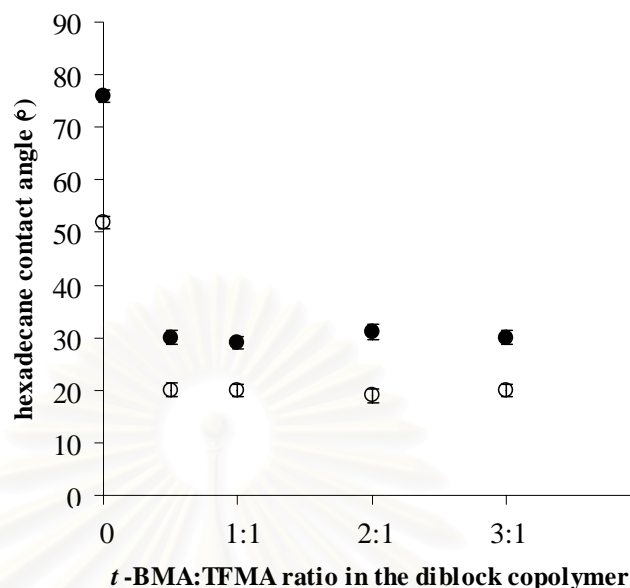


**Figure 4.14** Hexadecane contact angle of PTFMA-*b*-*Pt*-BMA brushes as a function of *t*-BMA:TFMA ratio:  $\theta_A$  (●),  $\theta_R$  (○).

The free PTFMA-*b*-*Pt*-BMA generated in solution by ATRP of *t*-BMA from the macroinitiator, PTFMA was characterized by  $^1\text{H-NMR}$  analysis. Figure 4.15 displayed a  $^1\text{H-NMR}$  spectrum of PTFMA-*b*-*Pt*-BMA (*t*-BMA:TFMA = 1:1) in comparison with those of PTFMA and *Pt*-BMA. The signal at 4.29 ppm due to 2 protons of  $-\text{CH}_2\text{CF}_3$  from the PTFMA block was observed along with the signals of 9 protons of  $-\text{C}(\text{CH}_3)_3$  from the *Pt*-BMA block at 1.50 ppm in the  $^1\text{H-NMR}$  spectrum of PTFMA-*b*-*Pt*-BMA. The data displayed in Table 4.1 strongly suggested that the copolymer composition in the diblock copolymer calculated from the relative peak integration of the  $^1\text{H-NMR}$  signal at 1.50 ppm ( $-\text{C}(\text{CH}_3)_3$  from the *Pt*-BMA block) and the one at 4.29 ppm ( $-\text{CH}_2\text{CF}_3$  from the PTFMA block) are in excellent agreement with the designated ratio of *t*-BMA:TFMA.

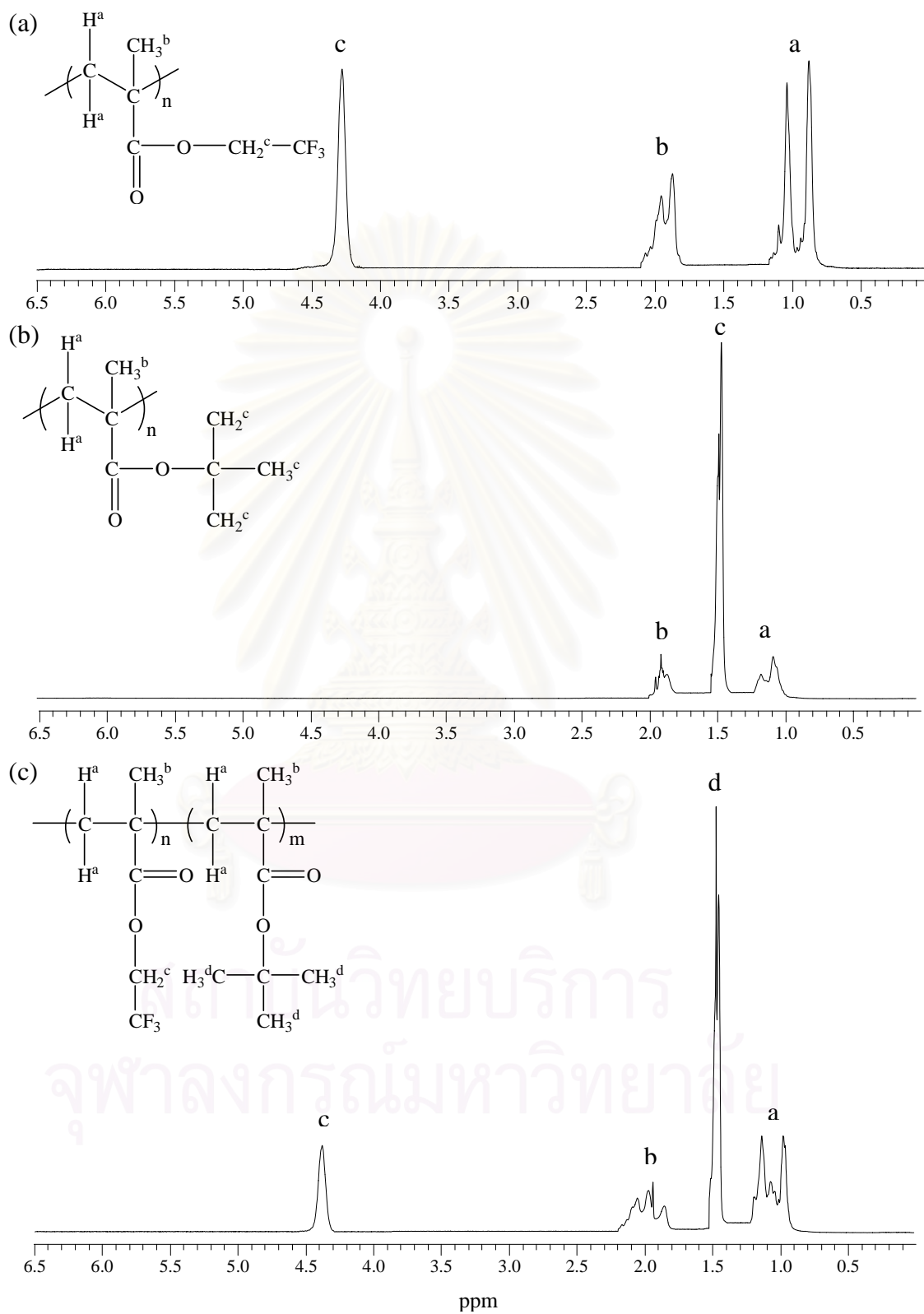
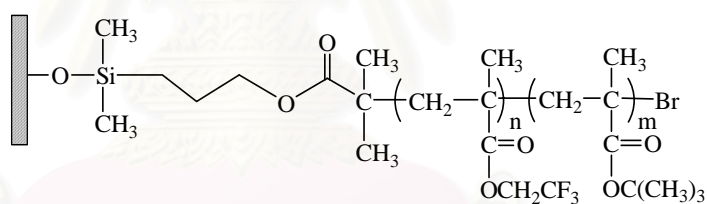


**Figure 4.15**  $^1\text{H}$ -NMR spectra of (a) PTFMA, (b) Pt-BMA, and (c) PTFMA-*b*-Pt-BMA (*t*-BMA:TFMA = 1:1) in solution.

**Table 4.1** Information from  $^1\text{H-NMR}$  spectrum of PTFMA-*b*-Pt-BMA

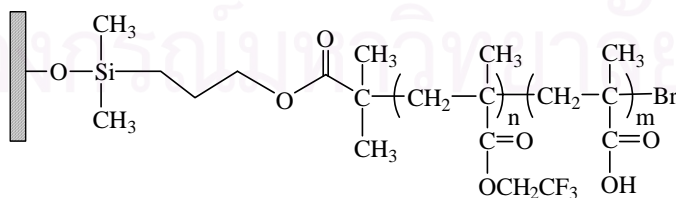
<i>t</i> -BMA:TFMA	Integration		Relative amount of unit		<i>t</i> -BMA:TFMA (from $^1\text{H-NMR}$ )
	$-\text{CH}_2\text{CF}_3$	$-\text{C}(\text{CH}_3)_3$	$-\text{CH}_2\text{CF}_3$	$-\text{C}(\text{CH}_3)_3$	
0.5:1	1.0	2.2	0.5	0.24	0.48:1
1:1	1.0	3.7	0.5	0.41	0.82:1
2:1	1.0	7.1	0.5	0.79	1.58:1
3:1	1.0	10.5	0.5	1.17	2.34:1

#### 4.4.2 Diblock Copolymer Brushes of PTFMA-*b*-PMAA



PTFMA-*block*-Pt-BMA brush on silicon-supported  
 $\alpha$ -bromoisobutyrate monolayer

trifluoroacetic acid/  
dichloromethane



PTFMA-*block*-PMAA brush on silicon-supported  
 $\alpha$ -bromoisobutyrate monolayer

Using the optimized condition for hydrolysis previously identified (5M TFA in dichloromethane, 4h, ambient temperature), the silicon-supported of PTFMA-*b*-PMAA brushes was converted from the silicon-supported PTFMA-*b*-Pt-BMA

brushes having *t*-BMA:TFMA =1:1. The change in water contact angles ( $\theta_A/\theta_R$ ) from  $90^\circ/70^\circ$  of the hydrophobic PtBMA to  $62^\circ/54^\circ$ , the values exactly matched the water contact angles of the silicon-supported PMAA brushes (See section 4.3.3), implied that the removal of the *t*-butyl groups from the outer block of Pt-BMA brushes by hydrolysis was complete and afforded PTFMA-*b*-PMAA brushes.

The hydrolysis of PTFMA-*b*-Pt-BMA was confirmed by  $^1\text{H-NMR}$  analysis. The disappearance of the signals of 9 protons from  $-\text{C}(\text{CH}_3)_3$  at 1.50 ppm of the Pt-BMA block and the emerging of the characteristic signals of PMAA (See section 4.3.3 for comparison) in  $^1\text{H-NMR}$  spectrum of the PTFMA-*b*-PMAA brushes (Figure 4.16) indicated that the *tert*-butyl groups of Pt-BMA were completely removed and the Pt-BMA block was transformed to the PMAA block. It should be underlined that the characteristic signals from PTFMA remained unaffected after hydrolysis.



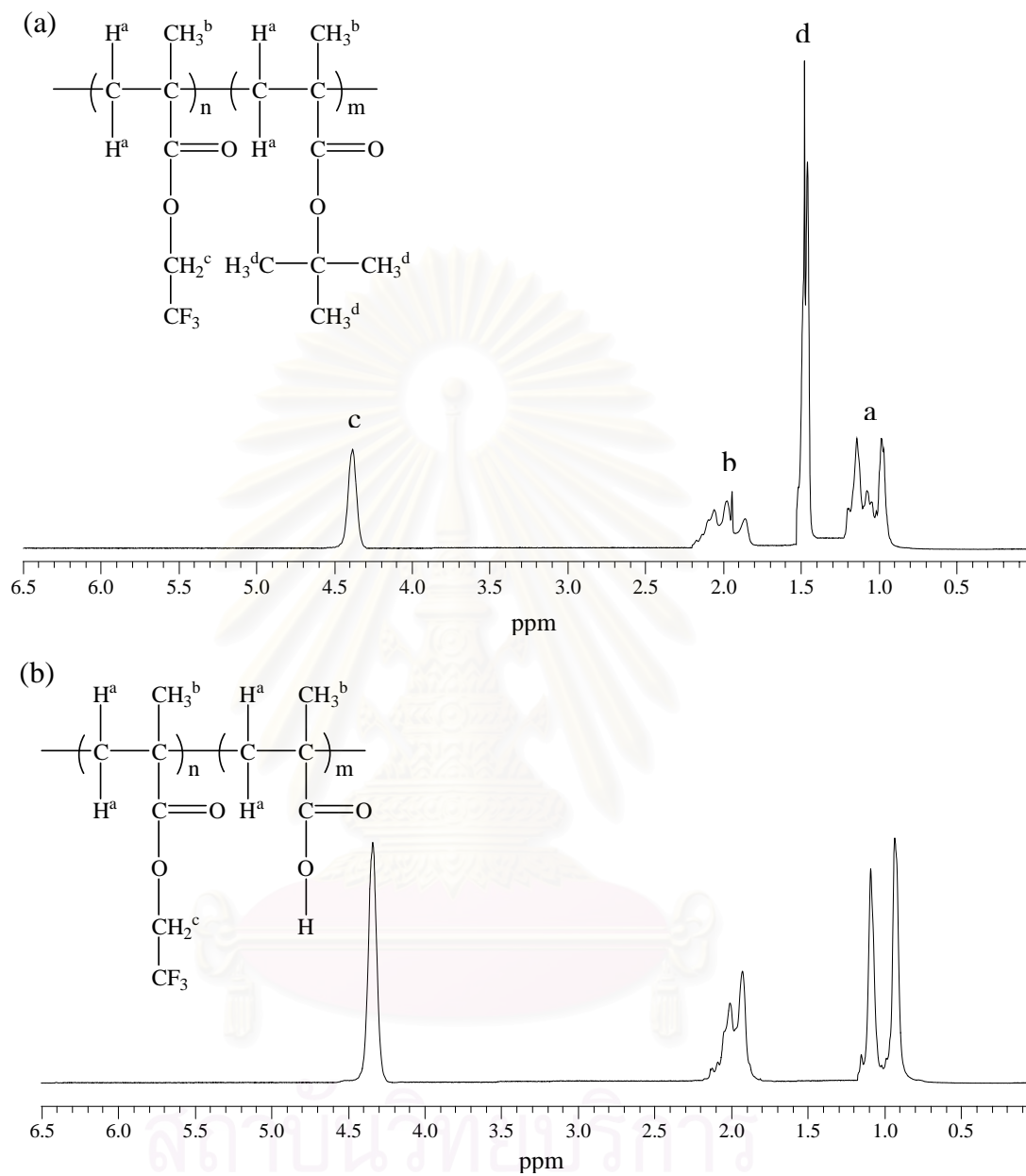


**Figure 4.16**  $^1\text{H-NMR}$  spectra of (a) PTFMA-*b*-Pt-BMA and (b) PTFMA-*b*-PMAA in solution.

#### 4.5 Surface Wettability of Diblock Copolymer Brushes in Response to Solvent Treatment

This part of research focuses on the surface properties of the diblock copolymer brushes upon exposure to  $\alpha,\alpha,\alpha$ -trifluorotoluene which is a good solvent for PTFMA, the inner block. The silicon-supported PTFMA-*b*-Pt-BMA brushes having *t*-BMA:TFMA = 1:1 was chosen as a model for studying effects of the treatment time on the surface wettability. The response can be monitored by water and hexadecane contact angle measurement as depicted in Figures 4.17 and 4.18. The switching of water and hexadecane contact angles indicated that the surface rearrangement has occurred in response to solvent treatment after 30 min. The contact angles have changed from 90°/70° (water) and 30°/20° (hexadecane) of the outer Pt-BMA block to 102°/79° (water) and 76°/52° (hexadecane) of the inner PTFMA block, respectively after the treatment.

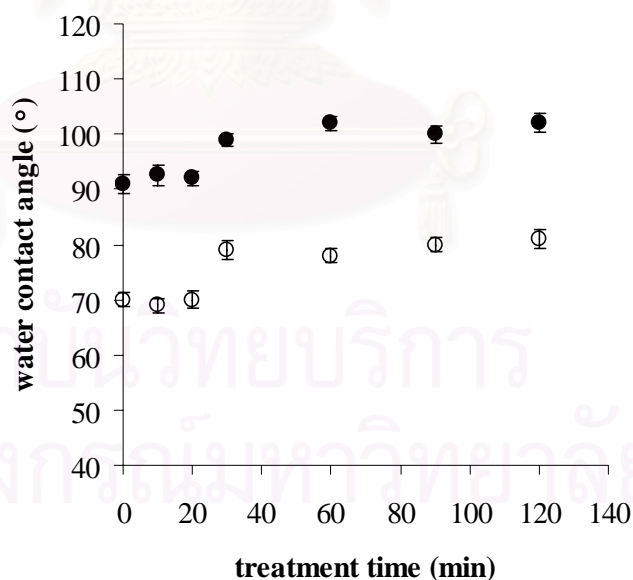


**Figure 4.17** Water contact angle of the silicon-supported PTFMA-*b*-Pt-BMA brushes (*t*-BMA:TFMA = 1:1) before and after treatment with  $\alpha,\alpha,\alpha$ -trifluorotoluene as a function of treatment time (min):  $\theta_A$  (●),  $\theta_R$  (○).

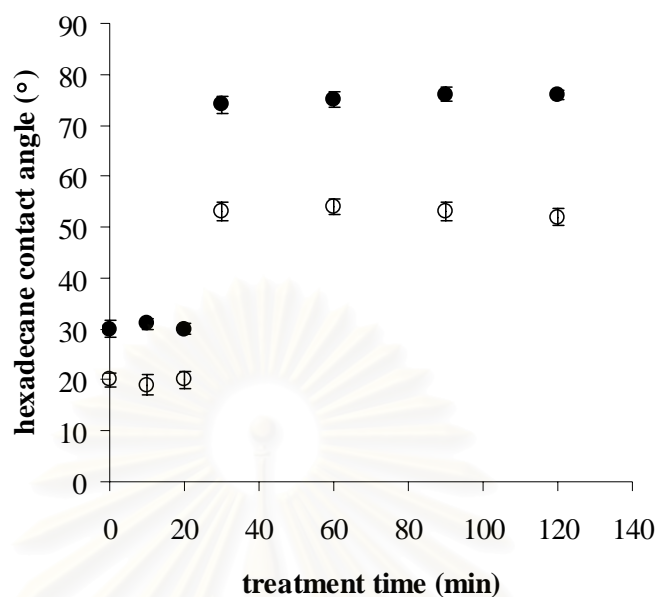


**Figure 4.18** Hexadecane contact angle of the silicon-supported PTFMA-*b*-Pt-BMA brushes (*t*-BMA:TFMA = 1:1) before and after treatment with  $\alpha,\alpha,\alpha$ -trifluorotoluene as a function of treatment time (min):  $\theta_A$  (●),  $\theta_R$  (○).

To investigate the influence of the relative block length of the diblock copolymer, the treatment time of 120 min was employed in order to obtain the optimal surface rearrangement. Figures 4.19 and 4.20 illustrate the changes of water and hexadecane contact angles, respectively. The surface-tethered PTFMA-*b*-Pt-BMA brushes of all compositions can rearrange in response to the solvent treatment except for the one having *t*-BMA:TFMA = 3:1. The outer block was perhaps too long to completely penetrate into the layer of the inner block. As a result, the top surface was mainly occupied by the outer block of Pt-BMA and the surface rearrangement was not detected.

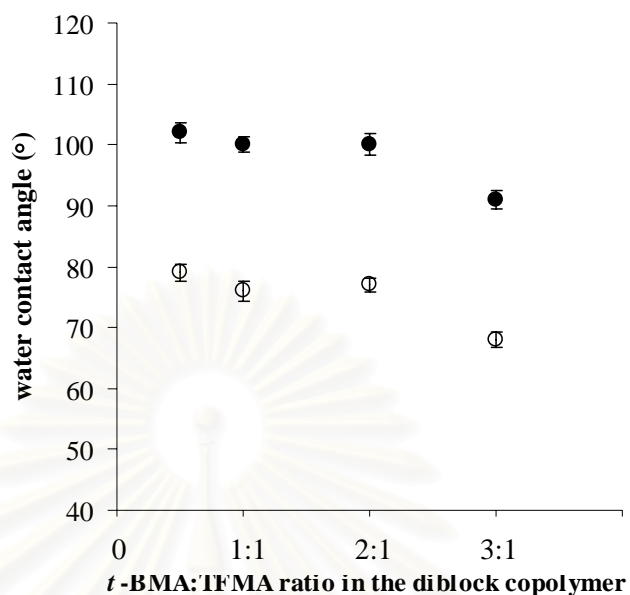


**Figure 4.19** Water contact angle of the silicon-supported PTFMA-*b*-Pt-BMA brushes after treatment with  $\alpha,\alpha,\alpha$ -trifluorotoluene for 120 min as a function of *t*-BMA:TFMA ratio in the diblock copolymer:  $\theta_A$  (●),  $\theta_R$  (○).

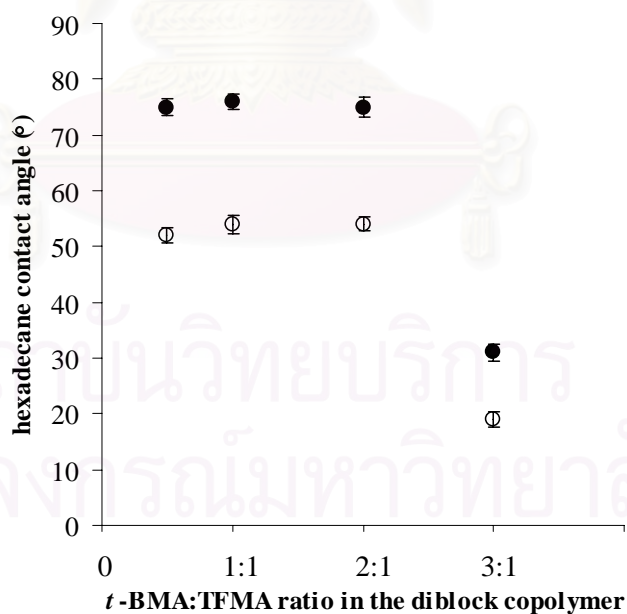


**Figure 4.20** Hexadecane contact angle of the silicon-supported PTFMA-*b*-Pt-BMA brushes after treatment with  $\alpha,\alpha,\alpha$ -trifluorotoluene for 120 min as a function of *t*-BMA:TFMA ratio in the diblock copolymer:  $\theta_A$  (●),  $\theta_R$  (○).

The reversibility of the response of the silicon-supported was also tested. Figures 4.21 and 4.22 show contact angles of the silicon-supported PTFMA-*b*-Pt-BMA brushes after 3 cycles of solvent treatment. One cycle consists of a treatment step followed by a drying step. The contact angles were measured both before and after each step. As soon as the treated solvent,  $\alpha,\alpha,\alpha$ -trifluorotoluene, was removed, the surface rearranged back to its original stage of having the outer block (Pt-BMA) of the copolymer exposed at the polymer/air interface.

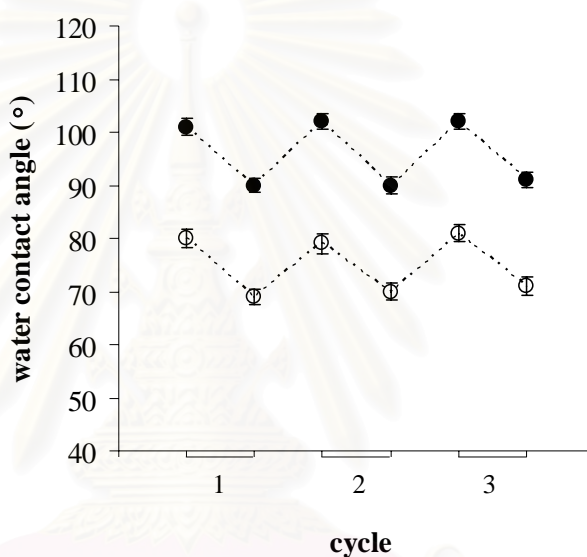


**Figure 4.21** Water contact angle of the silicon-supported PTFMA-*b*-Pt-BMA brushes after 3 cycles of solvent treatment:  $\theta_A$  (●),  $\theta_R$  (○).

สถาบันวิทยบริการ  
จุฬาลงกรณ์มหาวิทยาลัย

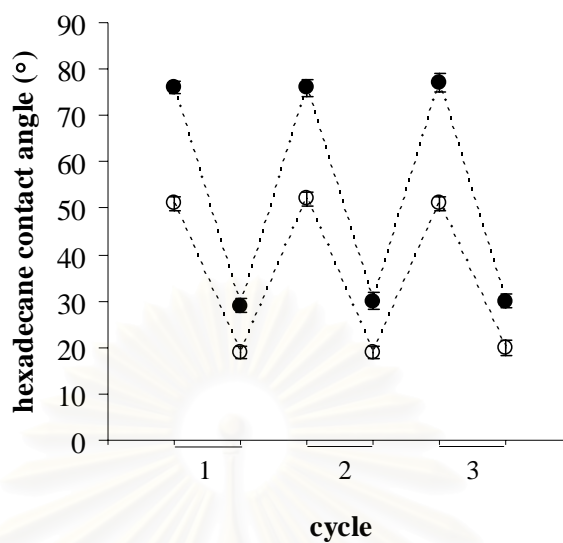


**Figure 4.22** Hexadecane contact angle of the silicon-supported PTFMA-*b*-Pt-BMA brushes after 3 cycles of solvent treatment:  $\theta_A$  (●),  $\theta_R$  (○).

Table 4.2 outlines water contact angle of the silicon-supported diblock copolymer brushes in comparison with the silicon-supported homopolymer brushes. The surface rearrangement was also realized for the silicon-supported PTFMA-*b*-PMAA brushes upon the solvent treatment.

**Table 4.2** Contact angle data of the silicon-supported polymer brushes

Silicon-supported polymer brushes	Water contact angle (°)	
	$\theta_A$	$\theta_R$
Si/SiO <sub>2</sub> -PTFMA	102	79
Si/SiO <sub>2</sub> -PMAA	62	74
Si/SiO <sub>2</sub> -PTFMA- <i>b</i> -Pt-BMA (1:1 by mole)	90	70
Si/SiO <sub>2</sub> -PTFMA- <i>b</i> -PMAA (1:1 by mole)	61	54
Si/SiO <sub>2</sub> -PTFMA- <i>b</i> -PMAA (1:1 by mole) (after treat with $\alpha,\alpha,\alpha$ -trifluorotoluene)	102	77

## CHAPTER V

### CONCLUSION AND SUGGESTION

By surface-initiated polymerization through atom transfer radical polymerization (ATRP) mechanism, the diblock copolymer brushes of poly(2,2,2-trifluoroethyl methacrylate) and poly(*tert*-butyl methacrylate) (PTFMA-*b*-*Pt*-BMA) grafted on the silicon oxide substrates were synthesized. The reaction progress can be monitored by ellipsometry, contact angle measurements, <sup>1</sup>H-NMR analysis and gel permeation chromatography (GPC). It has been demonstrated that the homopolymer brushes of poly(2,2,2-trifluoroethyl methacrylate) (PTFMA) and poly(*tert*-butyl methacrylate) (*Pt*-BMA) and PTFMA-*b*-*Pt*-BMA brushes successfully grew from silicon supported  $\alpha$ -bromoisobutyrate monolayer using CuBr/PMDETA as a catalytic system in the presence of 2-bromo-2-methyl-propionic acid propyl ester as a sacrificial initiator. Results from GPC and ellipsometric analyses prompted that  $M_w$  and the thickness of both PTFMA and *Pt*-BMA brushes can be separately controlled as a function of reaction time and monomer to “free” initiator ratio in solution. The linear dependence of molecular weight and thickness on polymerization time clearly suggested that polymerization is living in character. The growth of each block was uniform and the thickness of polymer brushes continuously increased after the outer block of *Pt*-BMA was consecutively added to the inner block of PTFMA.

Diblock copolymer brushes of poly(2,2,2-trifluoroethyl methacrylate) and poly(methacrylic acid) (PTFMA-*b*-PMAA) were prepared by hydrolysis of PTFMA-*b*-*Pt*-BMA to remove the *tert*-butyl groups from the *Pt*-BMA block. The condition for hydrolysis was optimized using the silicon-supported *Pt*-BMA as a substrate. According to contact angle analysis, the suitable condition was to treat the substrate in 5M trifluoroacetic acid in dichloromethane for 4h.



Surface properties of the diblock copolymer brushes upon a treatment with  $\alpha,\alpha,\alpha$ -trifluorotoluene, a good solvent for the inner block of PTFMA were studied. As analyzed by contact angle measurements using water and hexadecane as probe fluids, it was found that the diblock copolymer brushes underwent surface rearrangement in response to the solvent treatment. The switching of contact angles from ones of the outer block (*Pt*-BMA or PMAA) to ones of the inner block (PTFMA) within 30 min of treatment suggesting that the PTFMA block became the dominated block at the solid-air interface whereas the *Pt*-BMA block was buried in the subsurface in order to minimize the surface free energy of the system. The extent of rearrangement was, however, limited in the system of which the outer block was so long that there was no enough space to accommodate the rearrangement. Also, it has been demonstrated that the surface rearrangement of the diblock copolymer brushes was reversible. The original stage of having the outer block dominated at the solid-air interface was fully recovered after the treated solvent was removed.

## REFERENCES

1. Nakamura K.; Maruno T.; Murata N. "Synthesis and Properties of a Novel Fluorine-Containing Alicyclic Diepoxide" *Macromolecules* **1996**, *29*, 2006 - 2010.
2. Auman B. C.; Higley D. P.; Scherer K. V. Jr.; McCord E. F.; Shaw W. H. Jr. "Synthesis of a New Fluoroalkylated Diamine, 5-[1 H, H-2-Bis(trifluoromethyl)-Heptafluoropentyl]-1,3-Phenylenediamine and Polyimides Prepared Therefrom" *Polymer* **1995**, *36*, 651 - 656.
3. Möller M.; Hopken J. "Low surface energy Polystyrene" *Macromolecules* **1992**, *25*, 1461 - 1467.
4. [www.pcimag.com](http://www.pcimag.com)
5. Mama K. G.; Chapman T. M. "Determination of Low Critical Surface Tensions of Novel Fluorinated Poly(amide urethane) Block Copolymers. 2. Fluorinated Soft-Block Backbone and Side Chains" *Macromolecules* **1995**, *28*, 2081 - 2085.
6. Ciardelli F.; Aglietto M.; Mirabello M. D.; Passaglia E.; Giancristoforo S.; Castelvetro V.; Ruggeri G. "New Fluorinated Acrylic Polymers for Improving Weatherability of Building Stone Materials" *Prog. Org. Coat.* **1997**, *32*, 43 - 50.
7. Ober C. K.; Kramer E. J.; Iyengar D. R.; Perutz S. M.; Dai C. "Surface Segregation Studies of Fluorine-Containing Diblock Copolymers" *Macromolecules* **1996**, *29*, 1229 - 1234.

8. Santerre J. P.; Yip C. M.; McCloskey C. B. "Effect of Fluorinated Surface-Modifying Macromolecules on the Molecular Surface Structure of a Polyether Poly(urethane urea)" *Macromolecules* **2002**, *35*, 924 - 933.
9. Jennings G. K.; Brantley E. L. "Fluorinated Polymer Films from Acylation of ATRP Surface-Initiated Poly(hydroxyethyl methacrylate)" *Macromolecules* **2004**, *37*, 1476 – 1483.
10. Ober C. K.; Kramer E. J.; Andruzzi L.; Hexemer A.; Li X.; Galli G.; Chiellini E.; Fischer D. A. "Control of Surface Properties Using Fluorinated Polymer Brushes Produced by Surface-Initiated Controlled Radical Polymerization" *Langmuir* **2004**, *20*, 10498 – 10506.
11. Granville A. M.; Brittain W. J.; Boyes S. G.; Akgun B.; Foster M. D. "Synthesis and Characterization of Stimuli-Responsive Semifluorinated Polymer Brushes Prepared by Atom Transfer Radical Polymerization" *Macromolecules* **2004**, *37*, 2790 – 2796.
12. Baker G. L.; Bruening M. L.; Sun L. "Polymer Brush Membranes for Pervaporation of Organic Solvents from Water" *Macromolecules* **2005**, *38*, 2307 – 2314.
13. Szwarc, M.; Levy, M.; Milkovich, R. "Polymerization Initiated by Electron Transfer to Monomer a New Method of Formation of Block Polymers" *J. Am. Chem. Soc.* **1956**, *78*, 2656-2657.
14. Flory, P. J. "Principles of Polymer Chemistry" *Cornell Uni. Press*, Ithaca, NY. **1978**.
15. Webster, O. W. "Living Polymerization Methods" *Science* **1991**, *251*, 887 - 892.

16. Moad, G.; Rizzardo, E.; Solomon D. H. "Selectivity of the Reaction of Free Radicals with Styrene" *Macromolecules* **1982**, *15*, 909-914.
17. Georges, M. K.; Veregin, R. P. N.; Kazmaier, P. M.; Hamer, G. K. "Narrow Molecular Weight Resins by a Free-Radical Polymerization Process" *Macromolecules* **1993**, *26*, 2987-2988.
18. Kato, M.; Kamigaito, M.; Sawamoto, M.; Higashimura, T. "Polymerization of Methyl Methacrylate with the Carbon Tetrachloride/ Dichlorotris-(triphenylphosphine)ruthenium(II)/Methylaluminum Bis(2,6-di-*tert*-butylphenoxide) Initiating System: Possibility of Living Radical Polymerization" *Macromolecules* **1995**, *28*, 1721-1723.
19. Wang, J. S.; Matyjaszewski, K. "Controlled/"Living" Radical Polymerization. Atom Transfer Radical Polymerization in the Presence of Transition-Metal Complexes" *J. Am. Chem. Soc.* **1995**, *117*, 5614-5615.
20. Percec, V.; Barboiu, B. "'Living" Radical Polymerization of Styrene Initiated by Arenesulfonyl Chlorides and CuI(bpy)<sub>n</sub>Cl" *Macromolecules* **1995**, *28*, 7970-7972.
21. Wayland, B. B.; Poszmik, G.; Mukerjee, S. L.; Fryd, M. "Living Radical Polymerization of Acrylates by Organocobalt Porphyrin Complexes" *J. Am. Chem. Soc.* **1994**, *116*, 7943-7944.
22. Granel, C.; DuBois, P.; Jerome, R.; Teyssie, P. "Controlled Radical Polymerization of Methacrylic Monomers in the Presence of a Bis(ortho-chelated) Arylnickel(II) Complex and Different Activated Alkyl Halides" *Macromolecules* **1996**, *29*, 8576-8582.
23. Matyjaszewski, K. "Controlled Radical Polymerization" *ACS Symposium Series NO. 685 American Chemical Society: Washington, DC*, **1997**.

24. Matyjaszewski, K. "Mechanistic and Synthetic Aspects of Atom Transfer Radical Polymerization" *J. Macromol. Sci., Pure Appl. Chem.* **1997**, *A34*, 1785-1801.
25. Chambard, G.; Klumperman, B.; German, A. L. "Effect of Solvent on the Activation Rate Parameters for Polystyrene and Poly(butyl acrylate) Macroinitiators in Atom Transfer Radical Polymerization" *Macromolecules* **2000**, *33*, 4417-4421.
26. Matyjaszewski K.; Xia J. "Atom Transfer Radical Polymerization" *Chem. Rev.* **2001**, *101*, 2921 – 2990.
27. Percec, V.; Barboiu, B.; Neumann, A.; Ronda, J. C.; Zhao, M. "Metal-Catalyzed "Living" Radical Polymerization of Styrene Initiated with Arenesulfonyl Chlorides. From Heterogeneous to Homogeneous Catalysis" *Macromolecules* **1996**, *29*, 3665-3668.
28. Matyjaszewski K.; Xia J. "Controlled/ "Living" Radical Polymerization. Atom Transfer Radical Polymerization Using Multidentate Amine Ligands" *Macromolecules* **1997**, *30*, 7697 – 7700.
29. Zhao, B.; Brittain, W. J. "Polymer Brushes: Surface-Immobilized Macromolecules" *Prog. Polym. Sci.* **2000**, *25*, 677-710.
30. Raphael, E.; De Gennes, P. G. "Rubber-Rubber Adhesion with Connector Molecules" *J. Phys Chem* **1992**, *96*, 4002-4007.
31. Ji, H.; De Gennes, P. G. "Adhesion *via* Connector Molecules: The Many-Stitch Problem" *Macromolecules* **1993**, *26*, 520-525.
32. Amiji, M.; Park, K. J. "Surface Modification of Polymeric Biomaterials with Poly(ethylene oxide), Albumin, and Heparin for Reduced Thrombogenicity" *Biomater. Sci. Polym. Ed.* **1993**, *4*, 217-234.

33. van Zanten, J. H. "Terminally Anchored Chain Interphases: Their Chromatographic Properties" *Macromolecules* **1994**, *27*, 6797-6807.
34. Joanny, J. F. "Lubrication by Molten Polymer Brushes" *Langmuir* **1992**, *8*, 989-995.
35. Takei, Y. G.; Aoki, T.; Sanui, K.; Ogata, N.; Sakurai, Y.; Okano, T. "Dynamic Contact Angle Measurement of Temperature-Responsive Surface Properties for Poly(N-isopropylacrylamide) Grafted Surfaces" *Macromolecules* **1994**, *27*, 6163-6166.
36. Ito, Y.; Ochiai, Y.; Park, Y. S.; Imanishi, Y. "pH-Sensitive Gating by Conformational Change of a Polypeptide Brush Grafted onto a Porous Polymer Membrane" *J. Am. Chem. Soc.* **1997**, *119*, 1619-1623.
37. Ito, Y.; Park, Y. S.; Imanishi, Y. "Visualization of Critical pH-Controlled Gating of a Porous Membrane Grafted with Polyelectrolyte Brushes" *J. Am. Chem. Soc.* **1997**, *119*, 2739-2740.
38. Ito, Y.; Nishi, S.; Park, Y. S.; Imanish, Y. "Oxidoreduction-Sensitive Control of Water Permeation through a Polymer Brushes-Grafted Porous Membrane" *Macromolecules* **1997**, *30*, 5856-5859.
39. Velten, U.; Shelden, R. A.; Caseri, W. R.; Suter, U. W.; Li, Y. "Polymerization of Styrene with Peroxide Initiator Ionically Bound to High Surface Area Mica" *Macromolecules* **1999**, *32*, 3590-3597.
40. Velten, U.; Tossati, S.; Shelden, R. A.; Caseri, W. R.; Suter, U. W.; Hermann, R.; Müller, M. "Graft Polymerization of Styrene on Mica: Formation and Behavior of Molecular Droplets and Thin Films" *Langmuir* **1999**, *15*, 6940-6945.
41. Niu, Q. J.; Fréchet, J. M. J. "Polymers for 193-nm Microlithography: Regioregular 2-Alkoxycarbonylnortricyclene Polymers by Controlled

Cyclopolymerization of Bulky Ester Derivatives of Norbornadiene”  
*Angew Chem, Int Ed Engl* **1998**, *37*, 667-670.

42. Singhvi, R.; Kumar, A.; Lopez, G. P.; Stephanopoulos, G. N.; Wang, D. I. C.; Whitesides, G. M.; Ingber, D. E. “Engineering Cell-Shape and Function” *Science* **1994**, *264*, 696-698.
43. Chen, C. S.; Mrksich, M.; Huang, S.; Whitesides, G. M.; Ingber, D. E. “Geometric Control of Cell Life and Death” *Science* **1997**, *276*, 1425-1428.
44. Aksay, I. A.; Trau, M.; Manne, S.; Honma, I.; Yao, N.; Zhou, L.; Fenter, P.; Eisenberger, P. M.; Gruner, S. M. “Biomimetic Pathways for Assembling Inorganic Thin Films” *Science* **1996**, *273*, 892-898.
45. Balazs, A. C.; Singh, C.; Zhulina, E.; Gersappe, D.; Pickett, G. “Patterned Polymer Films” *MRS Bull* **1997**, *22*, 16-21.
46. Soga, K. G.; Zuckermann, M. J.; Guo, H. “Binary Polymer Brush in a Solvent” *Macromolecules* **1996**, *29*, 1998-2005.
47. Mansky, P.; Liu, Y.; Huang, E.; Russell T. P.; Hawker, C. “Controlling Polymer-Surface Interactions with Random Copolymer Brushes” *Science* **1997**, *275*, 1458-1460.
48. Zhao, B.; Brittain, W. J. “Synthesis of Tethered Polystyrene-*block*-Poly (methyl methacrylate) Monolayer on a Silicate Substrate by Sequential Carbocationic Polymerization and Atom Transfer Radical Polymerization” *J. Am. Chem. Soc.* **1999**, *1219*, 3557-3558.
49. Nakayama, Y.; Matsuda, T. “Surface Macromolecular Architectural Designs Using Photo-Graft Copolymerization Based on Photochemistry of Benzyl N,N-Diethyldithiocarbamate” *Macromolecules* **1996**, *29*, 8622-8630.

50. Ejaz, M.; Yamamoto, S.; Ohno, K.; Tsujii, Y.; Fukuda, T. "Controlled Graft Polymerization of Methyl Methacrylate on Silicon Substrate by the Combined Use of the Langmuir-Blodgett and Atom Transfer Radical Polymerization Techniques" *Macromolecules* **1998**, *31*, 5934-5936.
51. Husseman, M.; Malmström, E. E.; McNamara, M.; Mate, M.; Mecerreyes, D.; Benoit, D. G.; Hedrick, Mansky, P.; Huang, E. ; Russell, T. P.; Hawker, C. J. "Controlled Synthesis of Polymer Brushes by "Living" Free Radical Polymerization Techniques" *Macromolecules* **1999**, *32*, 1424-1431.
52. Huang, X.; Wirth, M. J. "Surface Initiation of Living Radical Polymerization for Growth of Tethered Chains of Low Polydispersity" *Macromolecules* **1999**, *32*, 1694-1696.
53. Sedjo, R. A.; Mirous, B. K.; Brittain, W. J. "Synthesis of Polystyrene-*block*-poly(methyl methacrylate) Brushes by Reverse Atom Transfer Radical Polymerization" *Macromolecules* **2000**, *33*, 1492-1493.
54. de Boer, B.; Simon, H. K.; Werts, M. P. L.; van der Vegte, E. W.; Hadziioannou, G. "'Living" Free Radical Photopolymerization Initiated from Surface-Grafted Iniferter Monolayers" *Macromolecules* **2000**, *33*, 349-356.
55. Fukuda T.; Tsujii Y.; Marutani E.; Yamamoto S.; Ninjbadgar T.; Takano M. "Surface-Initiated Atom Transfer Radical Polymerization of Methyl Methacrylate on Magnetite Nanoparticles" *Polymer* **2004**, *45*, 2231 – 2235.
56. Matyjaszewski, K.; Miller, P. J.; Shukla, N.; Immaraporn, B.; Gelman, A.; Luokala, B. B.; Siclovan, T. M.; Kickelbick, G.; Vallant, T.; Hoffmann, H.; Pakula, T. "Polymers at Interfaces: Using Atom Transfer Radical Polymerization in the Controlled Growth of Homopolymers and Block



Copolymers from Silicon Surfaces in the Absence of Untethered Sacrificial Initiator” *Macromolecules* **1999**, *32*, 8716-8724.

57. von Werene, T.; Patten, T.E. “Atom Transfer Radical Polymerization from Nanoparticles: A Tool for the Preparation of Well-defined Hybrid Nanostructures and for Understanding the Chemistry of Controlled/“Living” Radical Polymerizations from Surfaces” *J. Am. Chem. Soc.* **2001**, *123*, 7497-7505.
58. Brittain W. J.; Zhao B.; Zhou W.; Cheng S. Z. D. “AFM Study of Tethered Polystyrene-*b*-Poly(methyl methacrylate) and Polystyrene-*b*-Poly(methyl acrylate) Brushes on Flat Silicate Substrates” *Macromolecules* **2000**, *33*, 8821 – 8827.
59. Brittain W. J.; Zhao B.; Zhou W.; Cheng S. Z. D. “Nanopattern Formation from Tethered PS-*b*-PMMA Brushes upon Treatment with Selective Solvents” *J. Am. Chem. Soc.* **2000**, *122*, 2407 – 2408.
60. Brittain W. J.; Baum M. “Synthesis of Polymer Brushes on Silicate Substrates via Reversible Addition Fragmentation Chain Transfer Technique” *Macromolecules* **2002**, *35*, 610 – 615.
61. Brittain W. J.; Zhao B. “Synthesis, Characterization, and Properties of Tethered Polystyrene-*b*-Polyacrylate Brushes on Flat Silicate Substrates” *Macromolecules* **2000**, *33*, 8813 – 8820.
62. Bruening M. L.; Baker G. L.; Huang W.; Kim B. “Functionalization of Surfaces by Water-Accelerated Atom Transfer Radical Polymerization of Hydroxyethyl Methacrylate and Subsequent Derivatization” *Macromolecules* **2002**, *35*, 1175 - 1179.

63. Bruening M. L.; Baker G. L.; Huang W.; Kim B. "Synthesis of Triblock Copolymer Brushes by Surface-Initiated Atom Transfer Radical Polymerization" *Macromolecules* **2002**, *35*, 5410 - 5416.
64. Iyoda T.; Abe J.; Kawai T.; Kong X. "Amphiphilic Polymer Brushes Grown from the Silicon Surface by Atom Transfer Radical Polymerization" *Macromolecules* **2001**, *34*, 1837 - 1844.
65. [www.uta.edu/optics/research/ellipsometry/ellipsometry.htm](http://www.uta.edu/optics/research/ellipsometry/ellipsometry.htm)
66. Xiao, S. J. "Tailored Organic Thin Films on Gold and Titanium: Peptide-Grafting, Protein Resistance and Physical Characterization" Thesis; M. Sc. Chemistry, Fudan University, Shanghai China 1999.
67. Seymour, M. P. "Introduction to Polymers Chemistry" *Tokyo, McGraw-Hill Kogakusha* **1971**.
68. Karanam, S.; Goossens, H.; Klumperman, B.; Lemstra, P. "Controlled Synthesis and Characterization of Model Methyl Methacrylate/*tert*-Butyl Methacrylate Triblock Copolymers via ATRP" *Macromolecules*, **2003**, *36*, 3051-3060.
69. Mori, H.; Seng, D. C.; Zhang, M.; Muller, A. H. E. "Hybrid Nanoparticle with Hyperbranched Polymer Shells via Self-Condensing Atom Transfer Radical Polymerization from Silica surface" *Lungmuir* **2002**, *18*, 3682-3693.



## **APPENDICES**

สถาบันวิทยบริการ  
จุฬาลงกรณ์มหาวิทยาลัย



**APPENDIX A**

สถาบันวิทยบริการ  
จุฬาลงกรณ์มหาวิทยาลัย

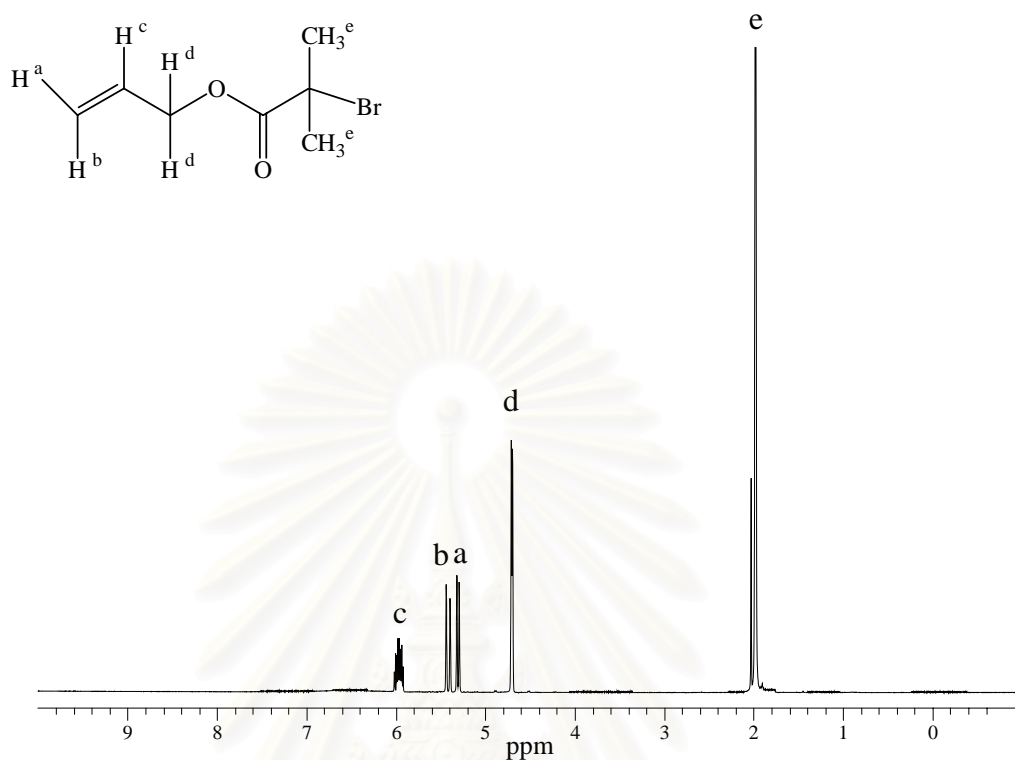


**Figure A-1**  $^1\text{H-NMR}$  spectrum (400 MHz,  $\text{CDCl}_3$ ) of 2-bromo-2-methylpropionic acid allyl ester (1).

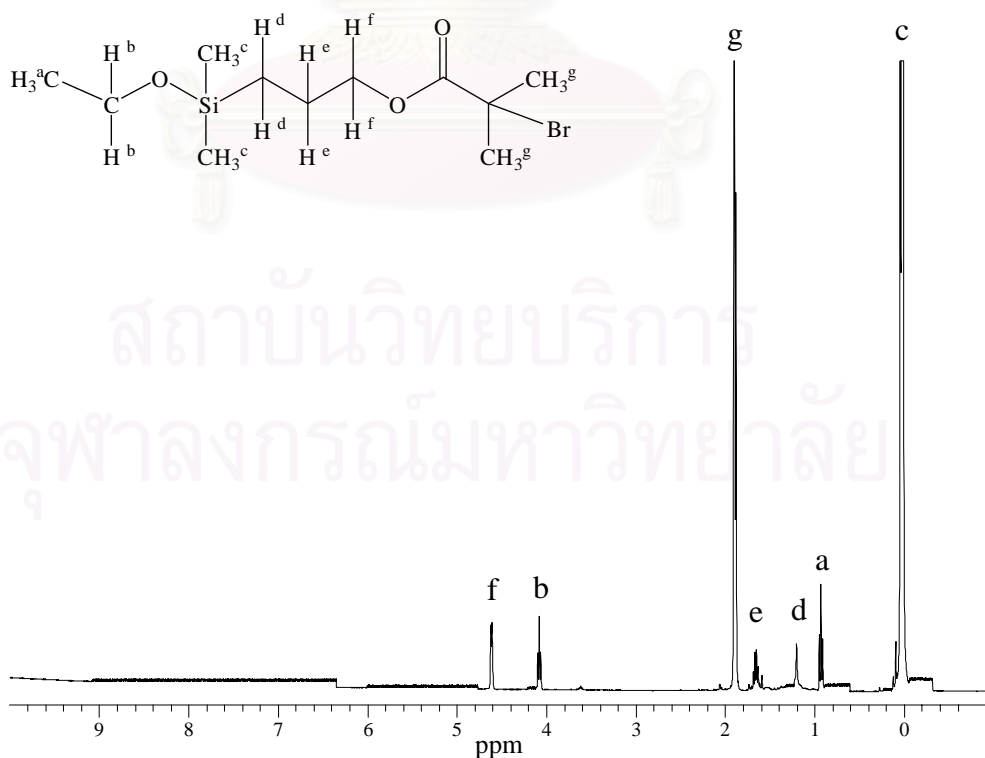


**Figure A-2**  $^1\text{H-NMR}$  spectrum (400 MHz,  $\text{CDCl}_3$ ) of 2-bromo-2-methylpropionic acid 3-(ethoxydimethylsilyl)propyl ester (2).

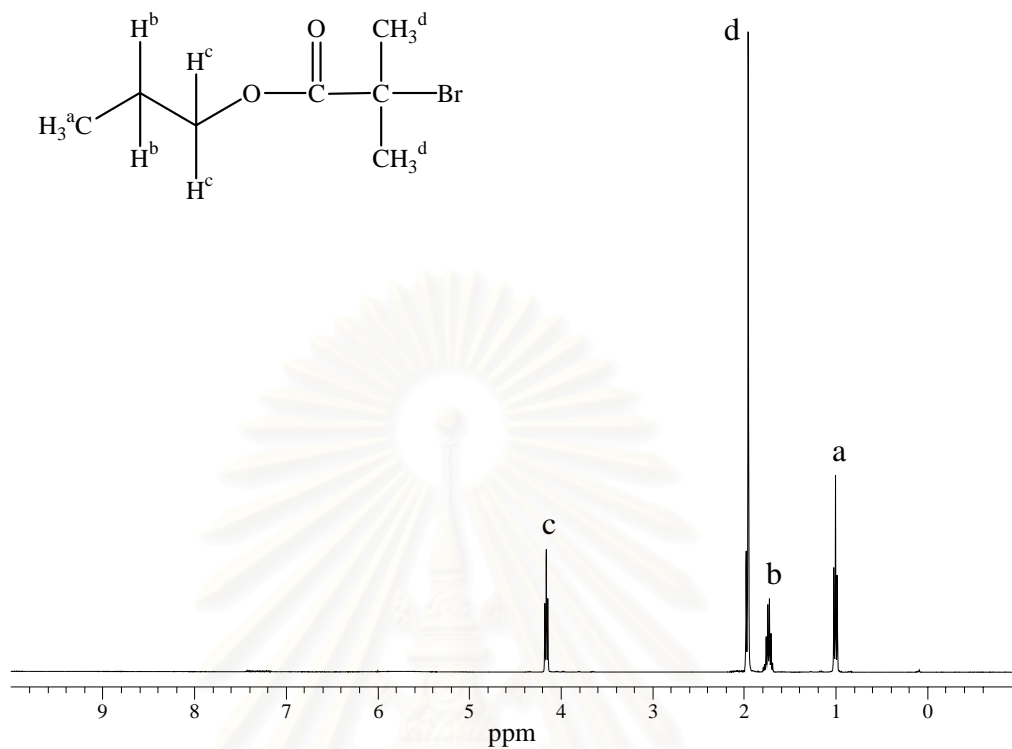
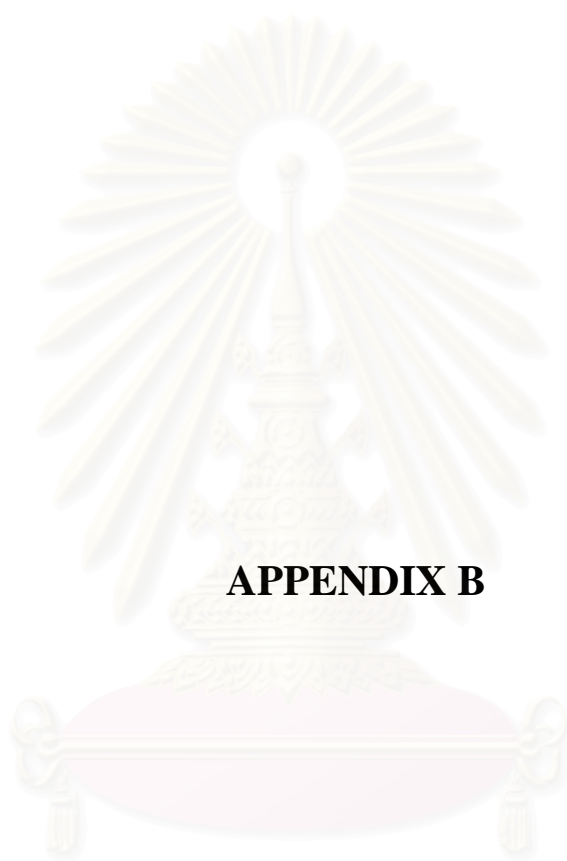


**Figure A-3**  $^1\text{H-NMR}$  spectrum (400 MHz,  $\text{CDCl}_3$ ) of 2-bromo-2-methylpropionic acid propyl ester (3).

สถาบันวิทยบริการ  
จุฬาลงกรณ์มหาวิทยาลัย



## APPENDIX B

สถาบันวิทยบริการ  
จุฬาลงกรณ์มหาวิทยาลัย

**Table B-1** Average thickness of Pt-BMA brushes for targeted DP = 100 and 200 calculated from ellipsometric data as a function of polymerization time.

Time (h)	Average thickness (nm)	
	targeted DP = 100	targeted DP = 200
2	2.0 ± 0.4	-
3	-	2.5 ± 0.4
4	3.0 ± 0.3	-
5	-	4.0 ± 0.4
8	5.5 ± 0.3	6.1 ± 0.2
16	9.0 ± 0.1	10.0 ± 0.1
24	12.0 ± 0.2	14.0 ± 0.1

**Table B-2** Advancing and receding water contact angle data of Pt-BMA brushes for targeted DP = 100 and 200 as a function of polymerization time.

Time (h)	$\theta_A/\theta_R$ (°)	
	targeted DP = 100	targeted DP = 200
0	70 ± 1.1/59 ± 1.2	70 ± 1.1/59 ± 1.2
2	87 ± 1.1/67 ± 1.2	-
3	-	88 ± 1.2/67 ± 1.1
4	89 ± 1.2/68 ± 1.1	-
5	-	90 ± 1.1/69 ± 1.2
8	89 ± 1.3/69 ± 1.1	90 ± 1.3/70 ± 1.2
16	90 ± 1.2/69 ± 1.2	90 ± 1.2/70 ± 1.2
24	90 ± 1.2/70 ± 1.1	91 ± 1.1/70 ± 1.2



**Table B-3** Average molecular weight and molecular weight distribution of Pt-BMA brushes for targeted DP = 100 and 200 analyzed by GPC as a function of polymerization time.

Time (h)	targeted DP = 100		targeted DP = 200	
	$\overline{M}_n \times 10^{-3}$	$\overline{M}_w/\overline{M}_n$	$\overline{M}_n \times 10^{-3}$	$\overline{M}_w/\overline{M}_n$
2	1.545	1.27	-	-
3	-	-	3.358	1.28
4	2.217	1.51	-	-
5	-	-	5.298	1.12
8	2.933	1.20	5.781	1.20
16	3.872	1.40	11.164	1.32
24	6.228	1.46	18.721	1.41

**Table B-4** Average thickness of PTFMA brushes for targeted DP = 100 and 200 calculated from ellipsometric data as a function of polymerization time.

Time (h)	Average thickness (nm)	
	targeted DP = 100	targeted DP = 200
4	2.5 ± 0.3	4.0 ± 0.2
8	4.4 ± 0.4	6.0 ± 0.4
16	7.5 ± 0.1	8.8 ± 0.1
24	10.0 ± 0.1	12.0 ± 0.3

**Table B-5** Advancing and receding water contact angle data of PTFMA brushes for targeted DP = 100 and 200 as a function of polymerization time.

Time (h)	$\theta_A/\theta_R$ (°)	
	targeted DP = 100	targeted DP = 200
0	$70 \pm 1.1/59 \pm 1.2$	$70 \pm 1.1/59 \pm 1.2$
4	$95 \pm 1.5/78 \pm 1.6$	$98 \pm 1.6/79 \pm 1.5$
8	$99 \pm 1.6/79 \pm 1.7$	$102 \pm 1.9/81 \pm 1.6$
16	$101 \pm 1.3/78 \pm 1.5$	$101 \pm 1.8/80 \pm 1.9$
24	$102 \pm 1.3/80 \pm 1.3$	$102 \pm 1.5/79 \pm 1.5$

**Table B-6** Average molecular weight and molecular weight distribution of PTFMA brushes for targeted DP = 100 and 200 analyzed by GPC as a function of polymerization time.

Time (h)	targeted DP = 100		targeted DP = 200	
	$\bar{M}_n \times 10^{-3}$	$\bar{M}_w/\bar{M}_n$	$\bar{M}_n \times 10^{-3}$	$\bar{M}_w/\bar{M}_n$
4	2.533	1.07	6.308	1.10
8	4.636	1.10	10.484	1.05
16	8.941	1.09	17.000	1.07
24	12.444	1.08	25.195	1.09

**Table B-7** Advancing and receding water contact angle data of Pt-BMA brushes after hydrolysis by a varied concentration of TFA in dichloromethane for 4h.

[TFA] (M)	$\theta_A/\theta_R$ (°)
0.0	93 ± 1.8/74 ± 2.5
0.5	86 ± 1.8/62 ± 1.6
1.5	82 ± 1.5/62 ± 2.3
2.5	69 ± 1.6/55 ± 1.9
5.0	62 ± 1.1/54 ± 2.1
7.5	60 ± 1.2/53 ± 1.6

**Table B-8** Advancing and receding water contact angle data of Pt-BMA brushes after hydrolysis by a varied hydrolysis time using 5M TFA in dichloromethane.

Time (h)	$\theta_A/\theta_R$ (°)
0	94 ± 1.5/66 ± 2.2
4	62 ± 1.1/53 ± 2.1
8	68 ± 1.2/58 ± 1.4
12	68 ± 1.9/57 ± 1.6
24	66 ± 1.8/55 ± 2.3

**Table B-9** Average thickness of PTFMA-*b*-Pt-BMA brushes calculated from ellipsometric data as a function of *t*-BMA:TFMA ratio.

<i>t</i> -BMA:TFMA	Average thickness (nm)
0:1	10.0 ± 0.1
0.5:1	14.0 ± 0.5
1:1	18.2 ± 0.4
2:1	22.0 ± 0.3
3:1	24.1 ± 0.5

**Table B-10** Advancing and receding water and hexadecane contact angle data of PTFMA-*b*-P*t*-BMA brushes as a function of *t*-BMA:TFMA ratio.

<i>t</i> -BMA:TFMA	$\theta_A/\theta_R$ (°)	
	water	hexadecane
0:1	102 ± 1.2/80 ± 1.2	76 ± 1.2/52 ± 1.2
0.5:1	92 ± 1.6/72 ± 1.3	30 ± 1.2/20 ± 1.3
1:1	92 ± 1.3/71 ± 1.6	29 ± 1.4/20 ± 1.2
2:1	91 ± 1.8/70 ± 1.2	31 ± 1.4/19 ± 1.3
3:1	90 ± 1.5/71 ± 1.2	30 ± 1.3/20 ± 1.2

**Table B-11** Advancing and receding water and hexadecane contact angle data of PTFMA-*b*-P*t*-BMA brushes (mole ratio = 1:1) before and after treatment with  $\alpha,\alpha,\alpha$ -trifluorotoluene as a function of treatment time.

Time (min)	$\theta_A/\theta_R$ (°)	
	water	hexadecane
0	91 ± 1.6/70 ± 1.3	30 ± 1.7/20 ± 1.3
10	93 ± 1.8/69 ± 1.3	31 ± 1.2/19 ± 1.5
20	92 ± 1.2/70 ± 1.6	30 ± 1.2/20 ± 1.6
30	99 ± 1.2/79 ± 1.7	74 ± 1.7/53 ± 1.8
60	102 ± 1.3/78 ± 1.3	75 ± 1.5/54 ± 1.6
90	100 ± 1.5/80 ± 1.2	76 ± 1.4/53 ± 1.7
120	102 ± 1.5/81 ± 1.6	76 ± 1.2/52 ± 1.6

**Table B-12** Advancing and receding water and hexadecane contact angle data of PTFMA-*b*-*Pt*-BMA brushes after treatment with  $\alpha,\alpha,\alpha$ -trifluorotoluene for 120 min as a function of *t*-BMA:TFMA ratio.

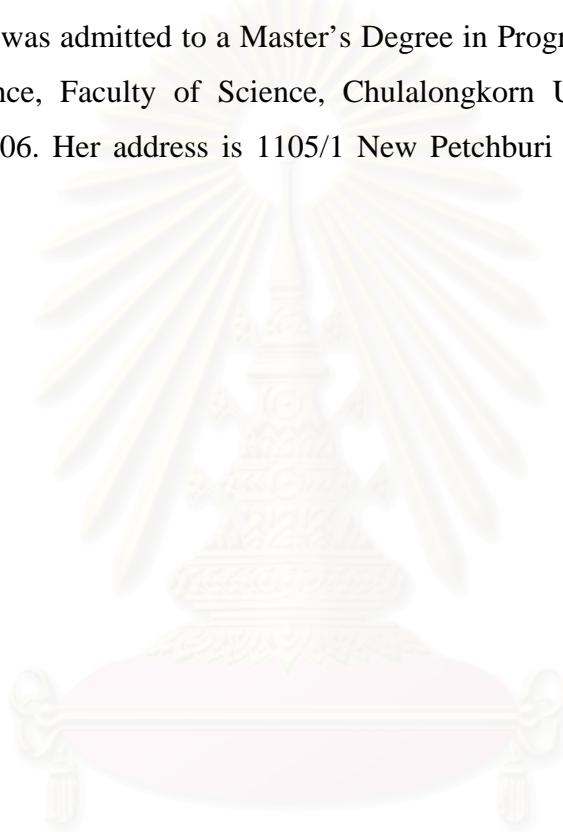
<i>t</i> -BMA:TFMA	$\theta_A/\theta_R$ (°)	
	water	hexadecane
0.5:1	102 ± 1.6/79 ± 1.3	75 ± 1.5/52 ± 1.3
1:1	100 ± 1.3/76 ± 1.6	76 ± 1.3/54 ± 1.6
2:1	100 ± 1.8/77 ± 1.2	75 ± 1.7/54 ± 1.2
3:1	91 ± 1.5/68 ± 1.3	31 ± 1.5/19 ± 1.3

**Table B-13** Advancing and receding water and hexadecane contact angle data of PTFMA-*b*-*Pt*-BMA brushes (mole ratio = 1:1) after 3 cycles of solvent treatment.

cycle	$\theta_A/\theta_R$ (°)	
	water	hexadecane
1	101 ± 1.5/80 ± 1.6	76 ± 1.4/52 ± 1.5
	90 ± 1.3/69 ± 1.5	29 ± 1.5/19 ± 1.3
2	102 ± 1.4/79 ± 1.8	76 ± 1.8/52 ± 1.4
	90 ± 1.7/70 ± 1.5	30 ± 1.9/19 ± 1.4
3	102 ± 1.4/81 ± 1.5	77 ± 1.9/51 ± 1.5
	91 ± 1.5/71 ± 1.7	30 ± 1.5/20 ± 1.6

## VITAE

Miss Sirorat Jeamrattanapitak was born on August 6, 1982 in Bangkok, Thailand. She received a bachelor degree of science from Department of Chemistry, Faculty of Science, Mahidol University, Rama VI, Bangkok Thailand in 2003. In the same year she was admitted to a Master's Degree in Program of Petrochemistry and Polymer Science, Faculty of Science, Chulalongkorn University and completed program in 2006. Her address is 1105/1 New Petchburi Road, Rajtavee, Bangkok 10400.



สถาบันวิทยบริการ  
จุฬาลงกรณ์มหาวิทยาลัย